



**HAL**  
open science

# Research on Performance Evaluation and Anti-scaling Mechanism of Green Scale Inhibitors by Static and Dynamic Methods

Dan Liu

► **To cite this version:**

Dan Liu. Research on Performance Evaluation and Anti-scaling Mechanism of Green Scale Inhibitors by Static and Dynamic Methods. Environmental Engineering. Ecole nationale supérieure d'arts et métiers - ENSAM, 2011. English. NNT : 2011ENAM0025 . pastel-00637079

**HAL Id: pastel-00637079**

**<https://pastel.hal.science/pastel-00637079>**

Submitted on 30 Oct 2011

**HAL** is a multi-disciplinary open access archive for the deposit and dissemination of scientific research documents, whether they are published or not. The documents may come from teaching and research institutions in France or abroad, or from public or private research centers.

L'archive ouverte pluridisciplinaire **HAL**, est destinée au dépôt et à la diffusion de documents scientifiques de niveau recherche, publiés ou non, émanant des établissements d'enseignement et de recherche français ou étrangers, des laboratoires publics ou privés.

École doctorale n° 432 : Sciences des Métiers de l'Ingénieur

**Doctorat ParisTech**

**T H È S E**

pour obtenir le grade de docteur délivré par

**l'École Nationale Supérieure d'Arts et Métiers**

**Spécialité " MECANIQUE MATERIAUX "**

*présentée et soutenue publiquement par*

**Dan LIU**

le 26 septembre 2011

**Research on Performance Evaluation and  
Anti-scaling Mechanism of Green Scale Inhibitors  
by Static and Dynamic Methods**

Directeur de thèse : **Franck HUI**

Co-encadrement de la thèse : **Jean LÉDION et Fengting LI**

**Jury**

**M. Hubert PERROT**  
**M. Georges MAURIN**  
**M. Mohamed TLILI**  
**M. Pierre LEROY**  
**M. Vincent JI**  
**M. Jean LEDION**  
**M. Franck HUI**  
**M. Olivier HORNER**

Directeur de Recherche, CNRS-Université Pierre et Marie-Curie  
Directeur de Recherche, CNRS-Université Pierre et Marie-Curie  
Maître de Conférences, CERTE, Tunisie  
Consultant, ARTS  
Professeur, Université Paris-Sud 11  
Expert, ARTS  
Chargé de Recherche, PIMM-CNRS-Arts et Métiers ParisTech  
Chef de projet, EDF

Président  
Rapporteur  
Rapporteur  
Examinateur  
Examinateur  
Examinateur  
Examinateur  
Invité

**T  
H  
È  
S  
E**

## **REMERCIEMENTS**

Ce travail a été réalisé au Laboratoire Procédés et Ingénierie en Mécanique et Matériaux (ancien Laboratoire d'Ingénierie des Matériaux, LIM) PIMM - CNRS UMR 8006 aux Arts et Métiers ParisTech. Je tiens à remercier Monsieur Thierry BRETHERAU, directeur du Laboratoire, pour m'y avoir accueilli. Les travaux de thèse ont été effectués sous la direction de Monsieur Jean LÉDION, expert (ARTS) et de Monsieur Franck HUI, Chargé de recherche au CNRS. Je les remercie sincèrement pour m'avoir initié à ce domaine de recherche original français et aux pensées et techniques d'études dont ils sont les promoteurs.

Que soit tout particulièrement remercié Monsieur Fengting LI, professeur au College of Environmental Science and Engineering de l'Université de Tongji (Chine) qui m'a fait confiance en me proposant ce travail qui faisait appel à une coopération franco-chinoise.

Ma gratitude va également à Monsieur G. MAURIN, Directeur de recherche au CNRS et à Monsieur M.TLILI, Maître de Conférences au Centre des Recherches et Technologies des Eaux (Tunisie) qui ont eu la tâche d'être rapporteurs de ce travail de thèse.

Je tiens aussi à remercier Monsieur H. PERROT, Directeur de recherche au CNRS, Monsieur P. LEROY, ancien directeur scientifique du CRECEP et Monsieur V. JI, Professeur à l'Université Paris-Sud 11, d'avoir bien voulu accepté d'être membres du jury, ainsi que Monsieur O. HORNER, Chef de projet chez EDF, qui a bien voulu s'intéresser à ces travaux.



# Résumé

Les exigences environnementales imposent de nombreux défis dans le domaine du traitement des eaux. Ainsi, le concept de « chimie verte » a-t-il été proposé et l'utilisation des produits chimiques « écologiques » est devenue une nécessité. Il est donc d'une importance primordiale d'élaborer des inhibiteurs d'entartrage « verts » afin de combattre les phénomènes d'entartrage qui ont des conséquences désastreuses, voire catastrophiques, dans certaines installations industrielles, comme les circuits de refroidissement des centrales nucléaires.

Dans cette étude, l'efficacité de différents inhibiteurs d'entartrage de  $\text{CaCO}_3$  a été évaluée dans un circuit de refroidissement simulé. En tant qu'inhibiteurs de précipitation de Ca-phosphonates, des homo-, co- et ter-polymères ont également été étudiés en matière de leur efficacité. En fait, l'ajout de ces polymères dans l'eau contenant des phosphonates peut réduire la précipitation du Ca-phosphonates et renforcer l'efficacité d'inhibition de l'entartrage du  $\text{CaCO}_3$ . L'effet synergétique de l'acide polyaspartique (PASP) et de l'acide polyepoxysuccinique (PESA) sur l'inhibition de l'entartrage a été étudié en utilisant à la fois des méthodes statique et dynamique. Les résultats obtenus montrent que l'efficacité inhibitrice du mélange PASP-PESA est supérieure à celle du PASP ou du PESA pris individuellement pour la précipitation de  $\text{CaCO}_3$ ,  $\text{CaSO}_4$  et  $\text{BaSO}_4$ . L'effet de la concentration des inhibiteurs, de la température et de la concentration de  $\text{Ca}^{2+}$  ont également été étudiés. Par ailleurs, l'analyse par MEB a bien montré la modification de morphologie des précipités en présence du PASP et du PESA.

Dans ce travail, on a également étudié les propriétés inhibitrices des ions  $\text{Cu}^{2+}$  et  $\text{Zn}^{2+}$  dans l'eau potable avec la méthode de Précipitation Contrôlée Rapide (PCR) développée dans le Laboratoire (LIM). Les résultats obtenus montrent que ces ions métalliques sont des inhibiteurs très efficaces à faible concentration. De plus, l'analyse par MEB et IR indiquent que ces ions peuvent affecter la morphologie cristalline du  $\text{CaCO}_3$ . Par ailleurs, l'influence de la température et du  $\text{CO}_2$  dissous sur le pouvoir entartrant de l'eau minérale de Salvetat (utilisée comme eau de référence), en présence des ions  $\text{Cu}^{2+}$  et  $\text{Zn}^{2+}$ , a été étudiée expérimentalement.

L'inhibiteur idéal serait un composé sous forme solide dont la solubilité serait très faible, mais largement suffisante pour assurer une inhibition totale de l'entartrage. Il pourrait ainsi être mis en contact directement avec l'eau à traiter sans que l'on ait à se soucier de sa concentration qui serait régulée automatiquement par sa solubilité. La synthèse de tels inhibiteurs a été réalisée et leur efficacité a été évaluée durant cette thèse. En fait, les inhibiteurs solides obtenus ont une solubilité de l'ordre de 1,5 mg/L dans l'eau du robinet de Paris et ils donnent une inhibition totale de  $\text{CaCO}_3$  dans la même eau avec une concentration seulement de 30 ppb ( $\mu\text{g/L}$ ). De plus, l'introduction de ces inhibiteurs solides peut être réalisée facilement par une cartouche.



## ABSTRACT

Increasing environmental concerns and discharge limitations have imposed additional challenges in treating process waters. Thus, the concept of “Green Chemistry” was proposed and green scale inhibitors became a focus of water treatment technology. Finding some economical and environmentally friendly inhibitors is one of the major research focuses nowadays.

In this dissertation, the inhibition performance of different phosphonates as  $\text{CaCO}_3$  scale inhibitors in simulated cooling water was evaluated. Homo-, co-, and ter-polymers were also investigated for their performance as Ca-phosphonate inhibitors. Addition of polymers as inhibitors with phosphonates could reduce Ca-phosphonate precipitation and enhance the inhibition efficiency for  $\text{CaCO}_3$  scale.

The synergistic effect of polyaspartic acid (PASP) and Polyepoxysuccinic acid (PESA) on inhibition of scaling has been studied using both static and dynamic methods. Results showed that the anti-scaling performance of PASP combined with PESA was superior to that of PASP or PESA alone for  $\text{CaCO}_3$ ,  $\text{CaSO}_4$  and  $\text{BaSO}_4$  scale. The influence of dosage, temperature and  $\text{Ca}^{2+}$  concentration was also investigated in simulated cooling water circuit. Moreover, SEM analysis demonstrated the modification of crystalline morphology in the presence of PASP and PESA.

In this work, we also investigated the respective inhibition effectiveness of copper and zinc ions for scaling in drinking water by the method of Rapid Controlled Precipitation (RCP). The results indicated that the zinc ion and copper ion were high efficient inhibitors of low concentration, and the analysis of SEM and IR showed that copper and zinc ions could affect the calcium carbonate germination and change the crystal morphology. Moreover, the influence of temperature and dissolved  $\text{CO}_2$  on the scaling potential of a mineral water (Salvetat) in the presence of copper and zinc ions was studied by laboratory experiments.

An ideal scale inhibitor should be a solid form compound having a very low solubility, but the value of this solubility is big enough to ensure a total scaling inhibition. A new type of scale inhibitor we synthesized possesses these properties. In fact, the synthesized inhibitor has a very poor solubility (about 1.5 mg/L) at 20°C for Paris’s tap water. Its anti-scaling properties have been evaluated by RCP method. A complete scaling inhibition was obtained with a concentration of 30  $\mu\text{g/L}$  (ppb) for Salvetat water at 30°C. Moreover, the introduction of the synthesized solid inhibitor to a water system can be easily realized by using a cartridge.

**Key Words:** circulating cooling water, green scale inhibitor, calcium carbonate, anionic polymer, polyaspartic acid, polyepoxysuccinic acid, metal ion, solid scale inhibitor



# Contents

<b>Chapter 1. Introduction.....</b>	<b>12</b>
1.1 Scaling .....	12
1.2 Hazard of scale.....	12
1.3 Formation of CaCO <sub>3</sub> scale .....	13
1.4 Inhibition of CaCO <sub>3</sub> formation .....	14
1.5 Evaluation methods for the scaling power of water.....	15
1.6 Methods of scale inhibition.....	19
1.7 Scale inhibitor .....	19
1.8 Green scale inhibitor .....	21
1.9 Mechanism of scale inhibition .....	22
<b>Chapter 2. Evaluation of anionic polymers as scale inhibitors on CaCO<sub>3</sub> and Ca-phosphonate precipitates.....</b>	<b>25</b>
2.1 Experimental.....	26
2.1.1 Main materials .....	26
2.1.2 Static tests for Ca-Phosphonate precipitation of various phosphonate inhibitors ..	27
2.1.3 Static tests for effects of polymeric inhibitors on Ca-Phosphonate formation.....	28
2.1.4 Static tests for inhibition efficiency of inhibitors on CaCO <sub>3</sub> scale formation .....	28
2.2 Results and Discussion .....	29
2.2.1 Static tests for Ca-phosphonates precipitation .....	29
2.2.2 Inhibition of Ca-Phosphonate precipitation .....	34
2.2.3 Inhibition of CaCO <sub>3</sub> scale formation by phosphonates and observed “threshold effect” .....	36
2.2.4 Inhibition of CaCO <sub>3</sub> scale formation by terpolymer .....	37
2.3 Summary .....	38
<b>Chapter 3. Performance of polyaspartic acid/ polyepoxysuccinic acid and their synergistic effect on inhibition of scaling .....</b>	<b>39</b>
3.1 Experimental.....	39
3.1.1 Materials .....	39
3.1.1.1 PASP .....	39
3.1.1.2 PESA.....	40
3.1.1.3 Water studied.....	40
3.1.2 Methods .....	41
3.1.2.1 Static tests for scale inhibition efficiency .....	41
3.1.2.2 Rapid controlled precipitation (RCP) tests .....	41
3.1.2.3 Continuous tests .....	43
3.2 Results and discussion .....	44
3.2.1 Comparison of anti-scaling performance of PASP and PESA .....	44
3.2.1.1 Static tests of scale inhibition.....	44
3.2.1.1.1 Inhibition of CaCO <sub>3</sub> scale .....	44
3.2.1.1.2 Inhibition of CaSO <sub>4</sub> ·2H <sub>2</sub> O scale .....	45
3.2.1.1.3 Inhibition of BaSO <sub>4</sub> scale.....	45

3.2.1.1.4 Inhibition of SrSO <sub>4</sub> scale.....	46
3.2.1.2 RCP tests.....	46
3.2.1.2.1 Inhibition effect of PASP.....	46
3.2.1.2.2 Inhibition effect of PESA.....	50
3.2.1.2.3 Comparison of anti-scaling performance.....	53
3.2.1.3 Anti-scaling mechanism.....	54
3.2.1.3.1 SEM analysis.....	54
3.2.1.3.2 XRD analysis.....	56
3.2.2 Synergistic effect of PASP and PESA on inhibition of scaling.....	59
3.2.2.1 Evaluation of scale inhibition performance by static tests.....	59
3.2.2.1.1 Research of synergistic effects on inhibition of CaCO <sub>3</sub> .....	59
3.2.2.1.2 Research of synergistic effects on inhibition of CaSO <sub>4</sub> ·2H <sub>2</sub> O.....	59
3.2.2.1.3 Research of synergistic effects on inhibition of BaSO <sub>4</sub> .....	60
3.2.2.2 Evaluation of scale inhibition performance by RCP tests.....	60
3.2.2.2.1 Effect of dosage of PASP combined with PESA on inhibition of CaCO <sub>3</sub> .....	60
3.2.2.2.2 Effect of Ca <sup>2+</sup> concentration on inhibition of CaCO <sub>3</sub> .....	64
3.2.2.2.3 Effect of temperature on inhibition of CaCO <sub>3</sub> .....	64
3.2.2.3 Evaluation of scale inhibition performance by continuous tests.....	66
3.3 Summary.....	69
<b>Chapter 4. Effects of Copper and Zinc Ion in Preventing Scaling of Drinking Water</b>	<b>71</b>
.....	.....
4.1 Experimental.....	71
4.1.1 Materials.....	71
4.1.1.1 Reagents.....	71
4.1.1.2 Water studied.....	71
4.1.2 Method.....	71
4.2 Results and discussion.....	71
4.2.1 Anti-scaling Tests of Zinc Ions of Different Concentrations.....	71
4.2.2 Anti-scaling Tests of Copper Ions of Different Concentrations.....	74
4.2.3 Comparison Between Inhibition Effectiveness of Zinc Ion and that of Copper Ion.....	76
4.2.4 Inhibition Mechanism of Scaling by Copper and Zinc Ions.....	78
4.2.5 Effects of temperature and dissolved CO <sub>2</sub> on the scaling of water in the presence of copper and zinc.....	80
4.2.5.1 Tests on scaling capacity of Salvetat water.....	81
4.2.5.1.1 The influence of temperature.....	81
4.2.5.1.2 The influence of dissolved CO <sub>2</sub> .....	81
4.2.5.2 Inhibition of scaling in the presence of copper.....	82
4.2.5.2.1 The influence of temperature.....	82
4.2.5.2.2 The influence of dissolved CO <sub>2</sub> .....	83
4.2.5.3 Inhibition of scaling in the presence of zinc.....	85
4.2.5.3.1 The influence of temperature.....	85
4.2.5.3.2 The influence of dissolved CO <sub>2</sub> .....	86

4.3 Summary.....	87
<b>Chapter 5. Evaluation of a new “green” solid scale inhibitor with real “threshold effect” .....</b>	<b>88</b>
5.1 Experimental.....	88
5.1.1 Materials .....	88
5.1.1.1 Test water .....	88
5.1.1.2 Synthesis of Solid inhibitor.....	88
5.1.2 Methods .....	88
5.1.2.1 RCP.....	88
5.1.2.2 Measurement of solubility .....	88
5.2 Results and discussion .....	88
5.3 Summary.....	88
<b>Conclusions &amp; Perspective .....</b>	<b>89</b>
Conclusions.....	89
Perspective .....	90
<b>References.....</b>	<b>91</b>



# Chapter 1. Introduction

Scaling in natural hard water is a major concern in different facets of industrial processes and domestic installations. Undesirable scale deposits often cause numerous technical and economical problems such as total or partial obstruction of pipes leading to a decrease in flow rate; reduced heat transfer as calcium carbonate precipitate is 15 to 30 times less conductive than steel; seizure of valves and clogging of filters, etc. In nuclear power plants, the power produced is often limited by scaling in cooling towers. In Great Britain, the non-productive expenses related to scaling were estimated at 600 million pounds per year. The same expenses are about 1.5 billion euros per year in France <sup>[1]</sup>. Hence, it is of vital importance to establish appropriate methods to study this phenomenon and find effective ways to prevent or combat it.

## 1.1 Scaling

Scaling is a phenomenon of precipitation or simple adhesion of calcium carbonate on the walls in contact with water containing calcium salts and magnesium in solution. Since the precipitation will bond on the surface of materials and form a relatively stable bond with the matrix, so scaling is obviously different with precipitating action which is just the loose solid aggregates in the liquid phase. Scaling is essentially linked to the formation of calcium carbonate ( $\text{CaCO}_3$ ). Scaling may contain other residues such as algae, calcium sulfate, clays and the brucite  $\text{Mg}(\text{OH})_2$ . But it is always calcium carbonate that precipitates first, usually in the colloidal form, because its solubility is lower than that of others <sup>[2]</sup>.

Scaling comes from the succession of two distinct phases: germination growth of colloidal particles linked to an electrochemical phenomenon and the setting of deposit on the surface due to electrostatic phenomenon.

**Nucleation:** The ions  $\text{Ca}^{2+}$  and  $\text{CO}_3^{2-}$  associate to form a polymer of ions. The nucleation may be spontaneous or provoked.

**Dehydration:** The polymer forms ion dehydration. Capturing other groups of ions  $\text{Ca}^{2+}$  and  $\text{CO}_3^{2-}$ , it will become electrically charged colloidal particles. Particulate matter remains in suspension as it is loaded.

**Growth:** The size increases by capturing new ions  $\text{Ca}^{2+}$  and  $\text{CO}_3^{2-}$ . After the nucleation, the growth occurs more easily than a new nucleation.

## 1.2 Hazard of scale

Water is the fundamental natural resource and the strategic economic resource. Water plays a central and general role in human activities, development of social economy and the ecological environment balance.

Recycling the industrial water has been an effective measure of mitigating the stress that the industrial water brings to the water source. But recycle of industrial water is easy to form scale in some operation stages due to the complexity of the water quality and the

operation conditions. The scale brings bad influence to the normal operation and threatens the safety of operation.

Cycling cooling water system is cooled through evaporating in the operational process. In the process, there will be different kinds of substances deposit on the surface of heat transfer. The deposit can be divided into four categories: scale, sludge, corrosion products and biological deposits. Normally, the main composition of scale is  $\text{CaCO}_3$  which is a kind of inorganic substance with low thermal conductivity. In the cycling cooling water system, the scale on the pipe wall of the heat exchanger will impede its heat transfer and low the cooling effect. In the pipe that transport the cooling water, the scale will decrease the sectional area of the pipe and reduce the flow quantity of the cooling water, even block up the channel and reduce the cooling effect as a result. The scale can also make oxygen concentration cell form on the surface of metal equipment and induce the corrosion of metals. So the form of scale can bring bad influence to the normal operation of devices and cause giant economic loss <sup>[3]</sup>.

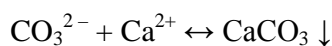
In a word, scale has great influence to industrial process, environment safety and economic benefits. Hence, it is of vital importance to establish appropriate methods to study this phenomenon and find effective ways to prevent or combat it.

### 1.3 Formation of $\text{CaCO}_3$ scale

The formation of calcium carbonate scale generally comprises two stages: germination and growth <sup>[4,5]</sup>.

#### (1) Germination

Germination consists in the appearance of a solid phase within a solution which is initially deprived of it. The appearance of the germs is done according to the chemical reaction:



When germination occurs in water and without contact with another surface, germination is known as homogeneous. On the other hand, in contact with a compound other than  $\text{CaCO}_3$ , which constitutes a solid surface, germination is known as heterogeneous. For the interaction between the germs of  $\text{CaCO}_3$  and the walls, when water is sufficiently calcifying (supersaturation coefficient  $\delta > 1$ ) and free from a significant quantity of impurities, colloidal calcium carbonate germs appear. They have a positive potential  $\zeta$  if such a germ is transferred in the vicinity of a metal wall. Therefore it can then be adsorbed on the surface, which has, in general, a negative electrochemical potential. Two cases are then possible:

- The germ strongly adheres to the wall and it is the starter of scaling of the metal wall.
- The germ (of a larger size than in the preceding case), which is transferred in the vicinity of the metal wall, is simply attracted without being really adsorbed. In this case, it can be used as site of growth of calcium carbonate, locally in excess (Fig.1.1).

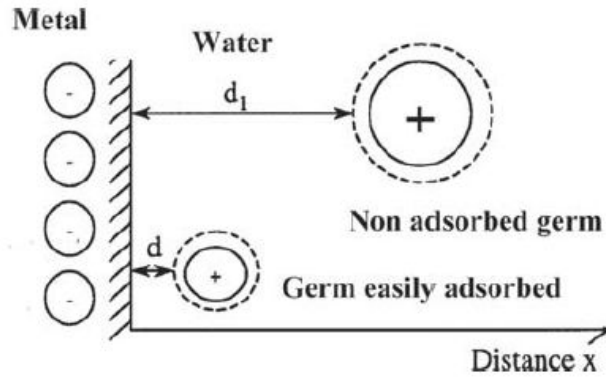


Fig.1.1 Adsorption of calcium carbonate germs on a metal wall

On the other hand, if one is in the presence of insulating surfaces, which are not metallic, the phenomenon remains similar even if the nature of surfaces involves a different type of adhesion. In the case of polymers, only attraction of the electrostatic type can be considered, because the reactivity of the majority of polymer surfaces is probably null with regard to the local modification of calcocarbonics balances.

(2) Growth of the deposits on the walls

In the case of the metal walls, as in the case of the insulating walls containing polymer, the first adsorbed germs can be used as site of growth for excesses of  $\text{CaCO}_3$  suitable for settling. But after covering the total surface, there is no more distinction to make between metal wall and insulating wall. Thus we are in the presence of a calcium carbonate wall which turns, in its turn, to behave like an insulating wall. It will be able to be used as site of growth or to continue to trap by the electrostatic effect the  $\text{CaCO}_3$  germs. The growth of the layer continues with this mechanism.

## 1.4 Inhibition of $\text{CaCO}_3$ formation

(1) Inhibition of the germination phase

At the top saturation rate of about 40, homogeneous germination corresponds to energy stabilization of the system and cannot thus be inhibited. But the majority of natural waters are metastable, their supersaturation generally lying between 1 and 40. In this case, precipitation, by mechanism of a radical type, can be inhibited by certain organic compounds present in natural water. The inhibitors of germination do not intervene with the growth once of the germs are produced.

(2) Inhibition of the growth

The best inhibitions were obtained for compounds such as polyphosphates and some compounds as organic phosphorus or polymeric acrylic resins. Indeed, they present a great affinity for solid  $\text{CaCO}_3$  on the surface of which they are absorbed by blocking active sites of germs in growth. Thus, this could involve a modification of the electric charge which, being initially positive, becomes negative. This leads then to a local reduction in the saturation rate of the medium which becomes lower than 1. The germination of  $\text{CaCO}_3$  is always possible but, as they appear, the germs are inhibited and cannot grow any more <sup>[6]</sup>.

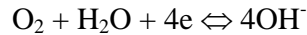
## 1.5 Evaluation methods for the scaling power of water

For decades, various attempts have been made to estimate the scaling power of natural waters and characterise the scaling formation mechanisms. We describe herein major different methods developed to date by emphasising whether they are representative with respect to a real-life scaling formation process.

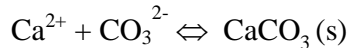
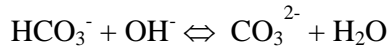
These methods can be roughly divided into two categories: electrochemical methods and non-electrochemical methods. The first one is made up of chronoamperometry, chronoelectro-gravimetry and electrochemical impedance technique which are all based on the reduction of the oxygen dissolved in the test water by polarizing a metallic electrode at a sufficiently negative potential. Among the non-electrochemical methods, we can enumerate the critical pH method, two thermal methods, an evaporation method, the LCGE method, the rapid controlled precipitation method, a polymer scaling test and a continuous test on tubes.

### (1) Electrochemical methods

The first electrochemical method, chronoamperometry <sup>[7]</sup>, has been proposed by Lédion. It is based on the electrochemical reduction of the oxygen dissolved in the test water by polarising a metallic electrode at a potential sufficiently negative according to:



The generation of hydroxide ions in the vicinity of the electrode can increase the local pH for several pH units and forces calcium carbonate to precipitate in a solid crystalline phase through two steps:



The limiting current intensity  $I_L$ , which is proportional to the flow of oxygen moving by convective diffusion towards the electrode, decreases whereas the active surface is progressively blocked by the growth of scale. Finally,  $I_L$  reaches a value close to zero when the surface is totally covered by the  $\text{CaCO}_3$  insulating layer.

The  $\text{CaCO}_3$  masse and the electrochemical impedance can also be measured with respect to time during scaling while the electrode was polarised at the limiting current for oxygen reduction. They are called the chronoelectrogravimetry and the electrochemical impedance technique respectively.

A typical chronoamperometric curve is shown in Fig.1.2. It is characterised by a falling current shape with time whose slope is related to the scaling rate. Lédion defined the scaling time,  $t_s$ , as the intersection of the tangent at the inflexion point of this curve and the time axis. It gives a rough estimate of the scaling potentiality of waters. The residual current  $i_{\text{res}}$  is somewhat related to the deposit morphology: the more compact and insulating the scale, the lower the residual current.

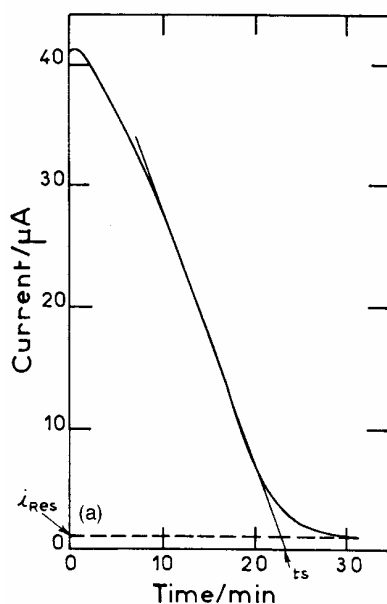


Fig.1.2 A typical chronoamperometric curve ( $t_s$ : scaling time;  $i_{res}$ : residual current)

Chronoelectrogravimetry <sup>[8]</sup> is the combination of the chronoamperometry and a quartz microbalance by which it is now possible to continuously follow extremely tiny mass changes. The frequency change,  $\Delta f$ , is proportional to the masse of scale deposited,  $\Delta m$ , on the electrode surface. Fig.1.3 shows a chronoelectrogravimetry curve which exhibits three steps in the scaling process.  $t_N$ , the nucleation time corresponding to the end of the first stage, is defined by the intersection of the linear part and the time axis;  $t_s$ , the scaling time corresponding to the end of the intermediate stage, is defined by the intersection of the linear part and the plateau.

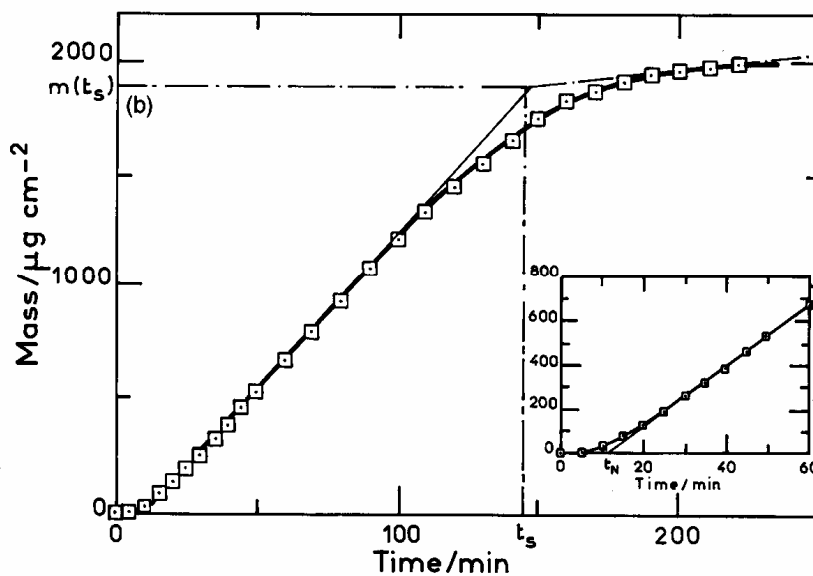


Fig.1.3 Chronoelectrogravimetric curve (variation of  $\text{CaCO}_3$  weight against time) for a natural water ( $t_N$ : nucleation time,  $t_s$ : scaling time)

Electrochemical impedance technique <sup>[9]</sup> shows two time constants more or less well separated during the scaling process: the high frequency time constant allows a pseudo high frequency resistance  $R_{HF}$  and a pseudo high frequency capacitance  $C_{HF}$  which are related to the coverage of the scale,  $C_{HF}$  can be obtained from  $2\pi f_{HF}R_{HF}C_{HF} = 1$ , as shown in Fig.1.4. Generally, the higher the  $R_{HF}$  value, the more compact and more adherent the scale deposit. The low frequency time constant is related to the oxygen diffusion in the bulk solution.

It is noted that even though the use of impedance technique can considerably improve the understanding of the electrochemical scaling process, this approach is much too complicated and time consuming to be used in practical situations.

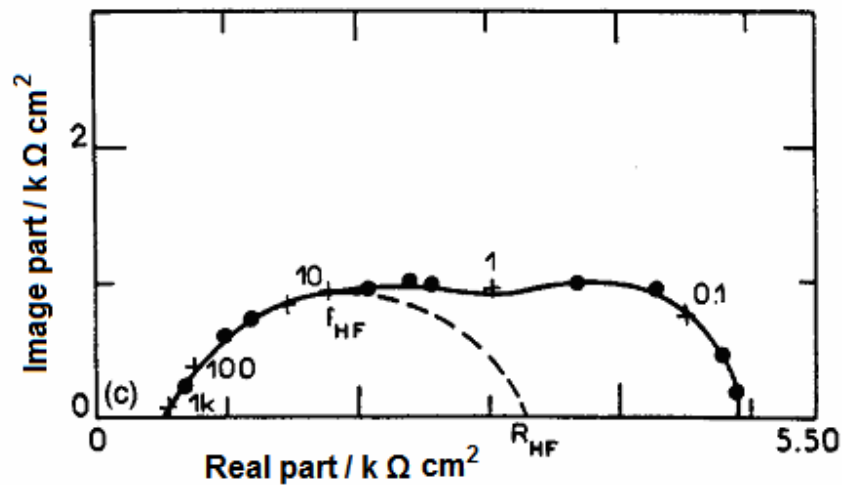


Fig.1.4 Electrochemical impedance diagram ( $R_{HF}$ : pseudo high frequency resistance;  $C_{HF}$ : pseudo high frequency capacitance)

## (2) Non-electrochemical methods

The critical pH method <sup>[10]</sup>, proposed by Feitler, is based on the fact that there is a critical pH above which scaling occurs. That is, when the actual pH exceeds the critical pH, precipitate forms in the bulk solution, and the pH undergoes a self-reduction.

Thermal method <sup>[11]</sup> is based on the temperature measurement of the wall of a tube in which the test water flows through. The tube is heated by an electric resistance surrounded externally. When scale deposits form on the tube wall, the heat transfer towards the water slows down and this leads to an increase of temperature on the tube wall.

Evaporation method <sup>[12]</sup> is based on the evaluation of the number of crystals,  $N$ , present in samples of supersaturated water (Fig.1.5). Two different types of analyses are carried out: a chemical analysis to determine the precipitated mass of  $CaCO_3$  and a morphometric analysis to define the mean characteristics of the crystals (diameter, shape and length).

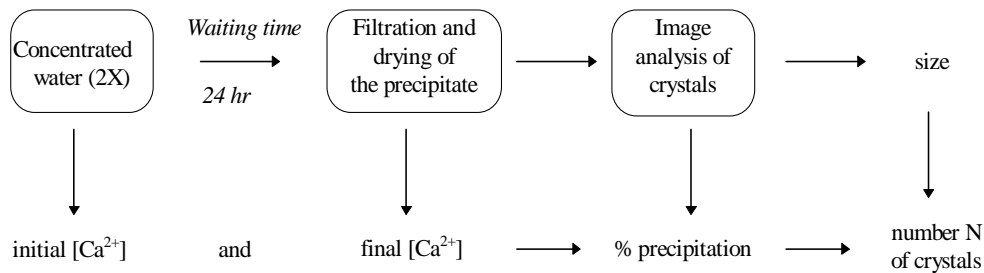


Fig.1.5 Test of scaling potentiality using Evaporation method

LCGE method <sup>[13]</sup>, proposed by Roques et al., aims at the dissociation of the different kinetic stages to isolate the most limiting one that is often the mass transfer on the solid-liquid interface.

Rapid controlled precipitation method (RCP) <sup>[14]</sup> is proposed by Lédion et al., which consists in degassing of CO<sub>2</sub> from the test water by a moderated agitation using a magnetic stirrer. In this way, the nucleation and the growth of CaCO<sub>3</sub> are initiated in a similar way of a natural scaling phenomenon. The water scaling capacity is then characterised by taking measurements of pH and resistivity as a function of time.

To simulate a real scaling procedure in hot water circuits, Lédion et al. have designed a test system called “continuous test rig” <sup>[15]</sup>.

By using the same CO<sub>2</sub> degassing procedure, Lédion et al. also proposed a gravimetry method called “polymer scaling test” <sup>[16]</sup>. It is based on electrostatic trapping of CaCO<sub>3</sub> nucleus by an insulating polyethylene wall. The experimental set-up is described in Fig.1.6. The specimen is a polyethylene tube. It is immersed in an austenitic stainless steel beaker containing the test water which is degassed by magnetic stirring. Test and reference specimens are cleaned prior to use followed by weighing on a balance accurate to a tenth of a milligram. After testing, the specimens are removed from the beaker lids, dried and then stabilised for a sufficient long time in the balance room and weighed. The weight gain due to the deposit was determined, taking into account the weight variation of the reference specimen.

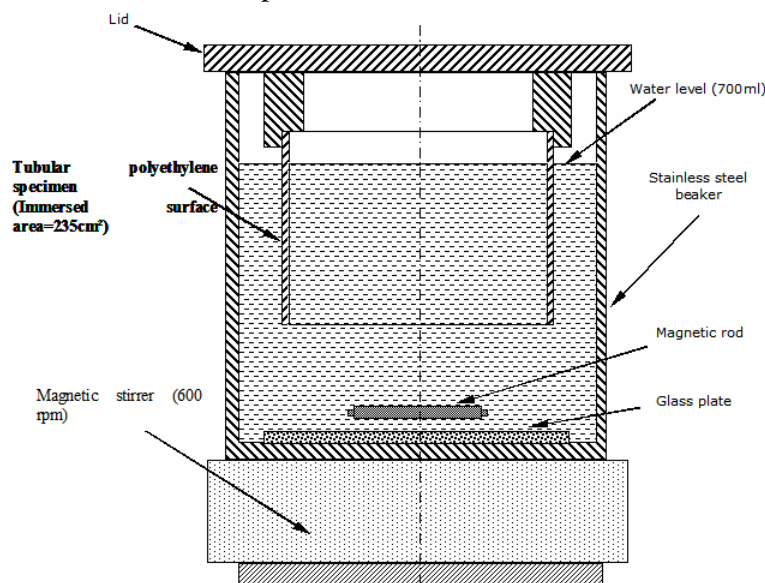


Fig.1.6 Experimental set-up of polymer test

All these methods have advantages and drawbacks, but their complementarity is often useful when we are confronted with the treatment of a real scaling problem. Nevertheless, the newest techniques have been developed in taking into consideration their representativeness in relation to a real-life scaling phenomenon, and if possible, to avoid major drawbacks of the previous methods. Hence, we can state that the methods such as the tests on polymers and on tubes as well as the Rapid Controlled Precipitation (RCP) allow to establish thermodynamic conditions where the scaling is formed with a degree of oversaturation much less than 40. In other words, the experimental conditions of these three methods lead to a real scaling but not a spontaneous and homogeneous precipitation of  $\text{CaCO}_3$ . Thus, the study of various proposed antiscaling treatments becomes entirely possible.

## 1.6 Methods of scale inhibition

Concerning the great harm that scale brings, scientists began the study of scale as early as a century ago and have invented various methods to prevent it. These methods can be divided into two broad categories: the physical methods and the chemical methods.

### (1) Physical methods

The physical methods mainly include ultrasonic wave method, permanent magnet method, electrostatic field method, high pressure high-frequency method, micro-electrolysis method, NMR method, anti-bond polymer layer, etc. However, the vast majority of the mechanism of physical methods is not clear so far, the effect is influenced greatly by water quality and the external factors, therefore, their practical application is very limited and treatment is often inefficient<sup>[17, 18]</sup>.

### (2) Chemical methods

The chemical methods include acid injection, ion exchange, quantitative complexation method, minimum inhibition method and so on. The first two methods require a large amount of agents, so the operating costs are high and also bring chemical pollution. Minimum inhibition method is the most economical way, but inhibitors often contain micro-inhibiting phosphorus that can cause eutrophication of water environment<sup>[19-21]</sup>.

On the other hand, the use of evaluation methods for the existing scale formation and scale inhibitor have generally very harsh conditions, so the concentration of inhibitor used is often too high, resulting in waste and pollution. In addition, it is very difficult to use these methods to infer the mechanism of its inhibition.

## 1.7 Scale inhibitor

The most common and effective scale control method in circulating cooling water, seawater desalination, boiler, and oil field is the use of scale inhibitors.

The development of inhibitor has experienced inorganic polyphosphate, organic phosphate, poly-carboxylic acid, binary and ternary phosphorus containing copolymer, binary and ternary non-phosphorus copolymer several stages. The research of inhibitors starts from the natural polymer, since the late 60s to the early 70s last century, the technique of inhibiting cooling water developed rapidly with the emergence of the

poly-acrylic acid and the poly-maleic acid, it promotes the development of a series of binary and synthetic copolymers. In the late 70s, phosphorous-containing polymer with the property of inhibition and corrosion was developed. In the 80s, there appeared a climax of development of sulfonic acid group containing polymer. In the late 80s to 90s, a climax of development of green chemistry emerged with the development of several environmentally friendly polymer inhibitors. This century, with the deep research and wide spread of green chemistry, the environmentally friendly green corrosion inhibitors that is non-phosphorous and bio-degradable become the main research direction of industrial water treatment, the use of water treatment agents step into a new age.

In the early days of industrial development, the inhibitor is inorganic compound. The inorganic poly-phosphate inhibitor, such as sodium tripolyphosphate, sodium hexametaphosphate, can inhibit the formation of scale. But the inorganic poly-phosphate will easily hydrolyze to orthophosphate; the improper use will induce the generation of  $\text{Ca}_3(\text{PO}_4)_2$  scale which is more difficult to treat, and speed the phosphorylation of water at the same time.

After the 1960s, the research of inhibitors focuses on the organic phosphoric acid corrosion inhibitors and the copolymer inhibitors at home and abroad. The organic phosphoric acid (phosphate), poly-carboxyl acid inhibitors, such as poly-acrylic acid, poly-maleic acid, compared with inorganic poly-phosphate inhibitors, have good chemical stability, good resistance to high water temperature, high alkalinity and are difficult to hydrolyze. They also have excellent inhibition performance to  $\text{CaCO}_3$  scale.

Binary copolymers, like phosphine poly-acrylic acid, phosphine poly-maleic acid, acrylic acid/methyl acrylate, which are developed in the late 1970s to the early 1980s and ternary copolymers, like acrylic acid/hydroxypropyl acrylate/methyl acrylate, acrylic acid/acrylamide methyl propane/hypo phosphorous acid, which are developed in the late 1980s are all developed for inhibiting the scale. This promotes the development of organic phosphoric acid (phosphate) copolymer—full phosphorous organic formula.

The development of inhibitors has experienced a change from chromium prescription to non-chromium prescription. In the non-chromium prescription, the inhibitors develop to be the full organic prescription that contains organic phosphine and polymer after dismissing poly-phosphate from phosphorous prescription.

#### (1) Organic phosphine inhibitors

Organic phosphine inhibitors are not only a kind of high efficient inhibitors, they can perform synergistic effects when complex formulating with other inhibitors. It means that the inhibition effects of complex formulation are greatly higher than the sum of effect of single inhibitor. The organic phosphine inhibitors include three types: organic phosphine acid, organic phosphonate and organic phosphonate ester, whose molecule structures are complex. The representatives of organic phosphine inhibitors are methylene phosphoric acid, same carbon diphosphate, carboxyl phosphoric acid, phosphoric acid containing atom sulfur, silicon, etc. The representatives of organic phosphonate are ethylenediamine tri-methylene potassium phosphate, amino tri-methylene zinc phosphate, etc. The representatives of organic phosphonate ester are polyoxyethylene phosphonate ester, amino methylene phosphonate ester, polyoxyethylene pyrophosphonate ester, etc.

#### (2) Polymer inhibitors

The hydrolysis of inorganic polyphosphate inhibitors limits its application. There is a kind of polymer inhibitor that does not hydrolyze in the water, generate precipitate and be limited with some conditions like temperature when applied. The kinds of these inhibitors are poly methyl acrylic acid, hydrolytic poly maleic anhydride, sodium poly acrylate, acrylic acid and acrylic acid amide copolymer, maleic anhydride and ethylene copolymer and so on.

In different kinds of inhibitors, the phosphorous-containing inhibitors are of high ratio. Their inhibition effect is high when used as single agent. In the complex formulation, they have synergistic effects. But phosphorous-containing compounds are the nutrition of algology in the water, they will promote the algology to grow fast and cover with the water surface, causing the water quality to get worse that is a threat to the environment protection <sup>[22]</sup>.

## 1.8 Green scale inhibitor

With people's consciousness of environmental protection strengthening, non-phosphorous or phosphorous-limited green inhibitors are the direction of development in the future. In 1990s, many companies began to develop non-phosphorus green scale inhibitors Polyepoxysuccinic acid (PESA) and Polyaspartic acid (PASP), showing green scale inhibitor has become the direction of water treatment chemicals. And nowadays PESA and PASP have been the main types of application internationally, because they have good biodegradability and compatibility function <sup>[23, 24]</sup>.

### (1) Polyepoxysuccinic acid (PESA)

PESA is a kind of biodegradable and environmentally friendly inhibitor with non-phosphorous, non-nitrogenous structure, which is shown in Fig.1.7.

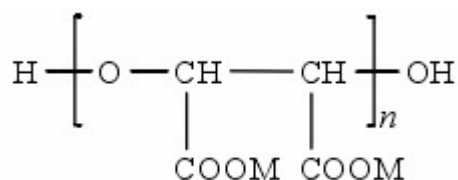


Fig.1.7 Structural formula of PESA

Where, the value n is normally 2~50, M is H<sup>+</sup> or water-soluble positive ions, like Na<sup>+</sup>, K<sup>+</sup>, NH<sub>4</sub><sup>+</sup>, etc.

PESA was developed by American company: the Prector & Gamble Company and the Betz Company in the late 1980s and the early 1990s respectively. Its structure shows, PESA is non-nitrogen, non-phosphorous organic compound which will not cause the water's eutrophication and is friendly to the environment. It has strong resistance to alkalinity and a good inhibition performance. Inserting oxygen atom in the polymer molecule makes its inhibiting performance greatly better than that of other organic phosphoric acid polymer inhibition, like sodium poly-acrylate, poly-maleic acid, and tartaric acid and so on. It has good thermal stability, good resistance performance for Fe<sup>3+</sup>, good biodegradability and strong chelation to Ca<sup>2+</sup>, Mg<sup>2+</sup> and Fe<sup>2+</sup>.

PESA has wide range of applications. It can be applied in the boiler water treatment, cooling water treatment, polluted water treatment, desalination of sea water and

membrane separation and so on. It can also be the non-phosphorus complexing agent in the detergent. It can help improve the quality of the detergent and is an important additive for the non-phosphorus detergent. Due to its clean operation of producing, PESA is considered as a kind of environmentally friendly green inhibitor <sup>[25]</sup>.

## (2) Polyaspartic acid (PASP)

PASP was produced by Donlar Company using two high efficient techniques in 1996. It is a kind of water soluble amino acid degradable polymer. Due to its unique biodegradability, it can replace many chemicals, like acrylic acid, which can pollute the environment in industrial activities. So PASP is a promising biopolymer material. PASP is a polymer glycidylated of the amino and the carboxyl of aspartic acid monomer. The molecular formula is  $C_4H_6NO_3(C_4H_5NO_3)_x C_4H_6NO_3$ , the molecular chain is  $\alpha$  chain and  $\beta$  chain, as Fig.1.8 shown.

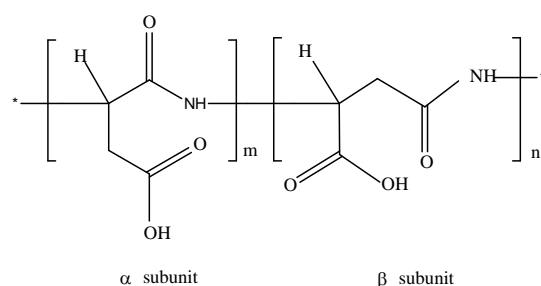


Fig.1.8 Structural formula of PASP

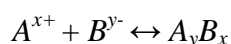
PASP is non-toxic, pollution-free and biodegradable. Many researches show, PASP has many advantages, such as good thermal stability, great performance of inhibiting, small dosage. It can chelate many multi-valence metallic ions, such as Calcium, Magnesium, Copper, Ferrum and so on. Especially, it can change the crystal structure of calcium salts and make them format soft scale, therefore, it has good scale inhibition performance.

The inhibiting performance for  $CaCO_3$  scale of PASP whose relative molecular mass is 4000 is better than that of poly-maleic acid and poly-acrylic acid. When the concentration of  $Ca^{2+}$  is  $1200mg \cdot L^{-1}$ , the inhibition rate can still hold to 50%. When the pH value is 10.5, the mass concentration of agent is  $3 mg \cdot L^{-1}$ , the inhibition rate can reach above 90%. When the temperature increases from 40 to 80 °C, the decreasing range with the increasing temperature is very small. So PASP can be applied as a water treatment agent for the water system with high temperature, high  $Ca^{2+}$  concentration <sup>[26]</sup>.

## 1.9 Mechanism of scale inhibition

The formation of scaling is a very complicated process that includes four phases: the ions in the water combine together and form salt molecule with little solubility; crystallization; molecules combine and arrange to form microcrystal, then generate crystal grains; amounts of crystals deposit and grow up to scale. Different shapes of scale form under different conditions.

For normal scaling reaction:



When the substances' ionic product exceeds its solubility constant, the precipitation

can generate probably. The necessary condition of precipitation is:

$$K_{sp(A_yB_x)} < [A^{x+}][B^{y-}]$$

Where,  $[A^{x+}]$  is the concentration of positive ions,  $\text{mol}\cdot\text{L}^{-1}$ ,  $[B^{y-}]$  is the concentration of negative ions,  $\text{mol}\cdot\text{L}^{-1}$ ,  $K_{sp(A_yB_x)}$  is the solubility product constant of  $A_yB_x$  under some certain temperature.

Influenced by several factors, the crystallization of substances in industrial water can generate precipitation only when it exceeds the certain oversaturation value. The super saturation value is called super saturation degree, its calculation is showed as:

$$S = \frac{[A^{x+}][B^{y-}]}{K_{sp(A_yB_x)}}$$

Nucleation is the first step of scaling. The nucleation speed is mainly influenced by super saturation degree (S). Though nucleation is possible under any conditions when  $S > 1$ , only when S exceeds some certain value, the crystallization speed increases abruptly. The value is called critical super saturation degree  $S'$ . Most compounds' critical super saturation degree of crystallization in the water solution is very large that can reach  $10^2 \sim 10^3$ .

$$S' = \frac{[A^{x+}][B^{y-}]}{K_{sp(A_yB_x)'}}$$

So adding inhibitors makes the inhibiting effect through increasing critical super saturation degree. The mechanisms of inhibition mainly are minimum suppression mechanism, lattice distortion mechanism, chelation, electric double layer mechanism, adsorption and dispersion mechanism [27].

#### (1) Minimum suppression mechanism

The generation of salt scale in the water experiences a process that first the seed crystal appears, then it grows to little crystal grains and the crystal grains concentrate together. The inhibitor is a kind of poisoning agent for seed crystal which can suppress or inhibit the growth of seed crystal. The salt scale cannot grow to scale deposition without certain amount of seed crystal in the water. Because this kind of inhibitors' mechanism is suppressing the generation of seed crystals, they don't have quantitative relation with salt scale compound molecule. Therefore, very little dosage of inhibitors can receive obvious inhibiting effects.

#### (2) Lattice distortion mechanism

The formation of scale deposition is a continuous growing process from seed crystal, bottom scale to secondary scaling. After the seed crystal appears, if it forms scale, it will need to adhere to the surface of solid around and become bottom scale. Bottom scale is the basis of continuous growth of seed crystal. Different kinds of salt scale that grow continually will sometimes adhere to some impurities, this process is secondary scaling, and they will continuously adhere to the bottom scale and become scale deposition finally.

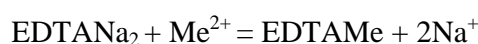
The mechanism of lattice distortion is that inhibitors can poison the grown little crystal and make the unit cell parameters in different axial change. As a result, the normal

growth of crystals is disturbed, and they cannot adhere to the solid surface to form bottom scale, then the growth of scale deposition loses its basis without bottom scale and the scale cannot form.

There isn't quantitative relation between this kind of inhibitor and salt scale compound molecule. Their dosage is little, so this kind of inhibitor is a high efficient inhibitor.

### (3) Chelation

There are two or more coordination bonds in the molecule of chelating agent or complexing agent. They are very easy to form stable soluble complex compound with positive ions which formulate scale in the water. The water loses these positive ions and the possibility of scale generation is decreased correspondingly. For example, the inhibiting mechanism of EDTA agent is:



Where,  $\text{Me}^{2+}$  represents the positive ions  $\text{Ca}^{2+}$ ,  $\text{Mg}^{2+}$ ,  $\text{Ba}^{2+}$  etc.

The reaction formula shows that the chemical reaction between the chelating agent and the scaling positive ions follows "law of constant composition", meaning one molecule  $\text{EDTANa}_2$  can only react with one scaling positive ion. Therefore, the quantity of this kind of inhibitor depends on the concentration of scaling positive ions in the water; the dosage of inhibitor is often very large.

### (4) Electric double layer mechanism

Gill, etc. think the inhibition performance for organic phosphonate is because the inhibitors concentrate in the diffusion boundary around where the crystal nucleus grows. It forms electric double layer and prevent scaling ions or molecule clusters from coagulating on the metal surface.

### (5) Adsorption and dispersion mechanism

When the anions which are generated by the poly-carboxylate polymer dissociating in the water solution collide with  $\text{CaCO}_3$  microcrystal, it appears physic-chemical adsorption phenomenon and makes electric double layer form on the surface of microcrystal. The chain structure of poly-carboxylate can absorb several microcrystals with the same charge; the static electricity repulsive force between them can prevent microcrystal from colliding with each other and also prevent big crystal's formation. When the adsorption production collides with other poly-carboxylate ions, it will transfer the adsorbed crystals to the ions and make the crystal grains disperse uniformly. Then the collision between the crystal grains and the metal surface will be impeded, the amount of crystal grains in the solution decreases and the  $\text{CaCO}_3$  are stable in the water as a result.

In fact, the same kind of inhibitor has different inhibition performance. In can not only make complex compound with scaling positive ions, but also adhere to the crystal nucleus and the crystal surface, making the effect of distortion and dispersion. Mostly, organic phosphine inhibitors mainly make effects of complexion and distorting. Macromolecule inhibitors' mechanism is dispersion action. But these mechanisms are with different factors and it becomes more complicated due to the existence of inhibitors, the inhibition performance is definite as a complexing function with different mechanisms. Hence, the research of mechanisms of inhibition needs a further development.

## Chapter 2. Evaluation of anionic polymers as scale inhibitors on CaCO<sub>3</sub> and Ca-phosphonate precipitates

Phosphonates are widely used as scale and corrosion inhibitors in a variety of fields including crude oil production, industrial equipment cleaning, and industrial water treatment [28-31]. They prevent hard water systems from depositing mineral scale and also protect against the corrosion of metal surfaces caused by mineral scale [31-37]. In an inadequately treated cooling system, the steel equipment undergoes scale and corrosion because of the interaction of the circulating water with dissolved oxygen and large concentrations of aggressive ions, such as calcium and sulphate [38-41], which form mineral scale made up of materials such as calcium carbonate [42], calcium sulfate [43,44], calcium phosphate [45], barium sulfate [46,47], strontium sulfate [48,49], and other insoluble salts [50-53]. Many serious or catastrophic operational problems can result from precipitation of this mineral scale.

Using phosphonates, R<sub>3</sub>C–P(O)(OH)<sub>2</sub>, as inhibitors is one method of preventing mineral scale and corrosion in cooling water systems. Some phosphonates which are commonly used in circulating water systems are displayed in Table 2.1. Phosphonates (R<sub>3</sub>C–P(O)(OH)<sub>2</sub>) differ structurally from polyphosphonates (R<sub>3</sub>C–O–P(O)(OH)<sub>2</sub>) in that they have a P-C bond rather than a P-O bond [53,54]. This structural difference gives phosphonates superior performance characteristics that include high chemical durability under extreme pH and temperature conditions, the ability to sequester metals, and a strong absorption capacity into metal coatings. In many cases, they are able to interfere with crystal growth of scale materials at concentrations far below stoichiometric levels of the reactive cations [55-57].

Phosphonates are generally considered to be CaCO<sub>3</sub> and CaSO<sub>4</sub> scale inhibitors as they have a high tolerance for calcium ions. However, in many applications where phosphonates are added to water treatment systems with high calcium ion concentrations, the phosphonates react stoichiometrically with the calcium ions and form insoluble Ca-phosphonate precipitates which share some of the same harmful effects as the other forms of scale being inhibited. Thus, in this paper the term “scale inhibition” will refer to the stoppage or decrease of both CaCO<sub>3</sub> scale and Ca-phosphonate precipitation. The insoluble Ca-phosphonate precipitates Ca-HEDP [58], Ca-ATMP [59], and Ca-DTPMP [60,61] have been investigated in oil field applications, but these studies were carried out with high phosphonate concentrations (> 1.5 × 10<sup>-1</sup> M) and high calcium ion concentration (> 6.25 × 10<sup>-2</sup> M).

Most studies have focused only on the mineral scale and corrosion inhibition efficiency of phosphonates, but comparatively few works have concentrated on the Ca-phosphonate precipitates themselves. The present work has two purposes: first to investigate the formation of Ca-phosphonate precipitates in different situations in order to check the calcium tolerance of several phosphonates (Table 2.1), and second to study the ability of anionic polymers (Table 2.2) to inhibit Ca-phosphonate precipitation. This

information should contribute to the understanding of the threshold effect of these phosphonates as inhibitors using static test experiments.

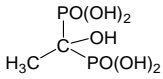
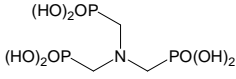
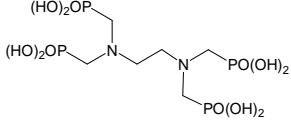
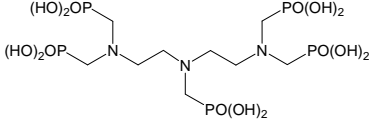
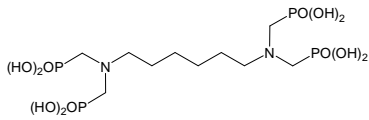
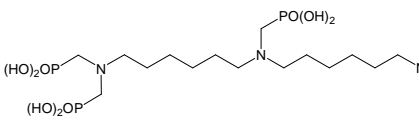
## 2.1 Experimental

### 2.1.1 Main materials

All chemicals in this study were analytical reagent grade, obtained from Sinopharm Chemical Reagent Shanghai Co. Ltd, China. Calcium stock solutions were prepared by dissolving calcium chloride dihydrate in distilled water, filtered through 0.22  $\mu\text{m}$  filter paper, and then analyzed by EDTA complexometric titration. Carbonic acid stock solutions were prepared by dissolving sodium bicarbonate in distilled water. Doubly distilled water was used as the solvent for all stock solutions.

The phosphonates used in this study were commercial grade and are shown in Table 2.1. HEDP, ATMP, EDTMP, DTPMP, HDTMP, and BHMTMPMP were purchased from Sigma-Aldrich Chemical Co., China. PBTCA and PAPEMP were obtained from Jianghai Chemical Group, China. The concentration of phosphonate solutions was standardized using the spectrophotometric method. Phosphonate was oxidized to orthophosphate by heating for 30 min in the presence of persulfate. The orthophosphate was then reacted with ammonium molybdate. This resulted in production of molybdophosphorus complex, which was reduced to phosphomolybdenum blue complex with ascorbic acid. The orthophosphate concentration was then measured colorimetrically.

Table 2.1 Abbreviations, names and structures of the phosphonate inhibitors covered in this investigation

Phosphonate	Name	Structure	Company
HEDP	1-hydroxyethylidene-1,1-diphosphonic acid		Sigma, China
ATMP	amino trimethylene phosphonic acid		Sigma, China
EDTMP	ethylene diamine tetra(methylenephosphonic acid)		Sigma, China
DTPMP	diethylenetriamine penta(methylenephosphonic acid)		Sigma, China
HDTMP	hexamethylenediaminetetra(methylene phosphonic acid)		Sigma, China
BHMTMPMP	bis (hexamethylene) triaminepentakis (methylene phosphonic acid)		Sigma, China

PBTCA	2-phosphonobutane-1,2,4-tricarboxylic acid		Jianghai Chemical Group, China
PAPEMP	polyamino polyether methylene phosphonate		Jianghai Chemical Group, China

n: 2~3

The polymeric inhibitors used in this study were either commercial or experimental grade. They include: PAA, AA/AMPS, AA/PPA/AMPS, PESA, and ESA/EBSA. Their chemical names and structures are shown in Table 2.2. PAA, AA/AMPS and AA/PPA/AMPS were obtained from Jianghai Chemical Group, China. PESA and ESA/EBSA were obtained from Meijing Environmental Protection material Co., Ltd., China. The polymer inhibitor concentrations were all calculated on a dry polymer basis.

Table 2.2 Abbreviations, names and structures of the polymer used as inhibitors covered in this investigation

Polymer	Name	Structure	Company
PAA	poly(acrylic acid)		Jianghai Chemical Group, China
AA/AMPS	acrylic acid/2-acrylamido-2-methylpropanesulfonic acid copolymer		Jianghai Chemical Group, China
AA/HPA/AMPS	acrylic acid/2-acrylamido-2-methylpropanesulfonic acid/2-hydroxypropylacrylate terpolymer		Jianghai Chemical Group, China
PESA	poly(epoxysuccinic acid)		Meijing material, China
ESA/EBSA	epoxysuccinic acid/4-poxyethyl benzenesulfonic acid copolymer		Meijing material, China

### 2.1.2 Static tests for Ca-Phosphonate precipitation of various phosphonate inhibitors

Static calcium phosphonate precipitation experiments were conducted in ground-glass stoppered 0.5 L flasks. Supersaturated solutions of calcium phosphonate

were prepared by adding a known volume of phosphonate solution to a bottle containing a known volume of double distilled water. After the temperature of the diluted phosphonate solution had stabilized, a known volume of calcium stock solution was added. The pH of each calcium phosphonate supersaturated solution was adjusted to 8.5 using dilute 0.5 M NaOH and/or HCl. The soluble phosphonate concentrations in the test solutions were monitored as a function of time during the precipitation process by filtering an aliquot of the solution through 0.22  $\mu\text{m}$  filter paper and analyzing the filtrate by the molybdenum blue method (section 2.1.1). The reaction duration for all experiments was fixed at 24 h.

### 2.1.3 Static tests for effects of polymeric inhibitors on Ca-Phosphonate formation

Similar to the experiments section 2.1.2, the static tests for the effects of polymeric inhibitors on Ca-phosphonate precipitation were performed in 0.5 L glass bottles held at a constant temperature. A known amount of polymer solution was added to the supersaturated solutions containing a certain amount calcium stock solution, then adjusted pH to 8.5 using dilute 0.5 M NaOH and/or HCl solution. The soluble phosphonate concentration in the test solutions was monitored as a function of time during the precipitation process by the molybdenum blue method. The reaction duration for all experiments was fixed at 24 h.

The Ca-phosphonate inhibition efficiency (%) of the polymer was calculated by the following equation,

$$\text{Ca - phosphonate inhibition efficiency (\%)} = \frac{[\text{phosphonate}]_{\text{final}} - [\text{phosphonate}]_{\text{blank}}}{[\text{phosphonate}]_{\text{initial}} - [\text{phosphonate}]_{\text{blank}}} \times 100\%$$

The terms  $[\text{phosphonate}]_{\text{final}}$  and  $[\text{phosphonate}]_{\text{blank}}$  refer to the phosphonate concentration of the sample after incubation for 24 h in the presence and absence, respectively, of the polymeric inhibitors. The term  $[\text{phosphonate}]_{\text{initial}}$  denotes the phosphonate concentration of the sample with polymeric inhibitors before incubation.

### 2.1.4 Static tests for inhibition efficiency of inhibitors on $\text{CaCO}_3$ scale formation

Similar to the two previously discussed methods, the static tests for the inhibition efficiency of the inhibitors on  $\text{CaCO}_3$  scale precipitation were performed. For each test, the phosphonate solution was first diluted. When its temperature had stabilized, a known volume of inhibitor stock solution was added and the solution pH was adjusted to 8.5 using dilute 0.5 M NaOH and/or HCl solution as necessary. The mixture was held at constant temperature as appropriate amounts of calcium and sodium bicarbonate stock solution were added, resulting in a supersaturated  $\text{CaCO}_3$  solution. The bottles were then incubated in a water bath for 18 h at 80  $^{\circ}\text{C}$ . After cooling, a fixed aliquot of solution was filtered through 0.22  $\mu\text{m}$  filter paper, and the calcium concentration in the filtrate was measured using the standard EDTA titration method.

The inhibition efficiency (%) of the inhibitor on  $\text{CaCO}_3$  scale precipitation was obtained by the following equation,

$$\text{CaCO}_3 \text{ inhibition efficiency (\%)} = \frac{V_1 - V_0}{V_2 - V_0} \times 100\%$$

where  $V_1$  and  $V_2$  are the amount of EDTA consumed after incubation for 18 h in presence and absence, respectively, of scale inhibitors.  $V_0$  is the amount of EDTA

consumed without scale inhibitor additives after incubation for 18 h.

## 2.2 Results and Discussion

### 2.2.1 Static tests for Ca-phosphonates precipitation

Static tests for Ca-HEDP, Ca-ATMP, Ca-EDTMP, Ca-DTPMP, Ca-HDTMP, Ca-BHMTMP, Ca-PBTCA, and Ca-PAPEMP precipitation were carried out with various levels of calcium ion (as  $\text{Ca}^{2+}$  ion) at pH 8.5 with heating at 50 °C for 24 h. The plots of residual phosphonates concentration as a function of time are shown in Figs.2.1-2.8.

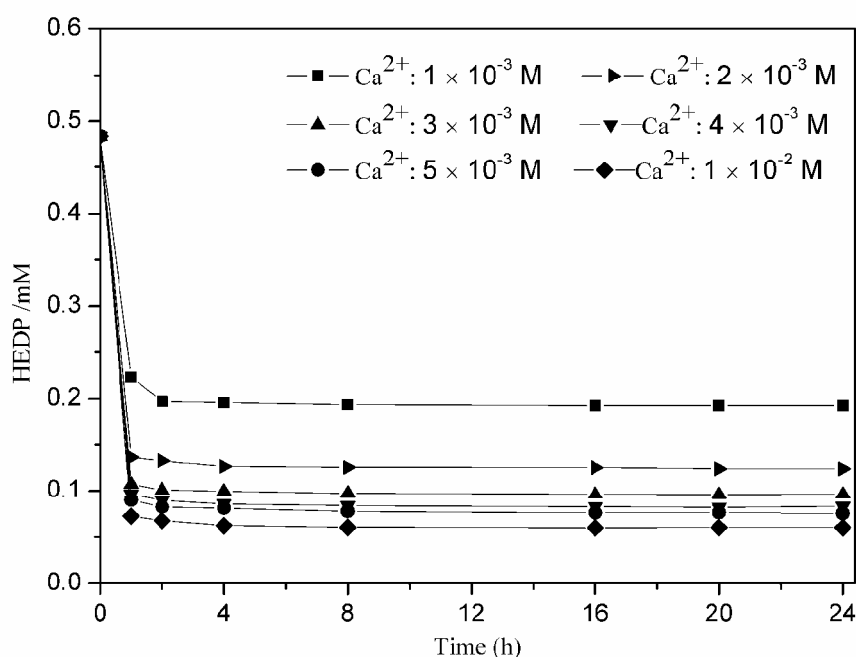


Fig.2.1 Variation of residual HEDP concentration in test solution with different  $\text{Ca}^{2+}$  concentrations. 0.48 mM of HEDP (as  $\text{PO}_4^{3-}$ ) was added into solution with different calcium ion concentration at 50 °C, pH 8.5, and 24 h

Fig.2.1 demonstrates that 50% of the HEDP precipitated out in the form of calcium phosphonate within 1 h for the solution with  $1.0 \times 10^{-3} \text{ M}$  calcium ion concentration. At higher calcium ion concentrations ( $4.0 \times 10^{-3} \sim 1.0 \times 10^{-2} \text{ M}$ ), larger than 80% Ca-HEDP precipitation was measured within 1 h. Thus, Ca-HEDP precipitation increases with calcium ion concentration. However, increasing the reaction time to 24 h did not significantly affect the residual HEDP concentration in the supersaturated calcium phosphonate solution.

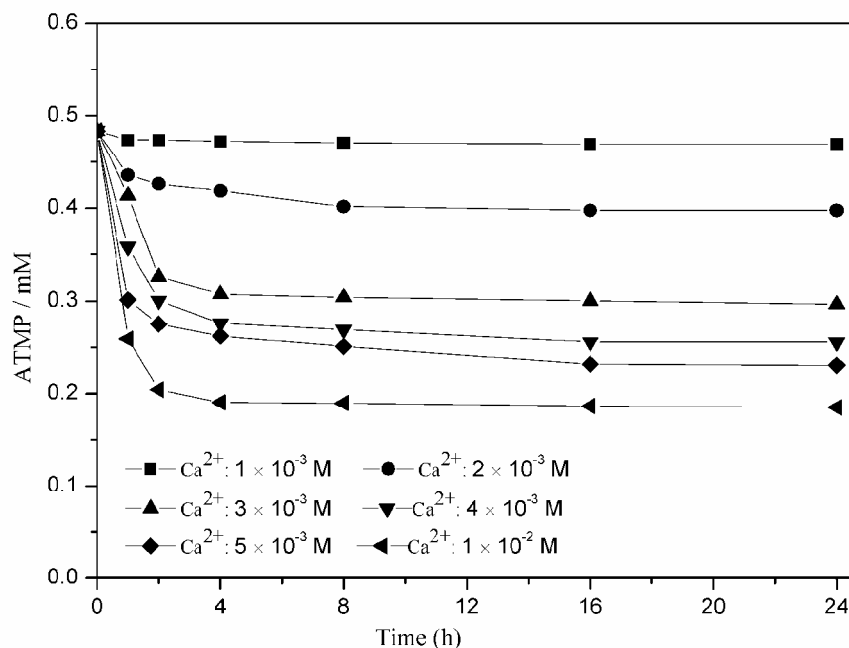


Fig.2.2 Variation of residual ATMP concentration in in test solution with different Ca<sup>2+</sup> concentrations.  
Test conditions: same as Fig.2.1

Fig.2.2 shows that only approximately 3% ATMP precipitated out as Ca-ATMP within 24 h for the solution with  $1.0 \times 10^{-3}$  M calcium ion. Increasing calcium ion concentration to  $1.0 \times 10^{-2}$  M resulted in the observation of 62% Ca-AMPT precipitation. It is apparent that, relative to HEDP, ATMP has a higher calcium ion tolerance in supersaturated solutions of calcium.

In assessing further differences in inhibition performance of the phosphonates, their molecular structures could be one of the important factors, there are only slight differences in molecular structure between EDTMP and HDTMP, and between DTPMP and BHMTMP (see Table 2.1). However, there are significant differences between the pairs themselves. Both pairs have different numbers of phosphonate functional groups attached to amine N atoms through methylene linkages. Additionally, the length of the polymethylene backbone connecting N atoms is different in each pairing. These structural differences appear to be significant, as discussed below.

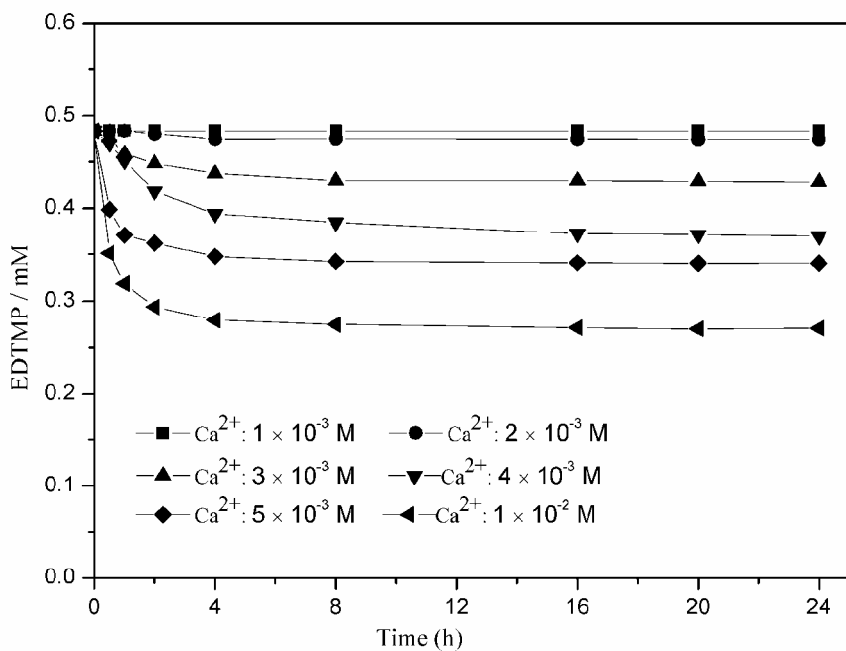


Fig.2.3 Variation of residual EDTMP concentration in test solution with different  $Ca^{2+}$  concentrations. Test conditions: same as Fig.2.1

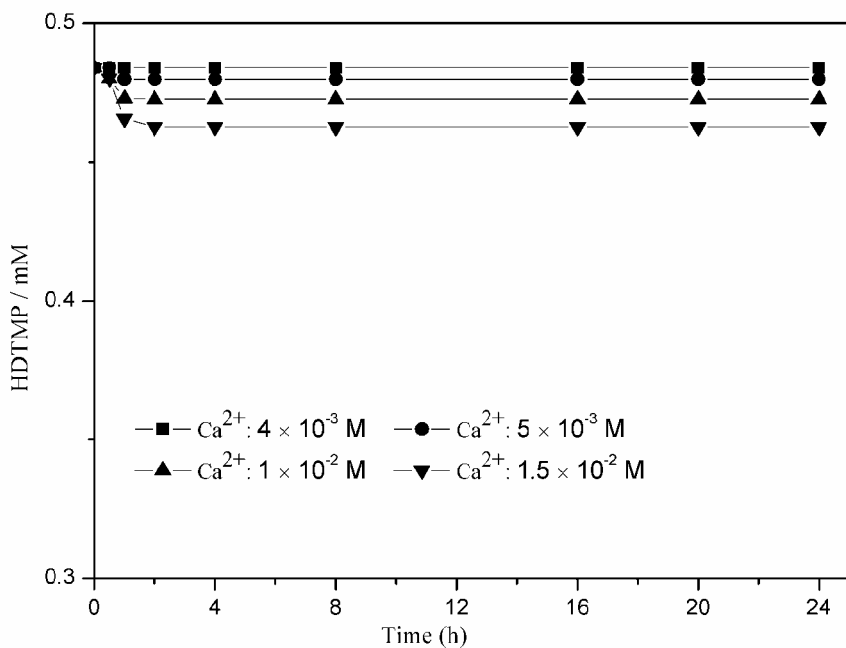


Fig.2.4 Variation of residual HDTMP concentration in test solution with different  $Ca^{2+}$  concentrations. Test conditions: same as Fig.2.1

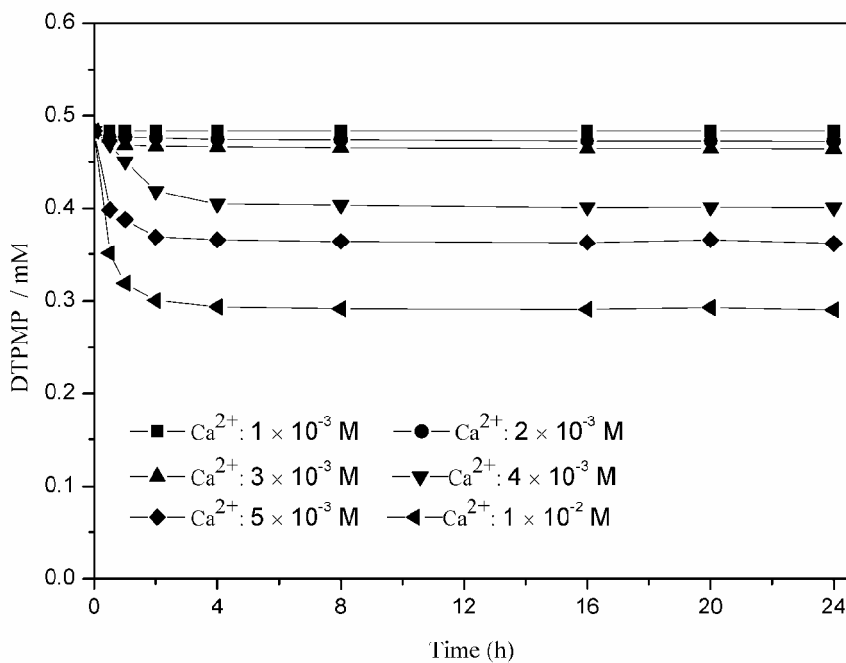


Fig.2.5 Variation of residual DTPMP concentration in test solution with different Ca<sup>2+</sup> concentrations. Test conditions: same as Fig.2.1

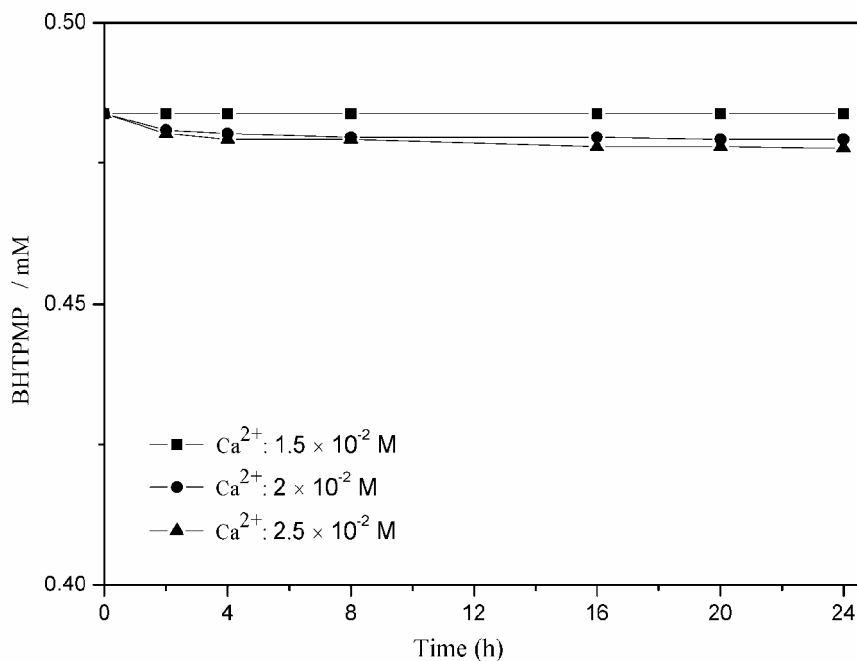


Fig.2.6 Variation of residual BHTPMP concentration in test solution with different Ca<sup>2+</sup> concentrations. Test conditions: same as Fig.2.1

Figs.2.3-2.6 show the extent of Ca-EDTMP, Ca-HDTMP, Ca-DTPMP, and Ca-BHMTMPMP precipitation at various calcium concentrations. There was no perceptible Ca-EDTMP, Ca-HDTMP, Ca-DTPMP, or Ca-BHMPMP precipitation with  $1.0 \times 10^{-3}$  M calcium ion concentration after 24 h. However, it is clear that increasing calcium ion

concentration could increase the precipitation of Ca-EDTMP and Ca-DTPMP. On the contrary, there were no Ca-HDTMP precipitate formations within 24 h until the calcium ion concentrations reached  $4.0 \times 10^{-3}$  M. Ca-BHMPMP precipitation does not appear at calcium ion concentrations as high as  $1.5 \times 10^{-2}$  M. This suggests that the binding capacity between calcium and various phosphates is dependent on the molecular structures of the phosphates.

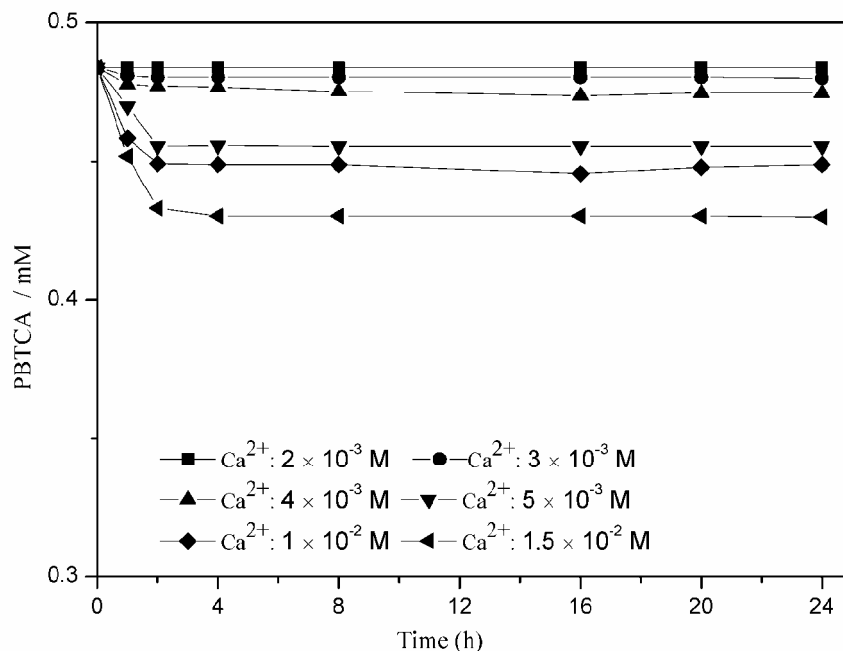


Fig.2.7 Variation of residual PBTCa concentration in test solution with different  $Ca^{2+}$  concentrations. Test conditions: same as Fig.2.1

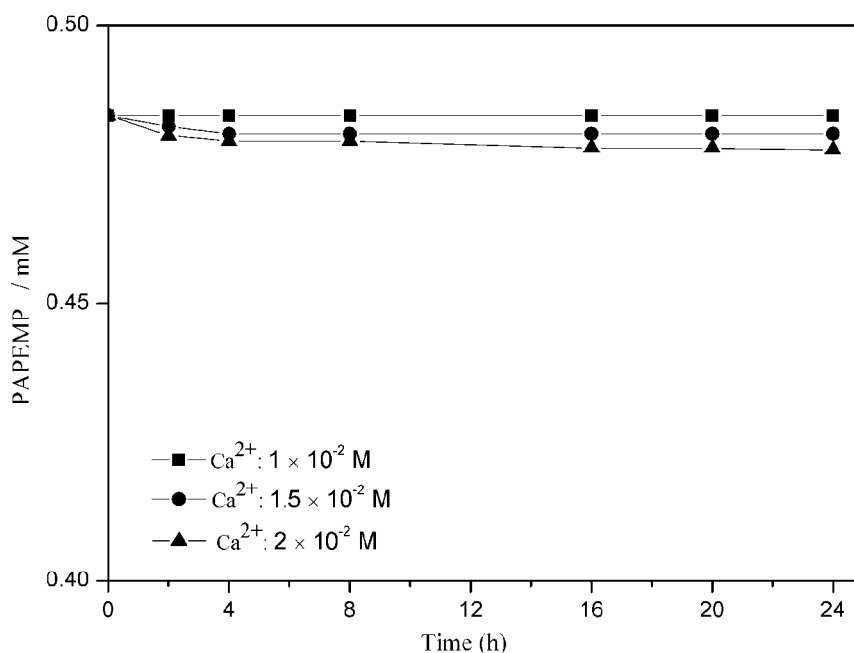


Fig.2.8 Variation of residual PAPEMP concentration in test solution with different  $Ca^{2+}$  concentrations. Test conditions: same as Fig.2.1

Fig.2.7 shows that no Ca-PBTCA precipitation formed in solutions with less than  $2.0 \times 10^{-3}$  M calcium ion. However, Ca-PBTCA precipitation increased slowly with increasing calcium ion concentrations from  $3.0 \times 10^{-3}$  M to  $1.5 \times 10^{-2}$  M. The formation of Ca-PAPEMP precipitate did not occur until the calcium concentration was at least  $1.5 \times 10^{-2}$  M (Fig.2.8), which within 24 h resulted in calcium 0.4% Ca-PAPEMP precipitation and then increased to 2.1% when treated with  $2.0 \times 10^{-2}$  M calcium ion.

As expected for all of the cases, the level of phosphonate precipitation increased with increasing calcium ion concentration. Ca-phosphonate precipitation occurred predominantly in the first few hours. For comparison, the percent precipitation of the phosphonates in the presence of  $5.0 \times 10^{-3}$ ,  $1.0 \times 10^{-2}$ , and  $1.5 \times 10^{-2}$  M calcium ion after 24 h is summarized in Table 2.3. Based on these data, the order of calcium ion tolerance for the phosphonates is as follows:

BHMTMPMP>PAPEMP>HDTMP>>PBTCA>DTPMP>EDTMP>ATMP> HEDP

Table 2.3 Insoluble Ca-phosphonate precipitation formed in various phosphonates solutions with different calcium concentration (as  $\text{Ca}^{2+}$  ion)

Phosphonates	% Ca-phosphonate precipitate		
	$5 \times 10^{-3}$ M (as $\text{Ca}^{2+}$ )	$1 \times 10^{-2}$ M (as $\text{Ca}^{2+}$ )	$1.5 \times 10^{-2}$ M (as $\text{Ca}^{2+}$ )
HEDP	84.46	87.60	—
ATMP	52.33	61.73	—
EDTMP	29.60	44.06	—
DTPMP	25.20	39.93	—
PBTCA	5.86	7.20	—
HDTMP	0.87	2.33	—
PAPEMP	0	0	0.66
BHMTMPMP	0	0	0

## 2.2.2 Inhibition of Ca-Phosphonate precipitation

Three polymers based on acrylic acid with various functionalities (Table 2.2) were investigated for their capability as inhibitors for Ca-HEDP precipitation. A series of experiments were performed at pH 8.5 with heating at  $50^\circ\text{C}$  for 24 h and in the presence of  $1.25 \times 10^{-2}$  M calcium ion and a range of polymer concentrations. As shown in Fig.2.9, the results indicate that acrylic acid homopolymer is not a particularly effective Ca-HEDP precipitation inhibitor. The inhibitory performance of the AA/AMPS copolymer was substantially better, while AA/AMPS/HPA terpolymer ( $5.0 \times 10^{-4}$  M) attained the best performance in this system as it achieved >90% inhibition of Ca-HEDP precipitation for at least 24 h.

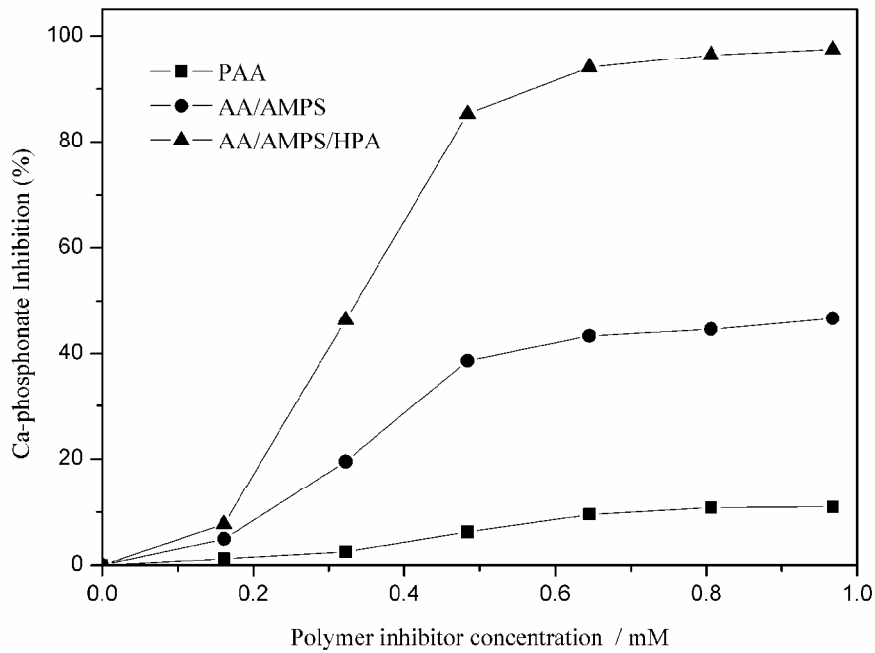


Fig.2.9 Effect of inhibiting Ca–HEDP precipitate in test solution with different polymers concentration. Test conditions:  $1.25 \times 10^{-2}$  M  $\text{Ca}^{2+}$  ion in solution and run at  $50^\circ\text{C}$ , pH 8.5, for 24 h

The results for the percent inhibition of Ca-HEDP, Ca-ATMP, Ca-EDTMP, Ca-DTPMP, and Ca-PBTCA precipitation under conditions identical to those of the acrylic acid based polymers are summarized in Fig.2.10. It is evident that for each of the phosphonates, the relative order of effectiveness of the three acrylic acid-based polymers follows the same trend as for the Ca-HEDP experiment. In addition, the Ca-phosphonate concentration in the supersaturated solution and the calcium ion tolerance of the phosphonate both had an effect on inhibition performance.

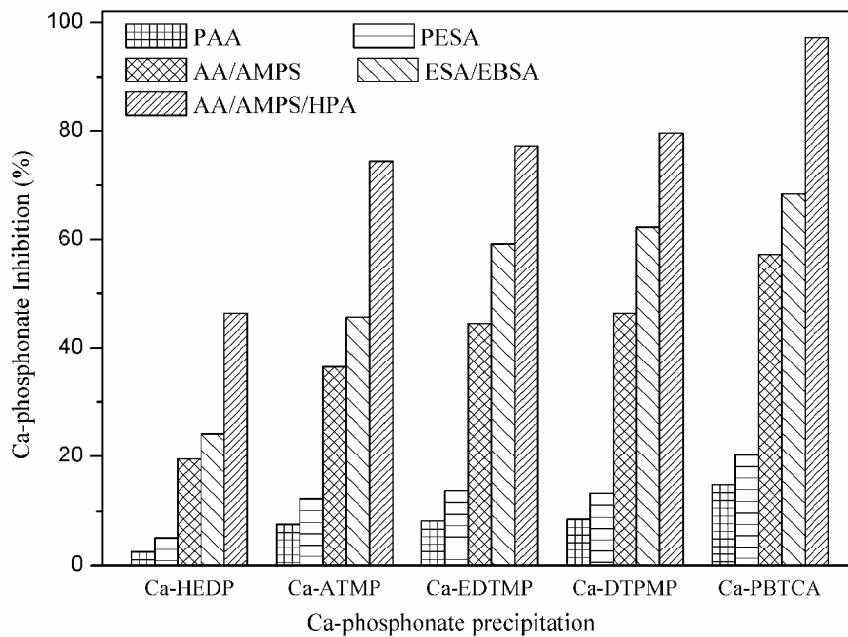


Fig.2.10 Effect of inhibiting Ca–phosphonates precipitate in test solution with different polymers. Test conditions: same as Fig.2.9

Other polymers with related monomer structure such as poly (epoxysuccinic acid) (PESA) and its copolymers, epoxysuccinic acid and 4-epoxy benzenesulfonic acid (ESA/EBSA), were also tested for their Ca-phosphonates precipitation inhibition capabilities. The results presented in Fig.2.10 indicate that ESA/EBSA copolymer is most effective in inhibiting Ca-phosphonate precipitation. Furthermore, the data demonstrate that the order of inhibition effectiveness is terpolymer > copolymer > homopolymer.

### 2.2.3 Inhibition of CaCO<sub>3</sub> scale formation by phosphonates and observed “threshold effect”

Phosphonates have been shown to be broadly effective in controlling scale and mild steel corrosion in industrial water treatment systems. They also were generally considered to be tolerant to calcium hardness. However, as mentioned in section 2.2.1, phosphonates can precipitate as Ca-phosphonates resulting in a negative effect on the inhibition of CaCO<sub>3</sub> scale formation under high hardness conditions.

To further clarify the influence of the formation of Ca-phosphonate on phosphonate’s ability to inhibit CaCO<sub>3</sub> scale formation, the phosphonates HEDP, PBTCa, and PAPEMP, with different calcium tolerances were investigated. A static test to determine the inhibition efficiency of phosphonates on CaCO<sub>3</sub> scale precipitation was conducted for 24 h at 80 °C and pH 8.50 under high hardness of [Ca<sup>2+</sup>] = 1.0 × 10<sup>-2</sup> M and [HCO<sub>3</sub><sup>-</sup>] = 6.67 × 10<sup>-3</sup> M.

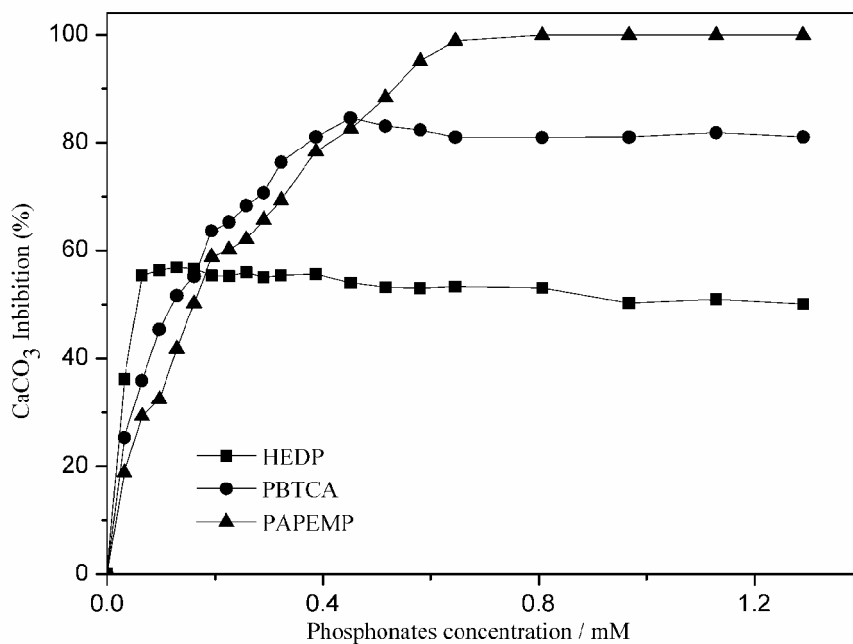


Fig.2.11 Effect of inhibiting CaCO<sub>3</sub> scale in test solution with different concentration of various phosphonate inhibitors (HEDP, PBTCa and PAPEMP). Test conditions: [Ca<sup>2+</sup>] = 1.0 × 10<sup>-2</sup> M, [HCO<sub>3</sub><sup>-</sup>] = 6.67 × 10<sup>-3</sup> M, pH 8.5, 80 °C, for 24 h

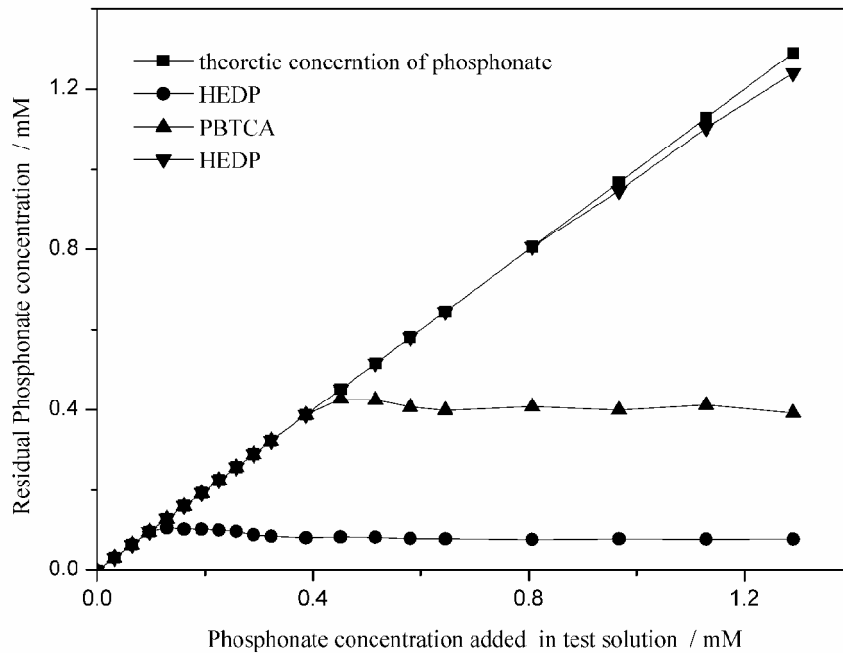


Fig.2.12 Sampling of theoretic phosphonates concentration compared to the residual phosphonates concentration as  $\text{CaCO}_3$  sclae inhibitor in static test solution for 24 h. Test conditions: same as Fig.2.11

Figs.2.11 and 2.12 reveal that HEDP and PBTCA exhibit an obvious “threshold effect,” meaning that the inhibition efficiency is not enhanced by increasing concentration where the dosage was exceed a certain value. The maximum inhibition efficiency of HEDP (56.8%) was appeared while the HEDP concentration was  $1.2 \times 10^{-4}$  M, PBTCA obtained the maximum inhibition efficiency (84.6%) when the concentration was  $4.5 \times 10^{-4}$  M, even if increased the concentration of HEDP and PBTCA, the inhibition efficiency did not increased any more. At the same time, the residual HEDP and PBTCA concentrations in solution were maintained about  $1.0 \times 10^{-4}$  M and  $4 \times 10^{-4}$  M respectively. In contrast, this threshold effect does not apply in the case of PPEMP as its inhibition efficiency increases proportionally to added phosphonate until it reaches nearly 100%. Nevertheless, the residual PPEMP concentration increased in proportion with the added dosage. Taking into account the considerable presence of Ca-phosphonates depositions in solution, as well as the remained concentration of the phosphonates (HEDP, PBTCA) which act as a  $\text{CaCO}_3$  scale inhibitor, the following postulation can be made: the formation of Ca-phosphonates can decrease the inhibition efficiency by reducing the phosphonates concentration which act as a  $\text{CaCO}_3$  scale inhibitor, thus exhibiting an apparent “threshold effect”.

#### 2.2.4 Inhibition of $\text{CaCO}_3$ scale formation by terpolymer

Fig.2.13 shows that the presence of terpolymer AA/AMPS/HPA increases the inhibition efficiency for preventing  $\text{CaCO}_3$  formation. For instance, the  $\text{CaCO}_3$  inhibition efficiency was about 52.2% and 98.3% respectively for  $1.9 \times 10^{-4}$  M of HEDP and  $1.9 \times 10^{-4}$  M of HEDP with  $4.8 \times 10^{-4}$  M terpolymer AA/AMPS/HPA. From the observation of results, the terpolymer AA/AMPS/HPA found to act as good inhibitor. These polymers

seem susceptible to increase the actual concentration of HEDP in the solution. Furthermore, considering the polymer AA/AMPS/HPA dispersant in static tests solution, the polymer AA/AMPS/HPA could markedly influence the solution surface and the interfacial process of combination of  $\text{Ca}^{2+}$  and HEDP. As such, the amount of Ca-HEDP precipitation decreased greatly and the residual HEDP concentration in solution increased, which lead to an improvement in inhibition efficiency. From the results obtained through this study, the association of phosphonates and anionic polymers constitute an attractive alternative for preventing  $\text{CaCO}_3$  scale in cooling water treatment system. Furthermore, the kinetic model of Ca-precipitation and inhibition mechanism should be completed.

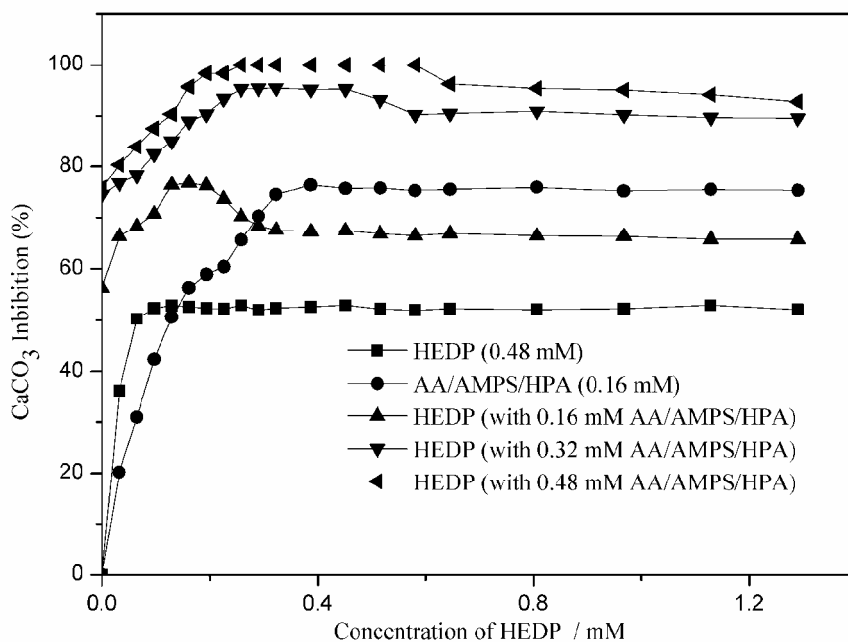


Fig.2.13 Impact of polymers (AA /AMPS/HPA) on the inhibition efficiency of HEDP in preventing  $\text{CaCO}_3$  scale. Test conditions: same as Fig.2.11

## 2.3 Summary

The order of solubility of the Ca-phosphonates was found to be as follows: BHMTMP > PAPEMP > HDTMP >> PBTCA > DTPMP > EDTMP > ATMP > HEDP. The formation of Ca-phosphonates precipitates plays an important role in inhibition performance for preventing  $\text{CaCO}_3$  scale.

Homopolymers of acrylic acid and epoxysuccinic acid were relatively ineffective as Ca-phosphonate precipitation inhibitors. However, copolymers and terpolymers show excellent inhibitory effectiveness. The inhibition order of the polymers for Ca-phosphonate precipitation was determined as follows: terpolymer > copolymer > homopolymer.

Using the anionic AA/AMPS/HPA terpolymer as Ca-phosphonate inhibitors was found to improve inhibition efficiency for preventing  $\text{CaCO}_3$  scale and reduce the threshold effect of the inhibition by phosphates. Moreover, the molecular structure of the polymers and concentration of the polymer are critical to their performance as inhibitors of Ca-phosphonate and  $\text{CaCO}_3$  precipitation.

## Chapter 3. Performance of polyaspartic acid/ polyepoxysuccinic acid and their synergistic effect on inhibition of scaling

One most promising method to retard or prevent scale formation involves the addition of inhibitors to the water in dosages of small concentrations. However, increasing environmental concerns and discharge limitations have imposed additional challenges in treating process waters. Thus, the concept of “Green Chemistry” was proposed and green scale inhibitors became a focus of water treatment technology [62-65].

Polyepoxysuccinic acid (PESA) and polyaspartic acid (PASP) are two representatives of green scale inhibitors because of their non-nitrogenous, non-phosphorus and biodegradable features. PASP has been widely used in the industry as the inhibitor of the salt crystallization and precipitation, or the water softener and corrosion inhibitor. PESA is a novel scale inhibitor first developed by Betzdearbon (U.S.), which has become one of the major research focuses in green inhibitors nowadays.

In this chapter, in order to simultaneously inhibit several typical scaling ( $\text{CaCO}_3$ ,  $\text{CaSO}_4$ ,  $\text{BaSO}_4$ ,  $\text{SrSO}_4$ ) and further improve the inhibition efficiency, the performance and applicability of PESA & PASP and their synergistic effect were studied using both static and dynamic methods.

### 3.1 Experimental

#### 3.1.1 Materials

##### 3.1.1.1 PASP

PASP was synthesized by the following method: Put 20g L-aspartic acid, 20g high purity water and small amount of phosphoric acid into the reactor, then react 2~4 hours under heated and pressurized condition, after cooling the reactants, we get viscous polymer. Then dilute the polymer and get different concentrations of polyaspartic acid solution. The synthetic principle of PASP and its physicochemical characteristics are shown in Fig.3.1 and Table 3.1 respectively.

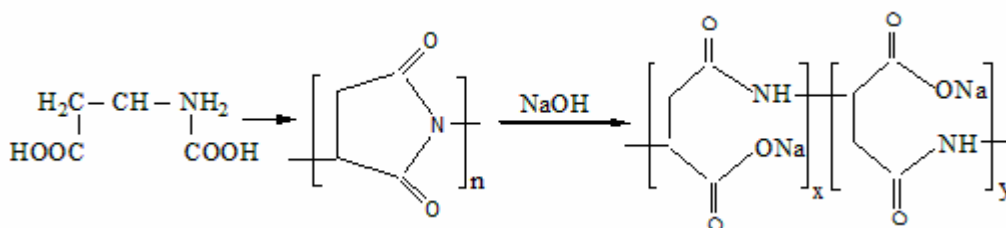


Fig.3.1 Synthetic principle of PASP

Table 3.1 Physicochemical characteristics of PASP

<b>Molecular formula</b>	$C_4H_6NO_3$ ( $C_4H_5NO_3$ ) $C_4H_6NO_4$	<b>Solid content %</b> $\geq$	32.0
<b>Molecular weight</b>	1000-5000	<b>Density (20°C) <math>g/cm^3</math></b> $\geq$	1.20
<b>Appearance</b>	Transparent amber liquid	<b>pH (1% solution)</b>	9.0-11.0

### 3.1.1.2 PESA

PESA, whose physicochemical characteristics is shown in Table 3.2, was prepared by the following steps according to the principle of Fig.3.2: Dissolve maleic anhydride in a certain amount of water, slowly add sodium hydroxide when cooling and stirring to make maleic anhydride change into maleate. Then heat maleate to 50~60 °C in water bath, add catalyst and mass fraction of 30% hydrogen peroxide to precede the epoxidation reaction of maleate, the reaction temperature is 60~70°C, the reaction time is 2~3 hours, after that we get epoxysuccinic acid. Then heat the temperature to 80~90°C, add a certain amount of catalyst and precede polymerization reaction for 2~3 hours, purify the reactants, get colorless or faint yellow viscous polyepoxysuccinic acid solution, its solid content can be regulated by controlling the amount of water.

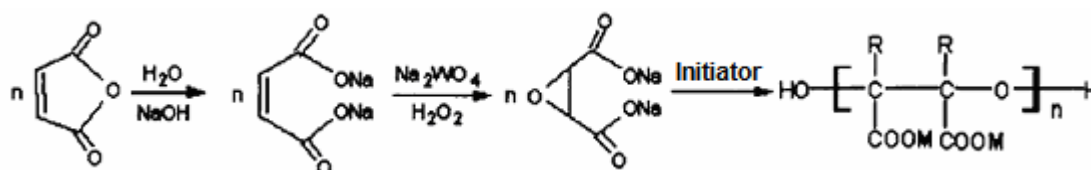


Fig.3.2 Synthetic principle of PESA

Table 3.2 Physicochemical characteristics of PESA

<b>Molecular formula</b>	$HO (C_4H_2O_5M_2)_n H$	<b>Solid content %</b> $\geq$	40.0
<b>Molecular weight</b>	400-1500	<b>Density (20°C) <math>g/cm^3</math></b> $\geq$	1.28
<b>Appearance</b>	Colorless or transparent amber liquid	<b>pH (1% solution)</b>	9.0-12.0

### 3.1.1.3 Water studied

To obtain a water whose scaling potential remained rigorously constant, it was decided to work with a mineral water named Salvetat, whose physicochemical characteristics <sup>[66]</sup> are shown in Table 3.3. Langelier index ( $I_L$ ) shows the water is liable to scaling.  $CaCO_3$  is thermo-dynamically liable to precipitate; it is simply metastable water.

Salvetat solutions of different volume percents (30 %, 50 % or 75 %) were prepared by diluting Salvetat with deionized water.

Table 3.3 Salvetat water analysis

Parameter	Value	Parameter	Value
T (°C)	18.8	Electrical conductivity (mS/cm)	1.328
pH	5.7	Hardness (°)	38
		Silica (mg/L)	72
Alkalinity ( $\times 10^{-3}$ mol/L)	13.4	Bicarbonate (mg/L)	820
Calcium (mg/L)	253	Sulphate (mg/L)	25
Sodium (mg/L)	7	Chloride (mg/L)	4
Magnesium (mg/L)	11	Nitrate (mg/L)	< 1
Potassium (mg/L)	3	Total anions (meq/L)	14.09
Total cations (meq/L)	13.95	180°C drying residue (mg/L)	850
pHeq	6.35	Degree of supersaturation ( $\delta$ )	0.23

### 3.1.2 Methods

#### 3.1.2.1 Static tests for scale inhibition efficiency

Static experiments were performed as described in GB/T 16632-1996 (China). A known amount of scale inhibitor solution was added to cation ( $M^{2+} = Ca^{2+}, Ba^{2+}, Sr^{2+}$ ) stock solution of certain volume in 0.5 L volumetric flasks, then adjusted pH to certain value using borax buffer solution, followed by dropping appropriate amounts of bicarbonate (or sulphate) stock solution and diluting, resulting in a supersaturated solution. The flasks were then incubated in a water bath for certain hours at constant temperature. After cooling, a fixed aliquot of solution was filtered through 0.22  $\mu m$  filter paper, and the  $M^{2+}$  concentration in the filtrate was measured by EDTA titration and spectrophotometric method [67].

The scale inhibition efficiency ( $E$ , %), which was calculated from the change in cation concentration, was obtained by the following equation:

$$E = \frac{X_2 - X_0}{X_1 - X_0} \times 100\%$$

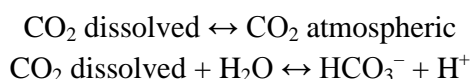
where  $X_2$  and  $X_0$  (mg/L) are the  $M^{2+}$  concentration in the water samples after incubation in presence and absence, respectively, of scale inhibitors;  $X_1$  (mg/L) is the  $M^{2+}$  concentration in the water samples treated with scale inhibitors before incubation.

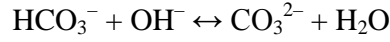
#### 3.1.2.2 Rapid controlled precipitation (RCP) tests

The RCP method was proposed by Lédion *et al.* [14, 68] and progressively improved in PIMM, which consists in degassing of  $CO_2$  from the test water by a moderated agitation using a magnetic stirrer. In this way, the nucleation and the growth of  $CaCO_3$  are initiated in a similar way of a natural scaling phenomenon. The water scaling capacity is then characterised by taking measurements of pH and resistivity as functions of time.

The principle of RCP was based on the following three steps [69]:

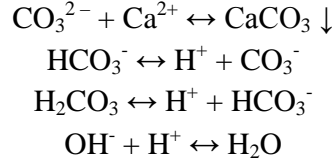
The first step:





This step was primarily the degassing of the dissolved  $\text{CO}_2$ , the equilibrium reactions were towards the left, so the concentration of the  $\text{OH}^-$  increased together with the pH values. In a way alike natural scaling phenomenon, the germination and the growth of calcium carbonate were initiated and the supersaturated coefficient began to increase.

The second step:



In this step, the dissolved carbon dioxide in the water became less and less. The adherent nucleation began to adsorb and form big particles. In this way, calcium carbonate precipitates began to produce in the solution. The concentration of  $\text{H}^+$  increased and the pH values decreased.

In the third step, the velocity of the degassing of dissolved carbon dioxide kept dynamic equilibriums with that of calcium carbonate precipitation and the pH values were stable. The capacity of the water scaling was characterized by measuring the pH and resistivity as a function of time. The resistivity measure was a necessary complement for pH measure.

In RCP, the following conditions should be satisfied: the suitable stirring velocity, the reasonable temperature and the solution composition, etc.

The experimental set-up of RCP is described in Fig.3.3. For the two flasks, one was filled with 300 mL Salvetat solution (untreated water); the other was filled with 300 mL Salvetat solution adding quantitative scale inhibitor (treated water). At a given temperature, the treated water and the reference water (untreated) were stirred simultaneously at a speed of 600 rpm in sequences of 1, 2, 3 or 5 min. After each sequence, the pH and the resistivity of the two waters were measured. The whole experiment normally lasted above 60 min.

Fig.3.4 illustrates an example of the variation of pH and resistivity with time for reference water and the same water treated by anti-scaling procedure. The maximum in the pH-time curves corresponds to the precipitation threshold in the water concerned. The start of precipitation is also indicated by a change in slope of the resistivity-time curves, while the slope beyond the inflection characterises the kinetics of the  $\text{CaCO}_3$  precipitation. However, experience shows that the onset of precipitation is determined more accurately from the pH curves, the resistivity curves being used essentially to analyse the rate of reaction.

The measured efficiency must incorporate both the nucleation and growth phases. The test time was therefore fixed and the area between the resistivity curves for treated and non-treated water was compared to the area beneath the resistivity curve for non-treated water. The efficiency,  $E$ , was then defined by

$$E_R(\%) = \frac{\int_0^t (R_{NT} - R_0) dt - \int_0^t (R_T - R_0) dt}{\int_0^t (R_{NT} - R_0) dt} \times 100 = A_a / (A_a + A_b)$$

where  $R_0$  is the initial resistivity;  $R_{NT}$  and  $R_T$  are the resistivity of the non-treated water and the treated water at time  $t$ , respectively;  $A_a$  and  $A_b$  represent the area of Part  $a$  and Part  $b$  correspondingly;  $c$  is the tangent of the beginning parts of the two curves of resistivity (Fig.3.4).

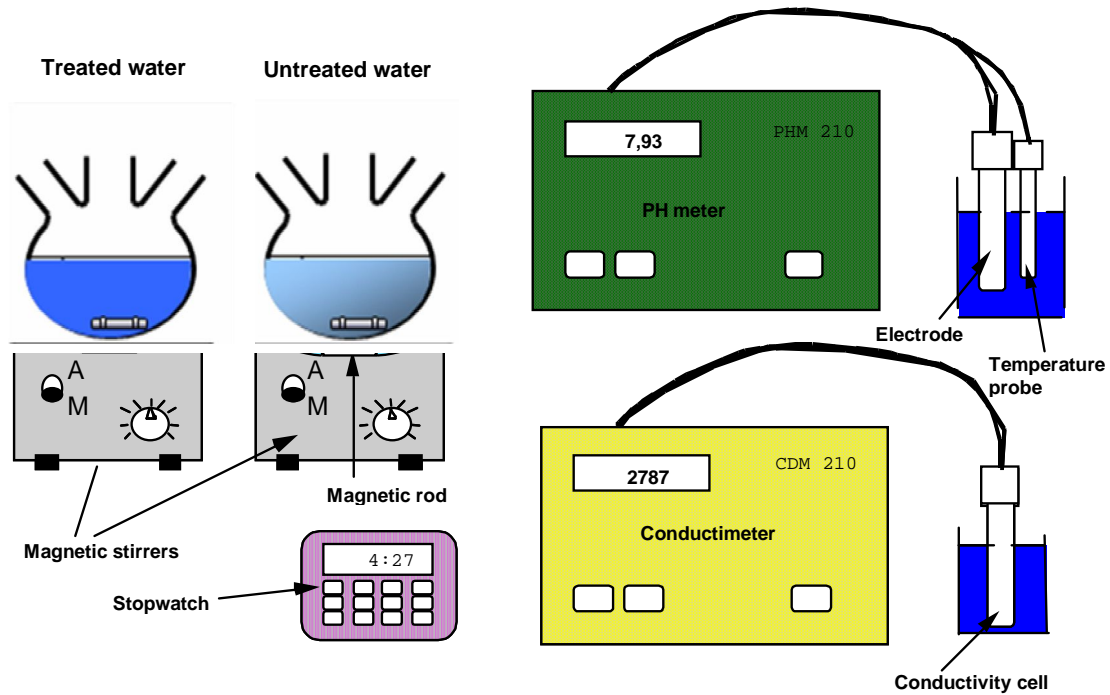


Fig.3.3 Experimental device of RCP

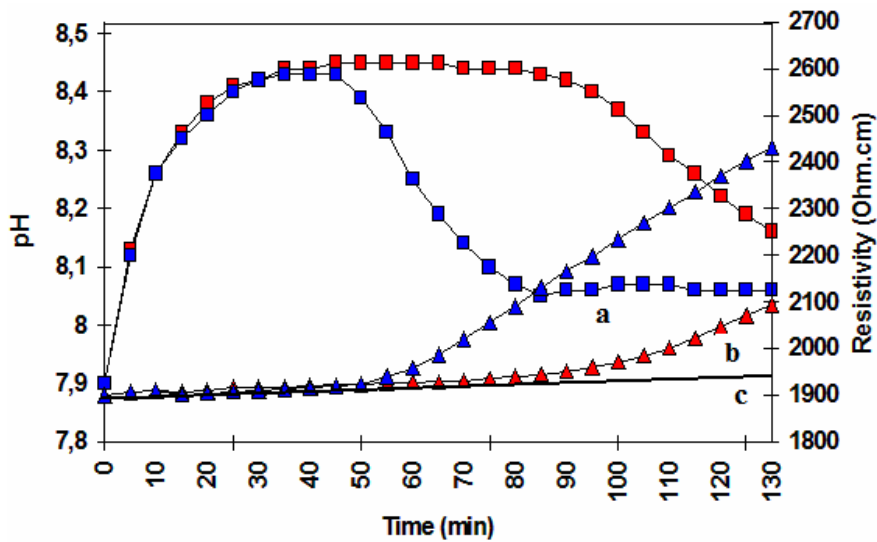


Fig.3.4 RCP curves: Variation of pH and resistivity versus time (Red: treated water; Blue: untreated water)

### 3.1.2.3 Continuous tests

To simulate a real scaling procedure in hot water circuits, Lédion *et al.* have designed a test system called “continuous test rig” which is shown schematically in Fig.3.5. The rig is designed so that the waters studied (Salvetat solution) begin slightly to

precipitate. This enables tests with a hot water circuit leading to scaling of the studied materials (austenitic stainless steel tubes:  $\Phi=2$  cm, length=10 cm). The tubes are mounted in series with plastic joints and their positions are changed every day by circular permutation, to compensate for possible variations in scale inhibitor concentration that could modify the scaling potential of the water at different points in the circuit. The temperature of the water was controlled by a thermostat bath at 40-60 °C, and the outlet flow rate was maintained at about 35 L/h. For each series of specimens, the tests lasted 30 days, with 8 hours exposure per day, i.e. a total of 240 hours. Scaling was evaluated by weighing on a balance accurate to a tenth of a milligram. To avoid unwanted scale nucleation due to water evaporation, the specimens were withdrawn after each exposure period, when the water had cooled to ambient temperature. They were then rinsed in deionized water and oven dried for 20 minutes at 50 °C. Weighing was performed after the tubes had cooled to the temperature of the balance room.

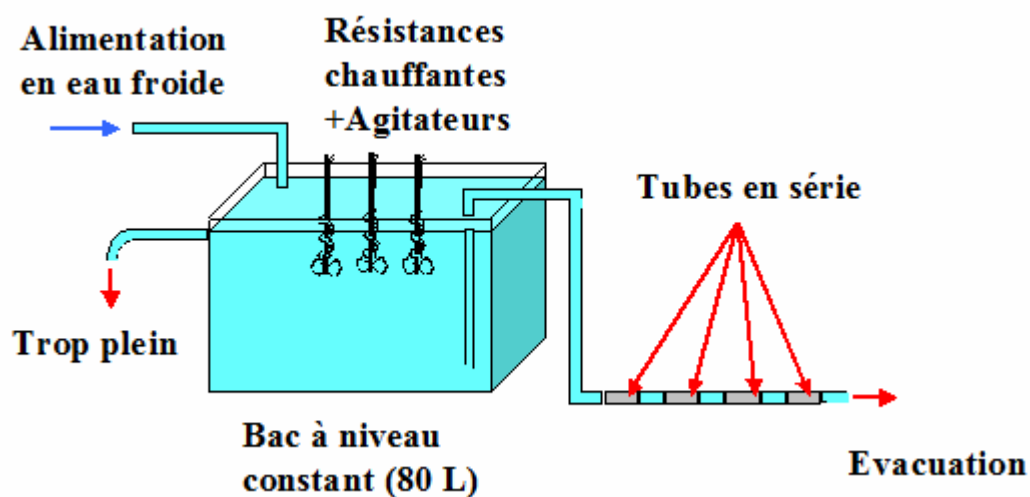


Fig.3.5 Experimental set-up of the continuous test rig

## 3.2 Results and discussion

### 3.2.1 Comparison of anti-scaling performance of PASP and PESA

#### 3.2.1.1 Static tests of scale inhibition

##### 3.2.1.1.1 Inhibition of $\text{CaCO}_3$ scale

For static tests on inhibition of  $\text{CaCO}_3$  ( $\text{Ca}^{2+}$ : 500 mg/L,  $\text{HCO}_3^{2-}$ : 750 mg/L, pH: 9, T: 80 °C, t: 8 h), as seen in Fig.3.6, PASP and PESA both have satisfactory inhibiting effect on  $\text{CaCO}_3$ , while PESA shows better performance than PSAP.

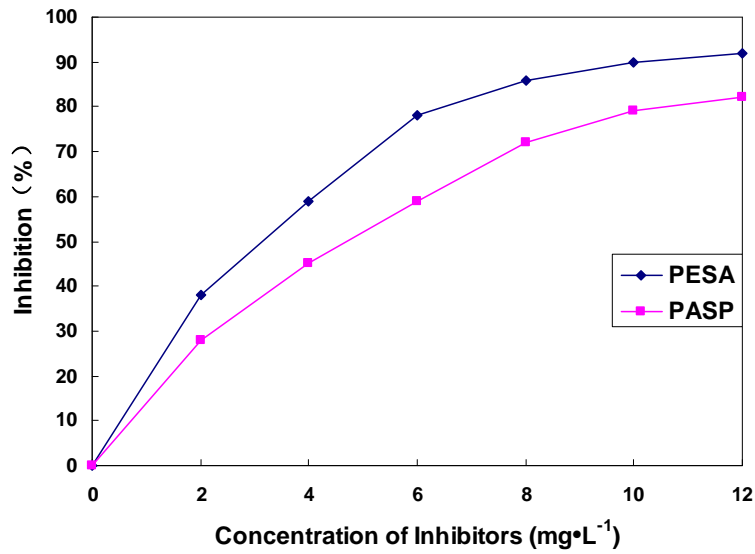


Fig.3.6 Variation of inhibition efficiency of CaCO<sub>3</sub> versus dosage of inhibitors

### 3.2.1.1.2 Inhibition of CaSO<sub>4</sub>·2H<sub>2</sub>O scale

For static tests on inhibition of CaSO<sub>4</sub>·2H<sub>2</sub>O (Ca<sup>2+</sup>: 2000 mg/L, SO<sub>4</sub><sup>2-</sup>: 4800 mg/L, pH: 7, T: 60 °C, t: 18 h), as seen in Fig.3.7, PASP shows excellent inhibiting performance on CaSO<sub>4</sub>·2H<sub>2</sub>O, while PESA has certain inhibition effect.

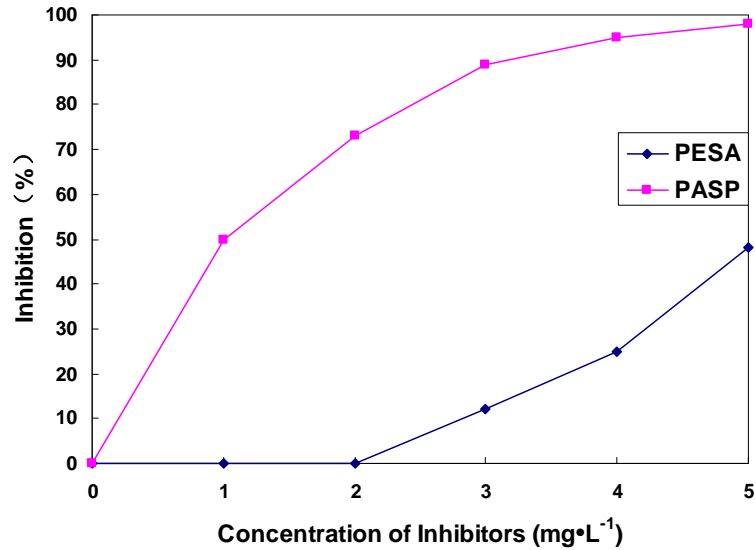


Fig.3.7 Variation of inhibition efficiency of CaSO<sub>4</sub>·2H<sub>2</sub>O versus dosage of inhibitors

### 3.2.1.1.3 Inhibition of BaSO<sub>4</sub> scale

For static tests on inhibition of BaSO<sub>4</sub> (Ba<sup>2+</sup>: 20 mg/L, SO<sub>4</sub><sup>2-</sup>: 100 mg/L, pH: 7, T: 65 °C, t: 18 h), as seen in Fig.3.8, PASP and PESA both have extremely good inhibiting effect on BaSO<sub>4</sub>, while PESA shows weaker performance than PASP.

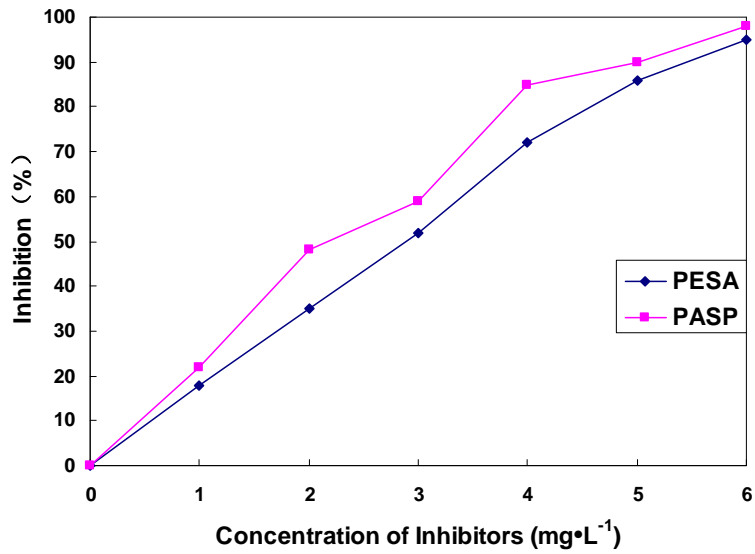


Fig.3.8 Variation of inhibition efficiency of BaSO<sub>4</sub> versus dosage of inhibitors

#### 3.2.1.1.4 Inhibition of SrSO<sub>4</sub> scale

For static tests on inhibition of SrSO<sub>4</sub> (Sr<sup>2+</sup>: 300 mg/L, SO<sub>4</sub><sup>2-</sup>: 1100 mg/L, pH: 7, T: 65 °C, t: 18 h), as seen in Fig.3.9, PASP and PESA both show quite strong inhibiting effect on SrSO<sub>4</sub>, while the performance of PESA is slightly superior to that of PASP.

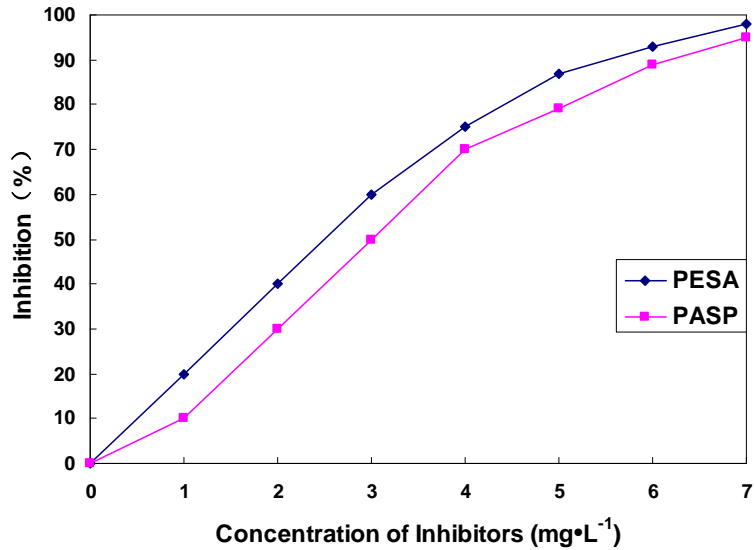


Fig.3.9 Variation of inhibition efficiency of SrSO<sub>4</sub> versus dosage of inhibitors

#### 3.2.1.2 RCP tests

##### 3.2.1.2.1 Inhibition effect of PASP

###### a. Influence of dosage

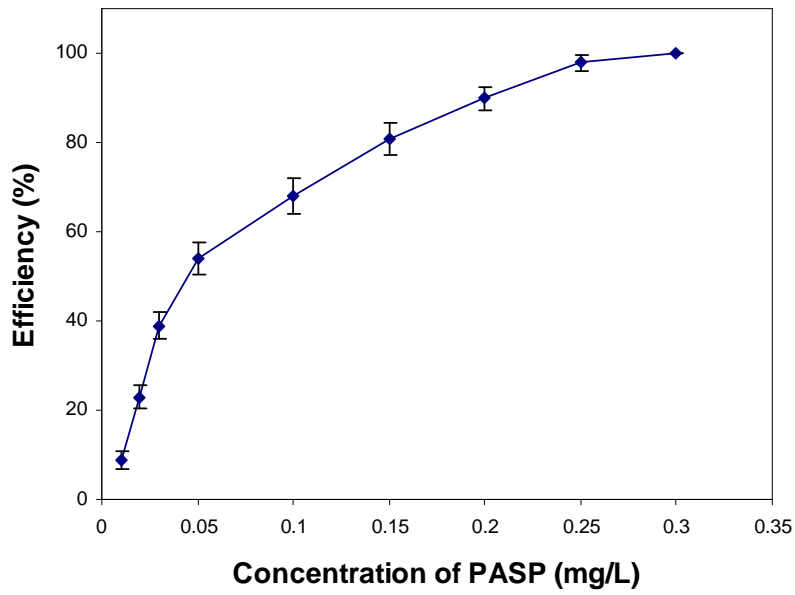


Fig.3.10 Variation of efficiency of inhibition versus dosage of PASP (50%Salvetat, t = 60 min)

As seen in Fig.3.10, when the concentration of PASP was lower than 0.01 mg/L, it hardly had any effect on the scaling. But when the dosage of PASP was above 0.3 mg/L, it showed total inhibition effectiveness in 60 min. While the concentration of PASP was between 0.01 mg/L and 0.3 mg/L, it could retard the precipitation of  $\text{CaCO}_3$ .

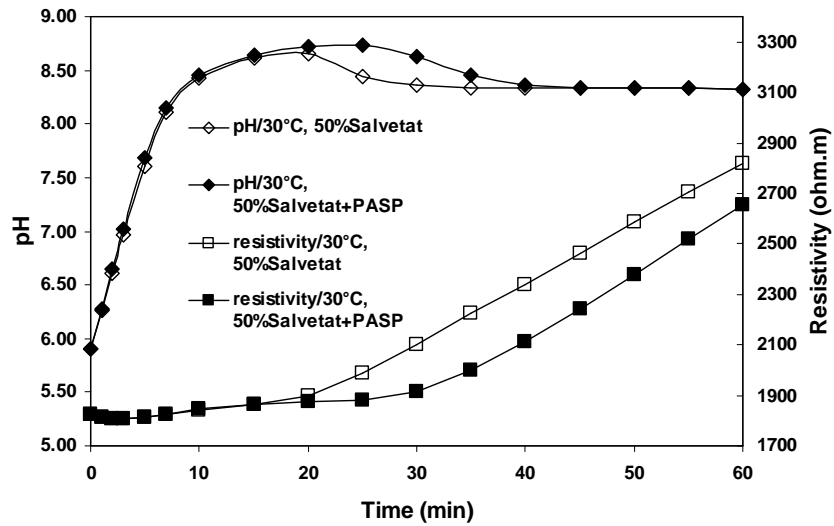


Fig.3.11 The curves of pH and resistivity versus time (PASP: 0.03 mg/L)

As seen in Fig.3.11, for the untreated water, the scaling time was 20min, after introducing 0.03 mg/L PASP, the retarding time was only 5min, it had weak effect on the inhibition of scaling.

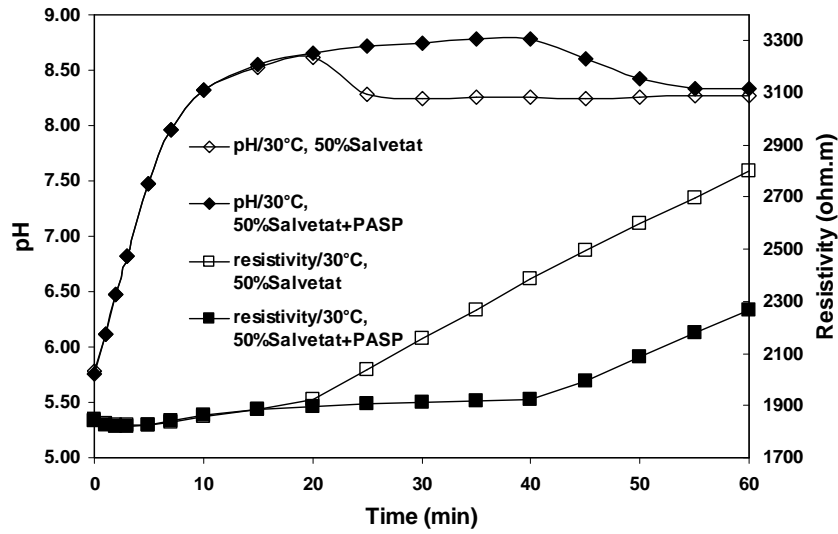


Fig.3.12 The curves of pH and resistivity versus time (PASP: 0.15 mg/L)

As seen in Fig.3.12, for the treated water, the pH began to fall 20 min later than that of untreated water, and the rate of precipitation, indicated by the slope of the resistivity curve, was considerably reduced, which showed that the greater the concentration of PSAP, the longer the scaling time lasted, the better its inhibition effectiveness.

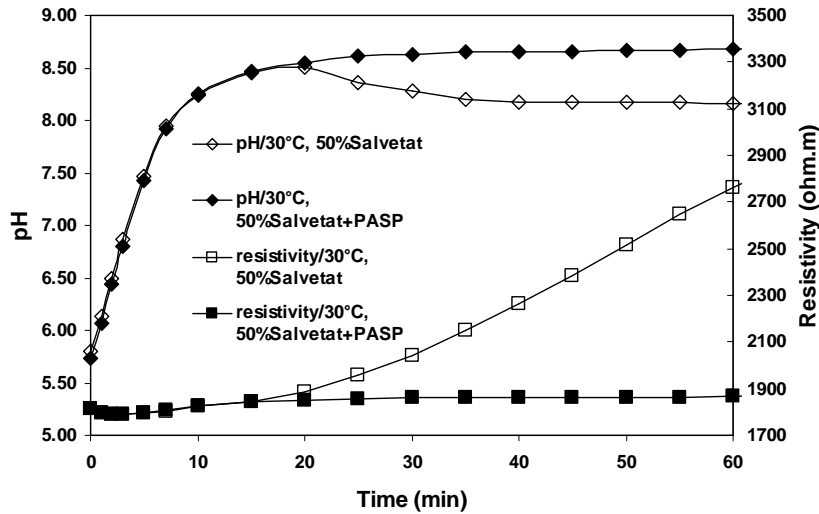


Fig.3.13 The curves of pH and resistivity versus time (PASP: 0.3 mg/L)

As seen in Fig.3.13, for the untreated water, the scaling time was 20 min, but for the treated water adding 0.3 mg/L PASP, the curve of pH-time and that of resistivity-time extend linearly towards the rights, no precipitate had yet appeared in 60 min, which showed that 0.3 mg/L PASP could inhibit the scaling of  $\text{CaCO}_3$  totally.

b. Influence of temperature

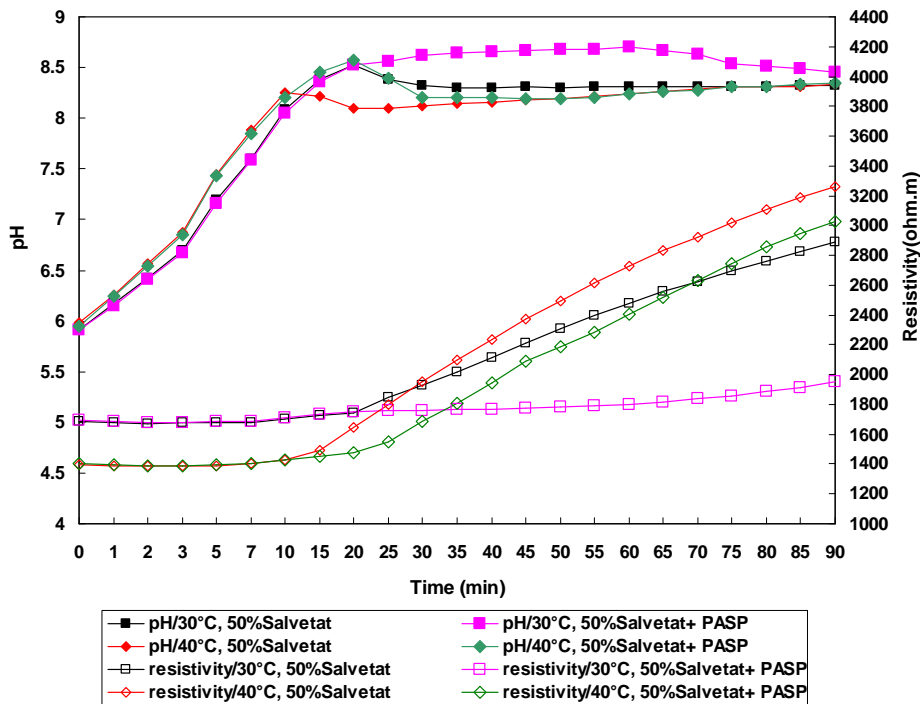


Fig.3.14 Influence of temperature on inhibition effect of PASP (0.28 mg/L)

At the temperature of 30 °C, as seen in Fig.3.14, for the untreated 50%Salvetat water, the scaling time was 20 min, for the treated water adding 0.28 mg/L PASP, the precipitate appeared at 60 min, that is, the retarding time of scaling is 40 min. However, when the temperature rose to 40 °C, for the untreated and treated water, the scaling time was 10 min and 20 min respectively, the precipitation of CaCO<sub>3</sub> was merely delayed for 10 min.

### c. Influence of Ca<sup>2+</sup> concentration

As seen in Fig.3.15, at the temperature of 30 °C, for 50 % Salvetat solution (Ca<sup>2+</sup>: 126.5 mg/L, HCO<sub>3</sub><sup>-</sup>: 410 mg/L), the scaling time of untreated and treated water was 20 min and 60 min respectively, the precipitate was delayed for 40 min. But for 75 % Salvetat solution (Ca<sup>2+</sup>: 189.75 mg/L, HCO<sub>3</sub><sup>-</sup>: 615 mg/L), the scaling time of untreated and treated water was 15 min and 20 min correspondingly, that is, the retarding time of precipitation by 0.28 mg/L PASP was only 5 min.

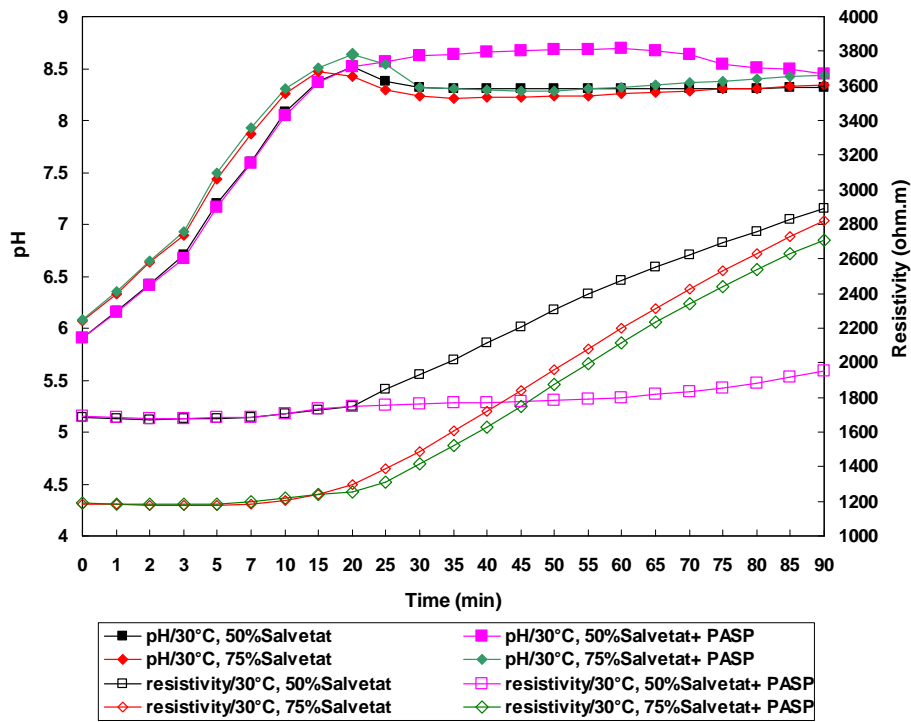


Fig.3.15 Influence of Ca<sup>2+</sup> concentration on inhibition effect of PASP (0.28 mg/L)

### 3.2.1.2.2 Inhibition effect of PESA

#### a. Influence of dosage

As seen in Fig.3.16, when the concentration of PESA was below 0.005 mg/L, it had little effect on the scaling and its inhibition effectiveness was poor. But when the dosage of PESA was increased to 0.025 mg/L, the inhibition effectiveness of PESA increased significantly.

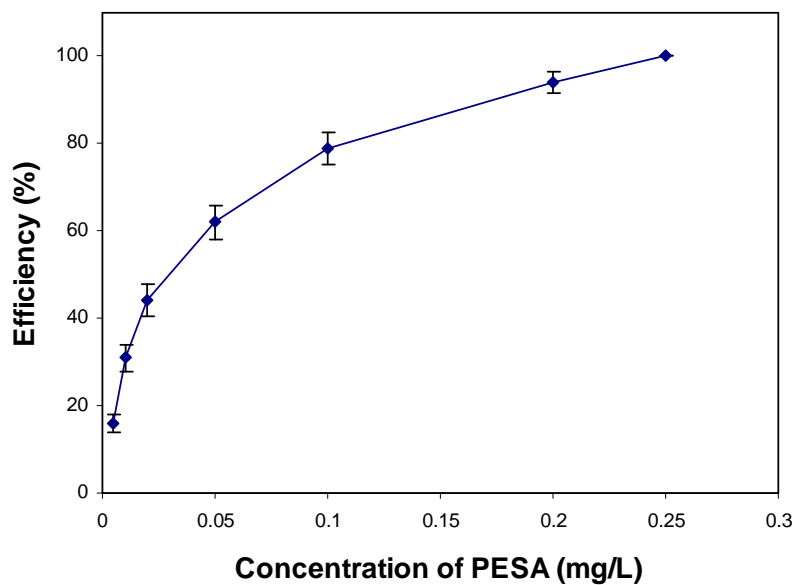


Fig.3.16 Variation of efficiency of inhibition versus dosage of PESA (50% Salvetat, t = 60 min)

As seen in Fig.3.17, for the untreated and treated water, the scaling times were 20 min and 25 min respectively, the retarding time was 5 min, which showed that 0.01 mg/L PESA had weak effect on the inhibition of scaling.

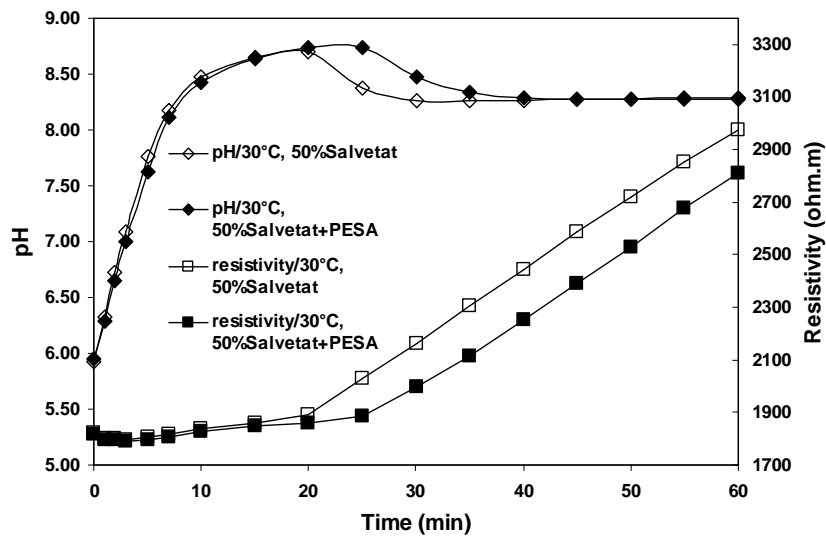


Fig.3.17 The curves of pH and resistivity versus time (PESA: 0.01 mg/L)

As seen in Fig.3.18, for the untreated water, the scaling time was 20 min, however, for the treated water adding 0.1 mg/L PESA, the precipitate began to appear slowly at 40 min, which indicated that with the increase of the concentration of PESA, its ability to inhibit the scaling of  $\text{CaCO}_3$  enhanced obviously.

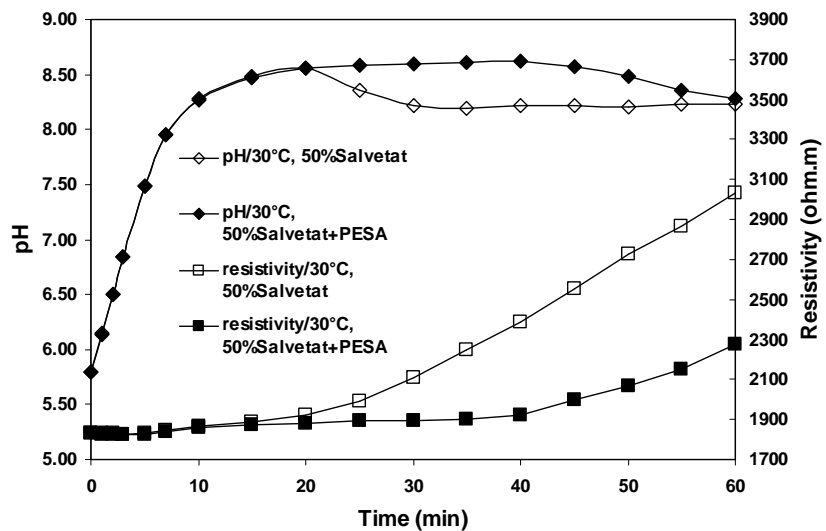


Fig.3.18 The curves of pH and resistivity versus time (PESA: 0.1 mg/L)

As seen in Fig.3.19, for the untreated water, the scaling time was 20 min, after introducing 0.25 mg/L PESA, no precipitate had yet appeared in 60 min, which showed total inhibition effectiveness of  $\text{CaCO}_3$ .

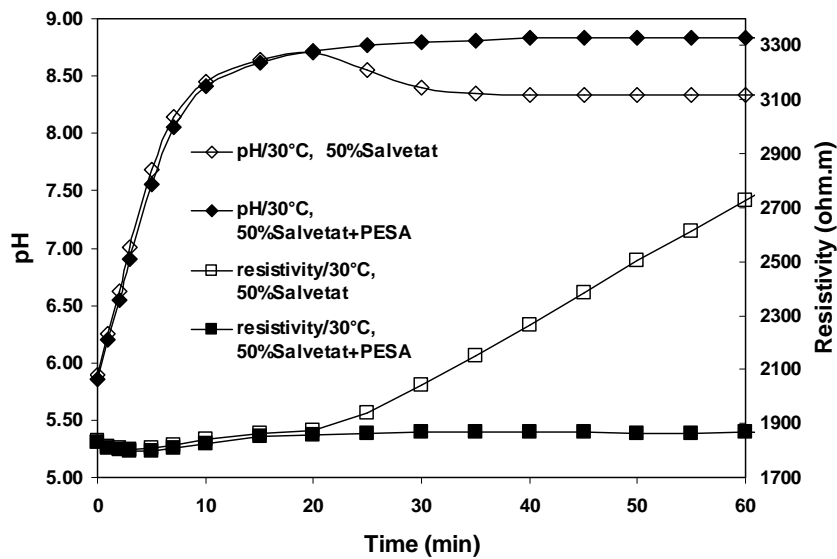


Fig.3.19 The curves of pH and resistivity versus time (PESA: 0.25 mg/L)

b. Influence of temperature

At the temperature of 30 °C, as seen in Fig.3.20, for the untreated 50%Salvetat water, the scaling time was 20 min, for the treated water adding 0.23 mg/L PESA, the precipitate appeared at 65 min, that is, the retarding time of scaling is 45 min. However, when the temperature rose to 40 °C, for the untreated and treated water, the scaling time was 10 min and 25 min respectively, the precipitation of CaCO<sub>3</sub> was delayed for 15 min.

c. Influence of Ca<sup>2+</sup> concentration

As seen in Fig.3.21, at the temperature of 30 °C, for 50 % Salvetat solution (Ca<sup>2+</sup>: 126.5 mg/L, HCO<sub>3</sub><sup>-</sup>: 410 mg/L), the scaling time of untreated and treated water was 20 min and 65 min respectively, the precipitate was delayed for 45 min. But for 75 % Salvetat solution (Ca<sup>2+</sup>: 189.75 mg/L, HCO<sub>3</sub><sup>-</sup>: 615 mg/L), the scaling time of untreated and treated water was 15 min and 25 min correspondingly, that is, the retarding time of precipitation by 0.23 mg/L PESA was 10 min.

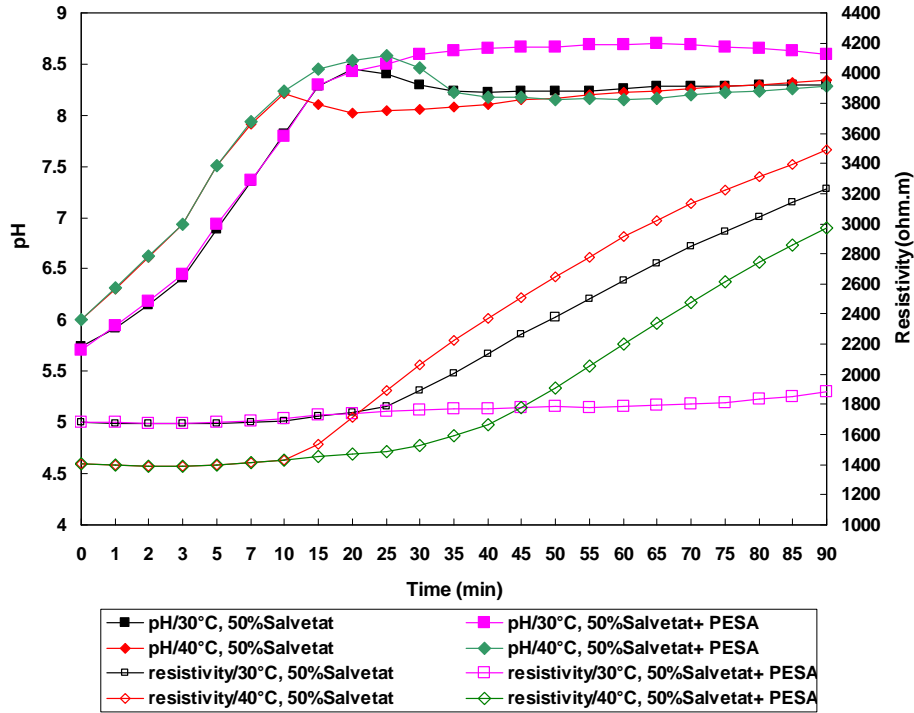


Fig.3.20 Influence of temperature on inhibition effect of PESA (0.23 mg/L)

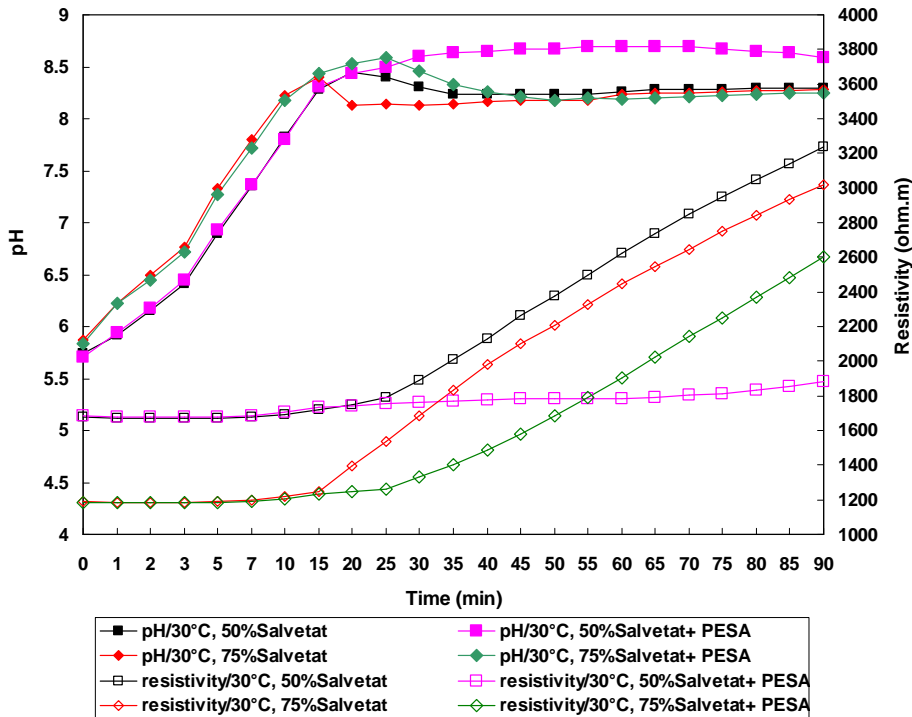


Fig.3.21 Influence of  $Ca^{2+}$  concentration on inhibition effect of PESA (0.23 mg/L)

### 3.2.1.2.3 Comparison of anti-scaling performance

As seen in Fig.3.22, the inhibition performance of PESA on  $CaCO_3$  is obviously superior to that of PASP, however, with the increase of dosage, their inhibiting effects become closer.

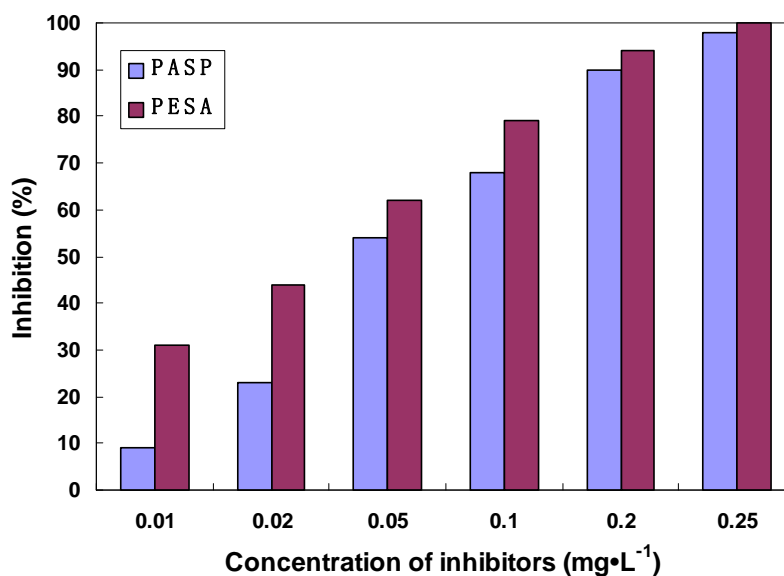


Fig.3.22 Comparison of anti-scaling effect of inhibitors on CaCO<sub>3</sub> (t = 60 min)

Compared with PASP, as seen in Table 3.4, PESA attains better inhibition effect at lower dosage. Thus the anti-scaling performance of PESA is superior to that of PASP for CaCO<sub>3</sub>.

Table 3.4 Anti-scaling effect of inhibitors on CaCO<sub>3</sub> (t = 90 min)

Inhibitor	Efficiency %	Efficiency %	Efficiency %
	(30 °C/ 50 % Salvetat)	(30 °C/ 75 % Salvetat)	(40 °C/ 50 % Salvetat)
0.28 mg/L PASP	88	12	36
0.23 mg/L PESA	94	48	52

### 3.2.1.3 Anti-scaling mechanism

#### 3.2.1.3.1 SEM analysis

Figs.3.23, 3.24, 3.25 are the scanning electron microscope photographs of calcium carbonate crystals of blank, dosing PESA, dosing PASP respectively. From the pictures, we can see that calcium carbonate crystal dosing no inhibitor is cube with regular shape and compact structure, but crystals formed in the solution dosing the scale inhibitors turn out to have irregular shape and loose structure. Similarly, we can see from Figs.3.26, 3.27, 3.28 that shape of calcium sulfate crystal dosing no inhibitor is regular needle-like and the surface is smooth and compact, while shape of crystal dosing inhibitor is irregular and the surface is rough and loose. Figs.3.29, 3.30, 3.31 are the scanning electron microscope photographs of barium sulfate crystals. Similarly, we can see from the figures that the shape of barium sulfate crystal dosing no inhibitor is regular and the structure is compact, while after dosing inhibitors crystals lose their original configuration and become loose and irregular. It can be seen from these figures no matter calcium carbonate, calcium sulfate or barium sulfate, after dosing inhibitors the original regular and compact crystal

structure would become irregular and compact and smooth surface would become rough and loose. According to dynamics theory of crystal growth, the growth of crystal is achieved through emergence and growth of level. In the tiny crystal growth process, if the tiny crystals adsorb scale inhibitors, in levels and dots battle doping crystal lattice, the crystal can not grow normally in accordance with array of crystal lattice strictly, which makes the crystals distort or internal stress of large crystals increase, resulting in fracture of crystal, thereby preventing microcrystalline from depositing into scale, to achieve the purpose of scale inhibiting.

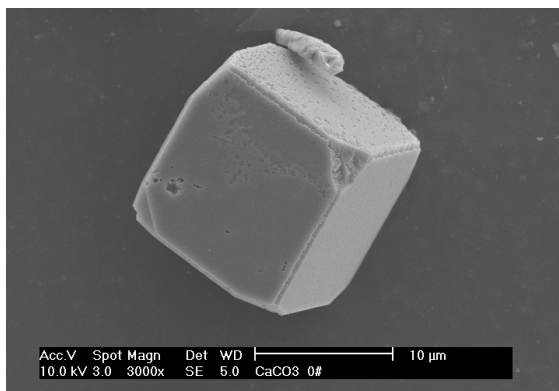


Fig.3.23 SEM image of CaCO<sub>3</sub> formed in the absence of inhibitor (blank solution, × 3000)

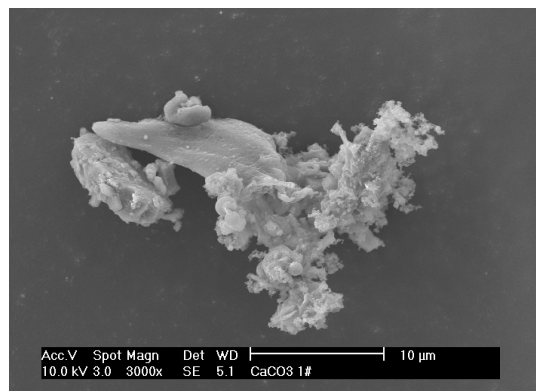


Fig.3.24 SEM image of CaCO<sub>3</sub> formed in the presence of PESA (× 3000)

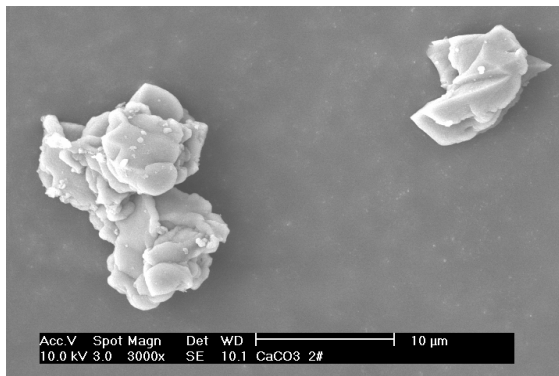


Fig.3.25 SEM image of CaCO<sub>3</sub> formed in the presence of PASP (× 3000)

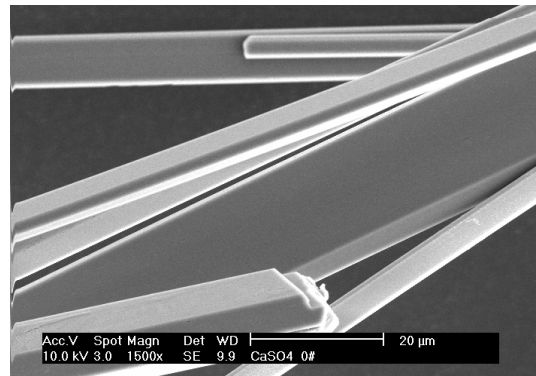


Fig.3.26 SEM image of CaSO<sub>4</sub> formed in the absence of inhibitor (blank, × 1500)

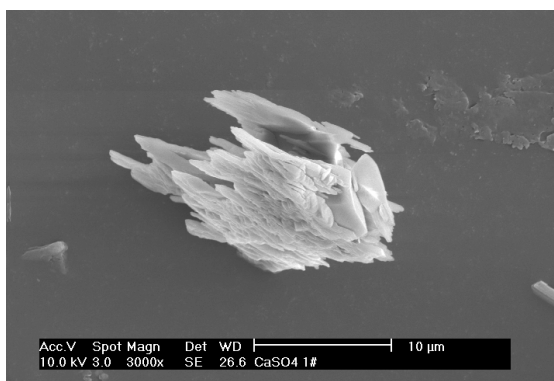


Fig.3.27 SEM image of  $\text{CaSO}_4$  formed in the presence of PESA ( $\times 3000$ )

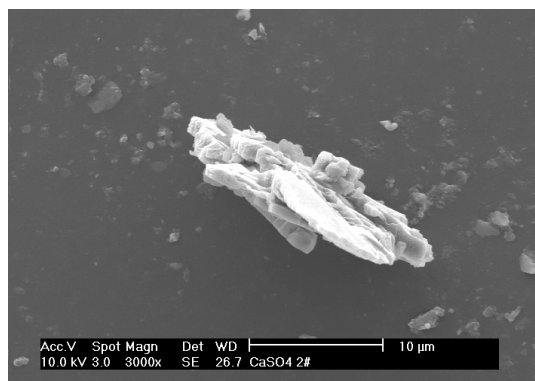


Fig.3.28 SEM image of  $\text{CaSO}_4$  formed in the presence of PASP ( $\times 3000$ )



Fig.3.29 SEM image of  $\text{BaSO}_4$  formed in the absence of inhibitor ( $\times 1500$ )

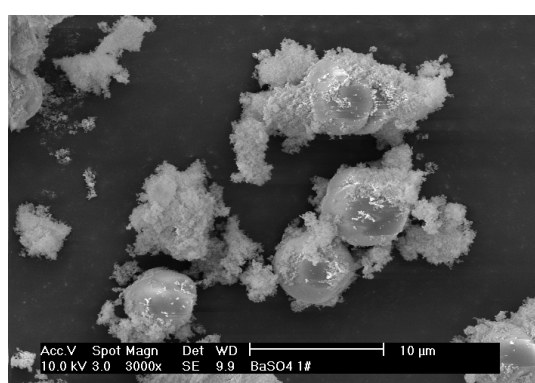


Fig.3.30 SEM image of  $\text{BaSO}_4$  formed in the presence of PESA ( $\times 3000$ )

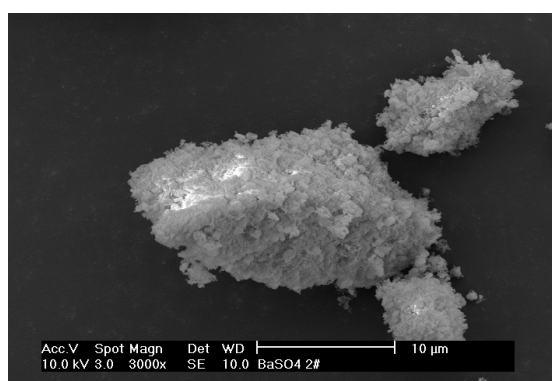


Fig.3.31 SEM image of  $\text{BaSO}_4$  formed in the presence of PASP ( $\times 3000$ )

### 3.2.1.3.2 XRD analysis

Fig.3.32 shows X-ray powder diffraction photographs of  $\text{CaCO}_3$  crystal formed in the blank supersaturated solution of calcium carbonate, supersaturated solution containing PESA and supersaturated solution containing PASP respectively.

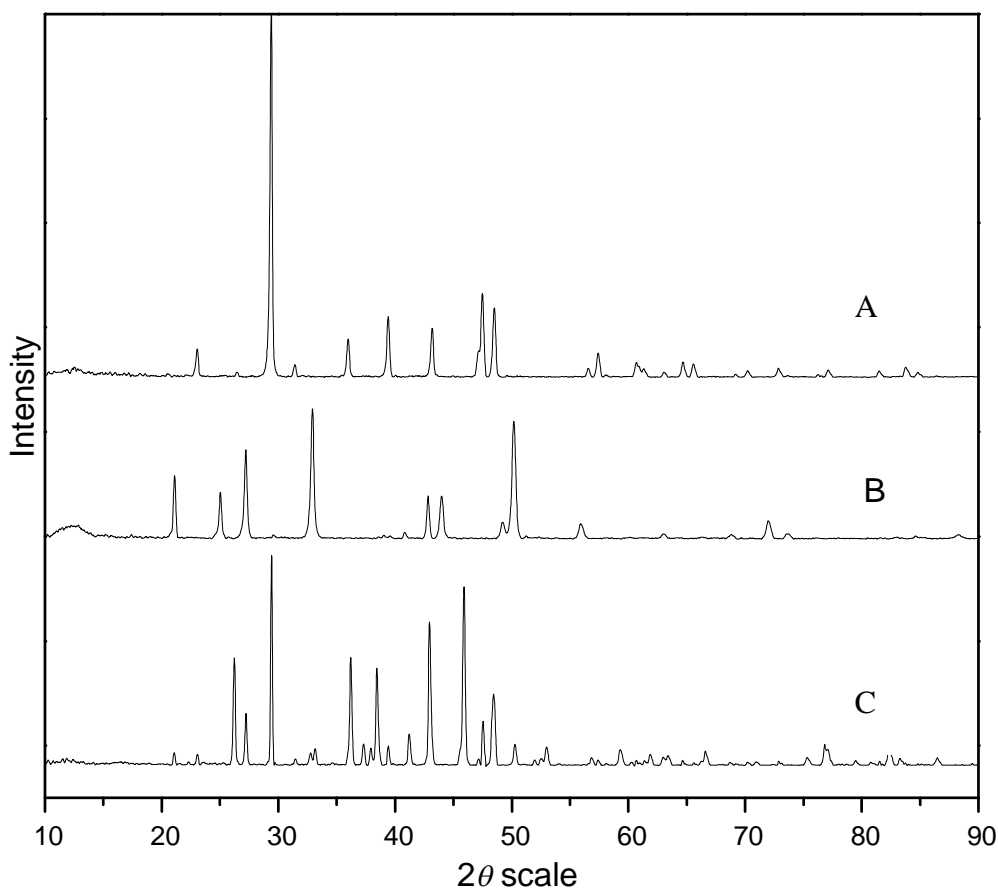


Fig.3.32 XRD photograph of  $\text{CaCO}_3$  crystal

(A: in the absence of inhibitor; B: in the presence of PESA; C: in the presence of PASP)

Compared with photograph A, it can be seen from B that diffraction peaks such as  $21.1^\circ$ ,  $25.05^\circ$ ,  $27.25^\circ$ ,  $32.9^\circ$ ,  $39.4^\circ$ ,  $50.2^\circ$  are significantly enhanced, and diffraction peaks such as  $26.2^\circ$ ,  $29.4^\circ$ ,  $36.2^\circ$ ,  $38.4^\circ$ ,  $43.0^\circ$ ,  $45.9^\circ$ ,  $48.5^\circ$  are significantly reduced. Compared with A, it can be seen from C that diffraction peaks such as  $29.4^\circ$ ,  $39.2^\circ$ ,  $47.5^\circ$  are significantly enhanced, and diffraction peaks such as  $26.2^\circ$ ,  $27.3^\circ$ ,  $36.2^\circ$ ,  $38.4^\circ$ ,  $43.0^\circ$ ,  $45.9^\circ$ ,  $48.5^\circ$  are significantly reduced. The changes of these peaks illustrate the modification of  $\text{CaCO}_3$  crystal habit. In the absence of inhibitors, calcite (A) is the main crystal form. However, calcite and vaterite (C) become the main polymorphs in the presence of PASP. In the presence of PESA, vaterite (B) is the main crystal form. These results show that the inhibitor PASP and PESA play a role of damaging and distorting  $\text{CaCO}_3$  crystals.

Fig.3.33 shows X-ray powder diffraction photographs of  $\text{CaSO}_4$  crystal formed in the blank supersaturated solution of calcium sulfate, supersaturated solution adding PESA and supersaturated solution adding PASP respectively.

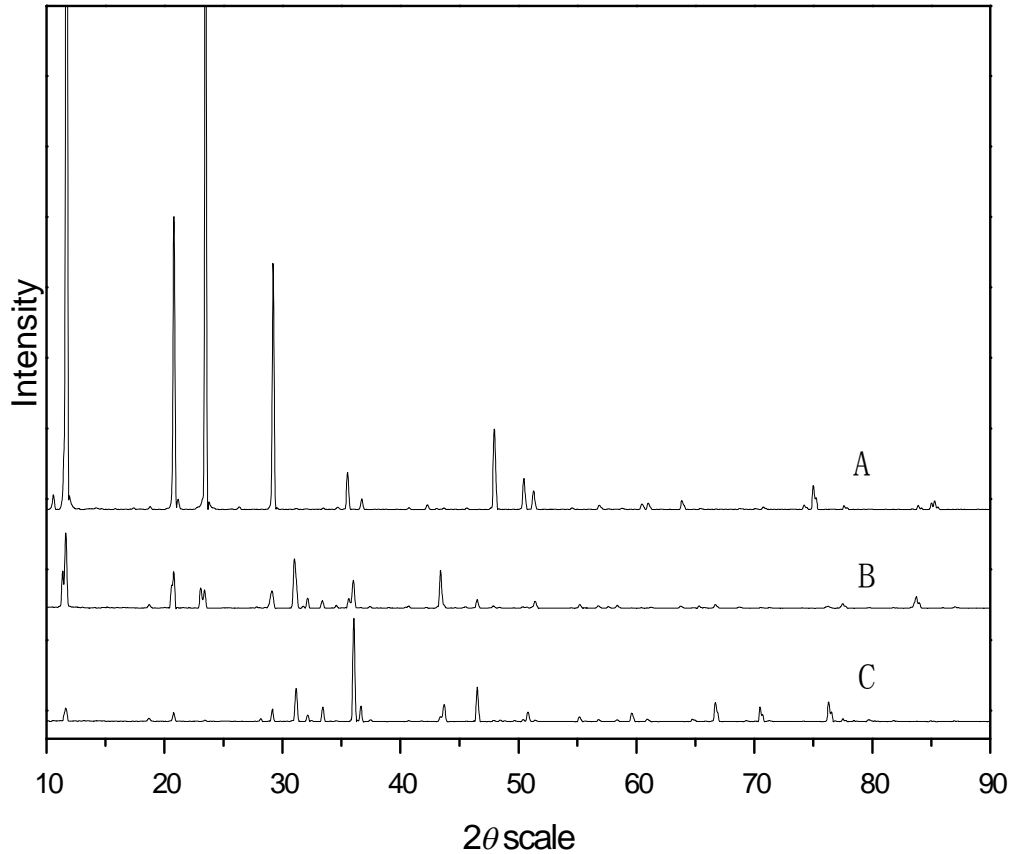


Fig.3.33 XRD photograph of  $\text{CaSO}_4$  crystal

(A: in the absence of inhibitor; B: in the presence of PESA; C: in the presence of PASP)

Diffraction peaks  $11.6^\circ$ ,  $20.8^\circ$ ,  $23.48^\circ$ ,  $29.15^\circ$ ,  $48.0^\circ$  in photograph A are very strong, which are characteristic peaks of calcium sulfate crystal. However, these diffraction peaks in B become very weak, and in C these peaks become much weaker and almost disappeared. In B and C, diffraction peaks  $31.05^\circ$ ,  $33.45^\circ$ ,  $43.4^\circ$ ,  $46.56^\circ$  are significantly enhanced. These changes of the peaks illustrate that calcium sulfate crystal changed a lot in the form and structure after adding inhibitor. Diffraction peaks such as  $11.6^\circ$ ,  $20.8^\circ$ ,  $23.48^\circ$ ,  $29.15^\circ$ ,  $31.05^\circ$  in B are stronger than that in C. but diffraction peaks such as  $35.98^\circ$ ,  $46.5^\circ$ ,  $66.75^\circ$ ,  $70.67^\circ$  in B are weaker than that in C, which illustrate that morphology changes of calcium sulfate crystal are different after adding PESA and PASP, but they both have changed the original crystal conformation, reduced the crystallinity degree and damaged the crystal structure of calcium sulfate. This make the structure of calcium sulfate loose and difficult to form a dense layer of fouling, sequentially prevent deposition.

According to crystal growth theory<sup>[70]</sup>, crystal growth has the habit effect that in the same external conditions, congeneric crystals grow the same shape in theory, which is also called crystal growth habit. Crystal habit is influenced by the factors of internal structure, in addition external environmental factors such as temperature, supersaturation, impurities also have impact on it. When other factors are same, impurities have significant impact on the relative growth rate of each crystal face of crystal, which results

in crystals different with the original crystal form. In the supersaturated solution containing inhibitors, inhibitors molecules that have the same effect as impurities are adsorbed to the crystal growth point, and then inhibit or slow the growth of crystals, so that the supersaturated solution is in a stable state temporarily. However the slowly growing surface in the absence of inhibitors absorbed has a certain growth in the period of induction, which can cover the inhibitors molecules adsorbed on the active site, so that the crystal can grow again, but orientation (habit) of crystal growth is destroyed, the crystal state is also distorted and skewed. So before and after adding inhibitors the structure of crystal changes and the lattice is distorted.

### 3.2.2 Synergistic effect of PASP and PESA on inhibition of scaling

#### 3.2.2.1 Evaluation of scale inhibition performance by static tests

##### 3.2.2.1.1 Research of synergistic effects on inhibition of $\text{CaCO}_3$

For static tests on inhibition of  $\text{CaCO}_3$  ( $\text{Ca}^{2+}$ : 96 mg/L,  $\text{CO}_3^{2-}$ : 151 mg/L, pH: 9, T: 50 °C, t: 16 h), the total dosage of PASP and PESA is 5 mg/L, as seen in Fig.3.34, PASP and PESA have obvious synergistic effect, the inhibitory effect of different ratios is better than that of PASP or PESA alone, and the optimal mass ratio of PASP and PESA is 1:1, the corresponding inhibition rate of  $\text{CaCO}_3$  attains to 84.5 %.

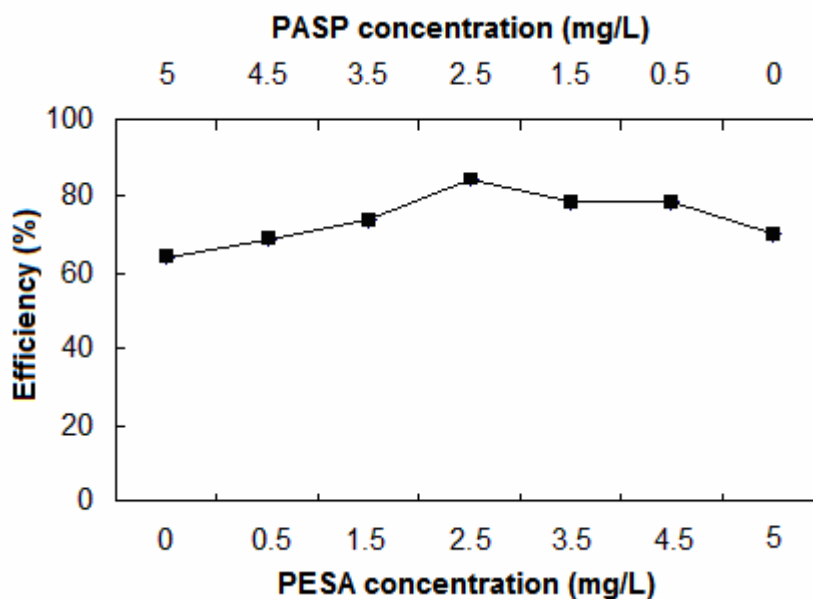


Fig.3.34 Synergistic effects of PASP and PESA on inhibition of  $\text{CaCO}_3$

##### 3.2.2.1.2 Research of synergistic effects on inhibition of $\text{CaSO}_4 \cdot 2\text{H}_2\text{O}$

As seen in Fig.3.35, the total concentration of PASP and PESA is 2 mg/L, the results of static tests on inhibition of  $\text{CaSO}_4 \cdot 2\text{H}_2\text{O}$  ( $\text{Ca}^{2+}$ : 1800 mg/L,  $\text{SO}_4^{2-}$ : 4300 mg/L, pH: 7, T: 80 °C, t: 16 h) showed that PASP and PESA had certain synergistic effect, when their mass ratio was 3:1, the corresponding inhibition effect is slightly better than that of PASP alone.

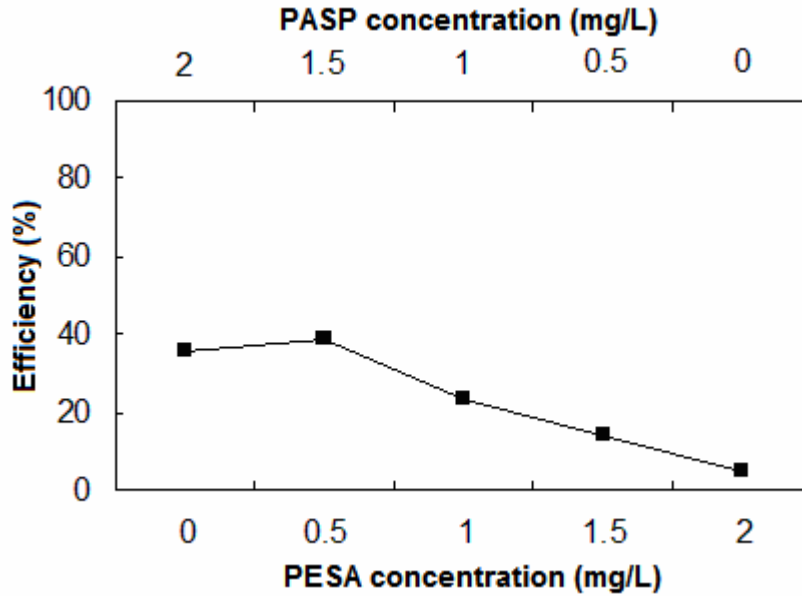


Fig.3.35 Synergistic effects of PESP and PESA on inhibition of  $\text{CaSO}_4 \cdot 2\text{H}_2\text{O}$

### 3.2.2.1.3 Research of synergistic effects on inhibition of $\text{BaSO}_4$

In the static tests for inhibition of  $\text{BaSO}_4$  ( $\text{Ba}^{2+}$ : 56.6 mg/L,  $\text{SO}_4^{2-}$ : 41.1 mg/L, pH: 7, T: 50 °C, t: 24 h), the total dosage of PESP and PESA is 1.5 mg/L, as seen in Fig.3.36, PESP and PESA show satisfactory synergistic effect, their optimal mass ratio was 1:2, the corresponding inhibitory efficiency of  $\text{BaSO}_4$  reaches up to 95.3 %.

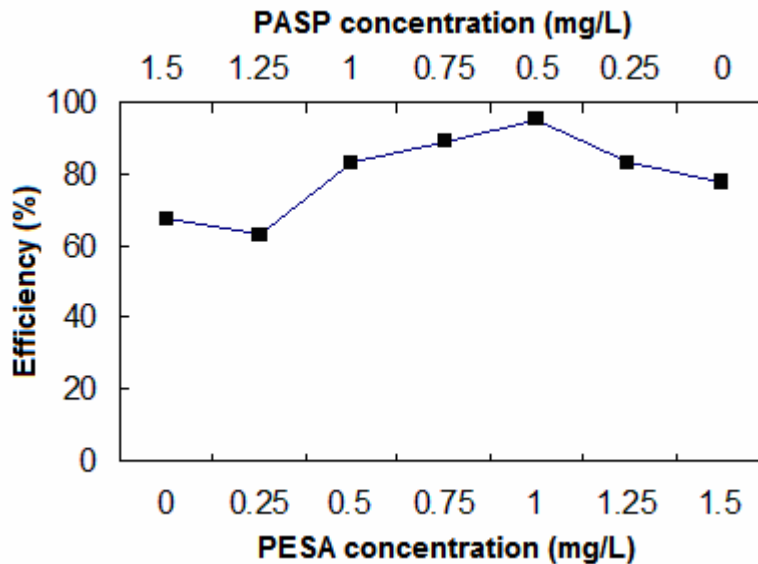


Fig.3.36 Synergistic effects of PESP and PESA on inhibition of  $\text{BaSO}_4$

### 3.2.2.2 Evaluation of scale inhibition performance by RCP tests

#### 3.2.2.2.1 Effect of dosage of PESP combined with PESA on inhibition of $\text{CaCO}_3$

At the temperature of 30 °C, for 50 % Salvetat solution adding (PESP+PESA) (1:1) (the mass ratio of PESP and PESA is 1:1), the results showed that with the rise in dosage of (PESP+PESA) (1:1), the inhibitory efficiency,  $E$  increased (Fig.3.37), the retarding

pH-time curve of the treated water slowly became a line and, correspondingly, the slope of the resistivity-time curve became smaller (Figs.3.38-3.41).

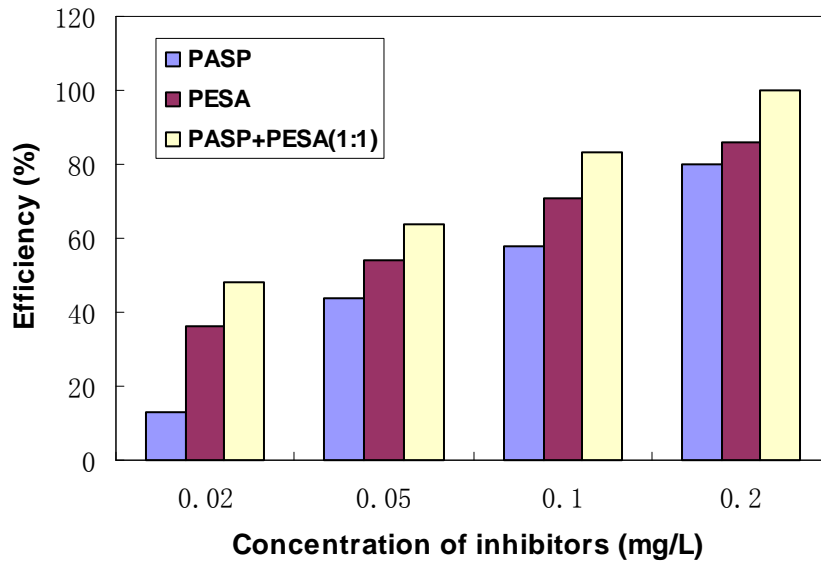


Fig.3.37 Comparison of anti-scaling effect of inhibitors

As shown in Fig.3.38, for the untreated water, the scaling time was 20 min, after introducing 0.02 mg/L (PASP+PESA) (1:1), the pH began to fall 15 min later than that of the untreated water, the calculated  $E$  was 48 %. However, if 0.02 mg/L PASP or PESA alone was added to 50 % Salvetat solution, the retarding time was 5 min and 10 min respectively, the corresponding inhibitory efficiency was 13 % and 36 %.

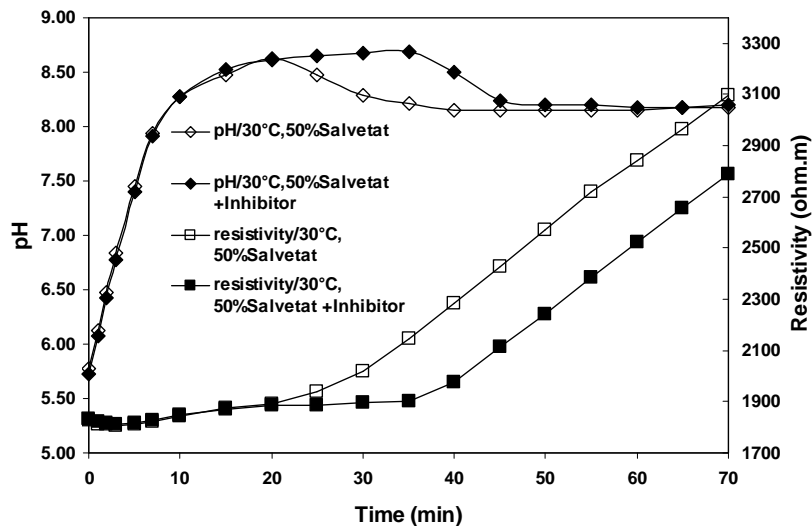


Fig.3.38 The curves of pH and resistivity versus time  
{ Inhibitor = 0.02 mg/L (PASP+PESA) (1:1) }

For the treated water with 0.05 mg/L (PASP+PESA) (1:1), as seen in Fig.3.39, the scaling time was 40 min and the inhibitory efficiency was 64 %. However, if treated with 0.05 mg/L PASP or PESA alone, the scaling time was 30 min and 35 min respectively, the corresponding  $E$  was 44 % and 54 %.

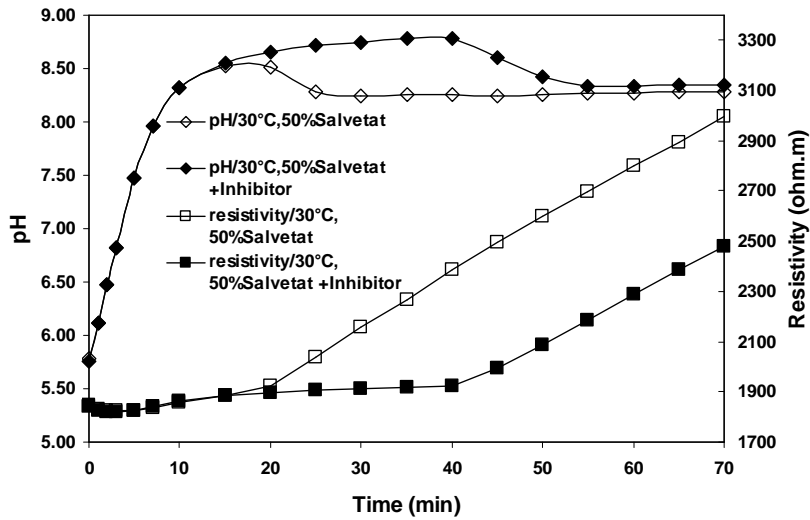


Fig.3.39 The curves of pH and resistivity versus time  
 {Inhibitor = 0.05 mg/L (PASP+PESA) (1:1)}

As shown in Fig.3.40, for the treated water adding 0.1 mg/L (PASP+PESA) (1:1), the retarding time was 25 min and the calculated  $E$  was 83 %. However, if treated with 0.1 mg/L PASP or PESA alone, the retarding time was 15 min and 20 min respectively, the corresponding  $E$  was 58 % and 71 %.

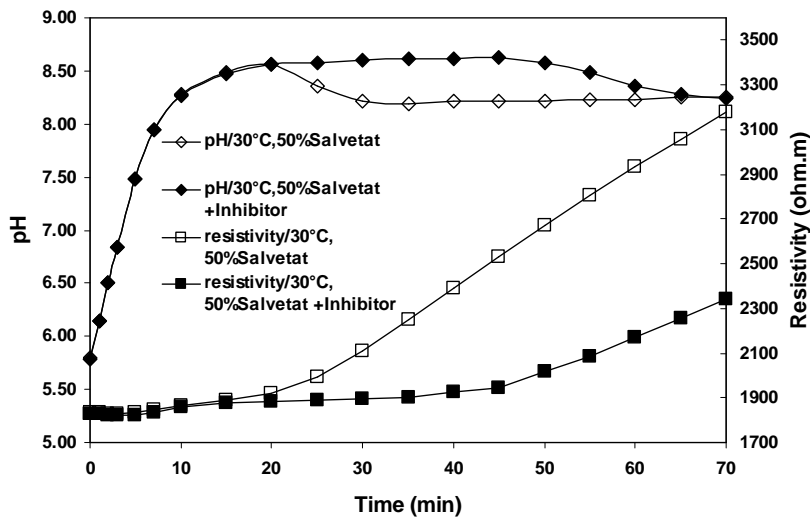


Fig.3.40 The curves of pH and resistivity versus time  
 {Inhibitor = 0.1 mg/L (PASP+PESA) (1:1)}

For the treated water with 0.2 mg/L (PASP+PESA) (1:1), as seen in Fig.3.41, the curve of pH-time and that of resistivity-time extended linearly towards the rights, no precipitate had yet appeared in 70 min, the total efficiency of 100 % was reached. However, if treated with 0.2 mg/L PASP or PESA alone, the scaling time was 40 min and 45 min respectively, the corresponding  $E$  was 80 % and 86 %.

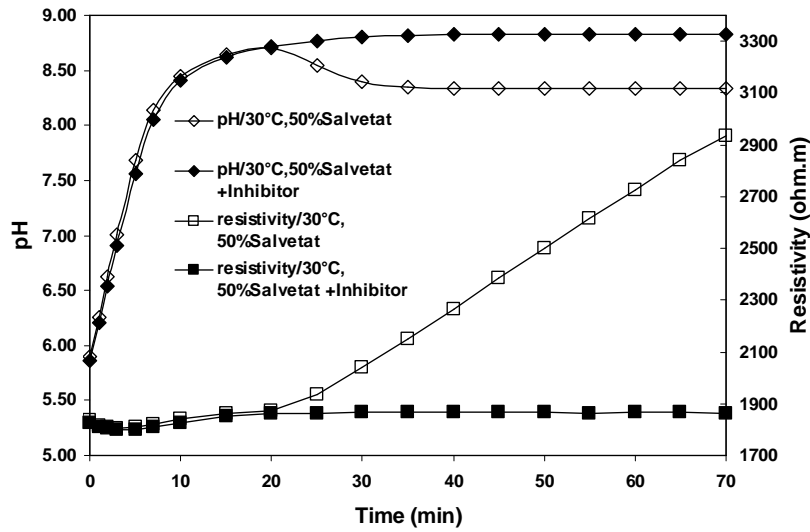


Fig.3.41 The curves of pH and resistivity versus time  
 {Inhibitor = 0.2 mg/L (PASP+PESA) (1:1)}

Table 3.4 Results of RCP tests of inhibitors of different concentration

Inhibitor	Scaling time (min)	Efficiency (%)
None	20	0
0.02 mg/L PASP	25	13
0.05 mg/L PASP	30	44
0.10 mg/L PASP	35	58
0.20 mg/L PASP	40	80
0.02 mg/L PESA	30	36
0.05 mg/L PESA	35	54
0.10 mg/L PESA	40	71
0.20 mg/L PESA	45	86
0.02 mg/L PASP+PESA (1:1)	35	48
0.05 mg/L PASP+PESA (1:1)	40	64
0.10 mg/L PASP+PESA (1:1)	45	83
0.20 mg/L PASP+PESA (1:1)	None	100

Table 3.5 Comparison of the dosage of inhibitors corresponding to Efficiency %

Inhibitor	Concentration/ mg/L	Concentration/ mg/L
	(E = 0%) ≤	(E = 100%) ≥
PASP	0.010	0.30
PESA	0.005	0.25
PASP+PESA (1:1)	0.004	0.20

By comparing the inhibitory efficiency of the same dosage (Table 3.4, Fig.3.37), it could be found that the anti-scaling performance of (PASP+PESA) (1:1) was superior to that of PASP or PESA alone. Moreover, as seen in Table 3.5, the concentration of (PASP+PESA) (1:1) needed to attain the same efficiency was lower than that of PASP or PESA alone.

### 3.2.2.2.2 Effect of $Ca^{2+}$ concentration on inhibition of $CaCO_3$

As seen in Fig.3.42, at the temperature of 30 °C, for 50 % Salvetat solution ( $Ca^{2+}$ : 126.5 mg/L,  $HCO_3^-$ : 410 mg/L), the scaling time of untreated water was 20 min, after introducing 0.2 mg/L (PASP+PESA) (1:1), there was no precipitate appearing in 70 min. But for 75 % Salvetat solution ( $Ca^{2+}$ : 189.75 mg/L,  $HCO_3^-$ : 615 mg/L), the scaling time of untreated and treated water was 15 min and 40 min correspondingly, that is, the retarding time of precipitation by 0.2 mg/L (PASP+PESA) (1:1) was only 25 min. However, if the concentration of (PASP+PESA) (1:1) increased to 0.3 mg/L, the scaling of  $CaCO_3$  could be totally inhibited in 70 min.

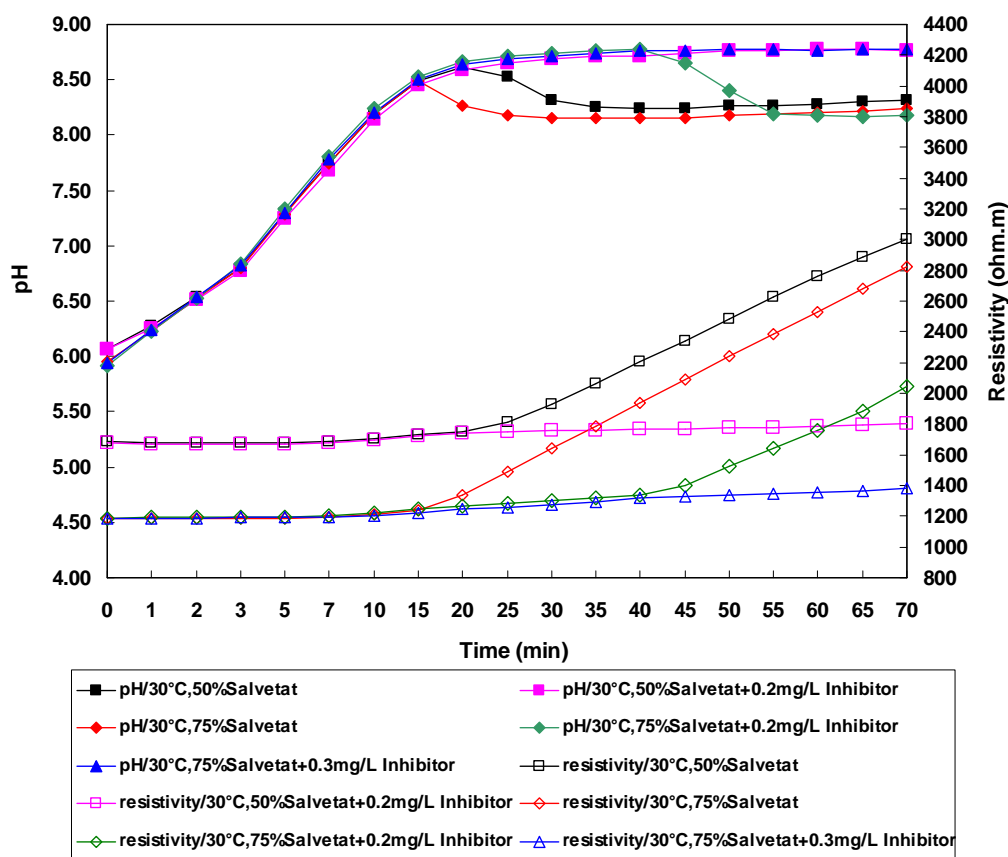


Fig.3.42 Influence of  $Ca^{2+}$  concentration on synergistic inhibition effect of PASP and PESA  
{Inhibitor = (PASP+PESA) (1:1)}

### 3.2.2.2.3 Effect of temperature on inhibition of $CaCO_3$

At the temperature of 30 °C, as seen in Fig.3.43, for the untreated water, the scaling time was 20 min, for the treated water adding 0.2 mg/L (PASP+PESA) (1:1), no precipitate had yet appeared in 70 min. However, when the temperature rose to 40 °C, for

the untreated and treated water, the scaling time was 15 min and 45 min respectively, the precipitation of  $\text{CaCO}_3$  was merely delayed for 30 min by 0.2 mg/L (PASP+PESA) (1:1), only if the concentration of (PASP+PESA) (1:1) reached up to 0.25 mg/L, the inhibitory efficiency of 100 % could be attained in 70 min.

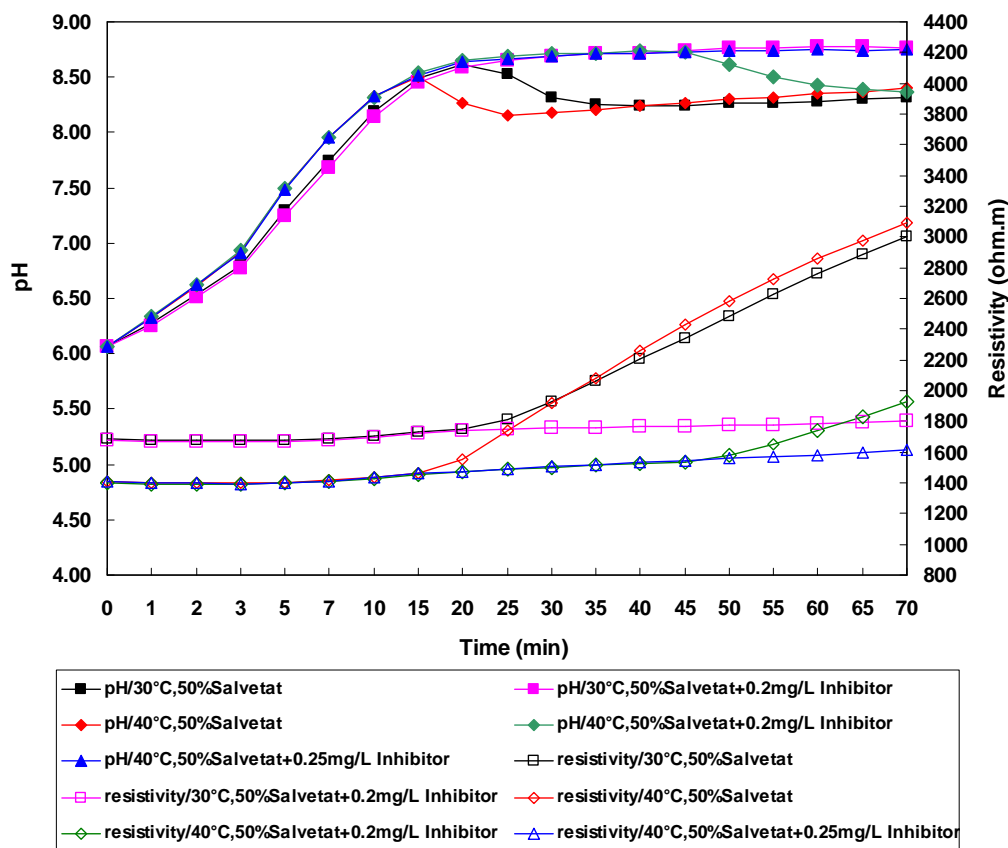


Fig.3.43 Influence of temperature on synergistic inhibition effect of PASP and PESA {Inhibitor = (PASP+PESA) (1:1)}

Figs.3.44 and 3.45 show the scanning electron microscope (SEM) micrographs of  $\text{CaCO}_3$  formed in the Salvetat water at 30 °C. It can be seen that in the presence of (PASP+PESA) (1:1),  $\text{CaCO}_3$  loses its sharp edges, the original regular crystalline structure becomes irregular, and the smooth and compact crystal surface becomes rough and loose. During  $\text{CaCO}_3$  crystal growth, the inhibitor molecules are adsorbed in a different concentration onto the various types of crystal faces, since each type of face has a different surface lattice structure and thus a different distribution of adsorption sites. A different degree of growth retardation for each type of crystal face results in alteration of the crystal shape during outgrowth. The habit-modifying influence of an inhibitor can be so pronounced that one or more crystal faces either appear or disappear with advancing outgrowth of the crystals. The crystal morphology is then changed.

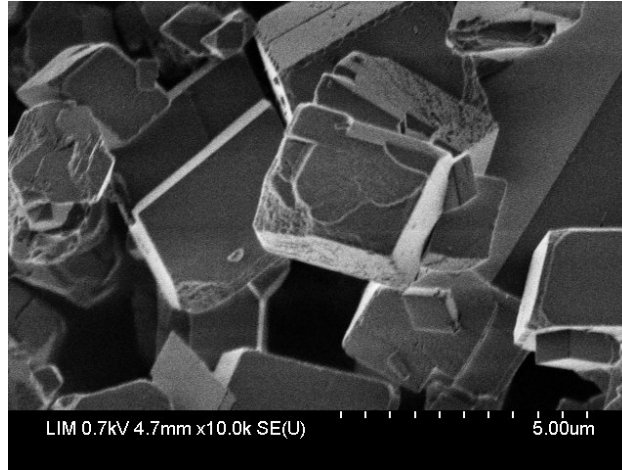


Fig.3.44 SEM micrographs of CaCO<sub>3</sub> formed in the Salvetat water

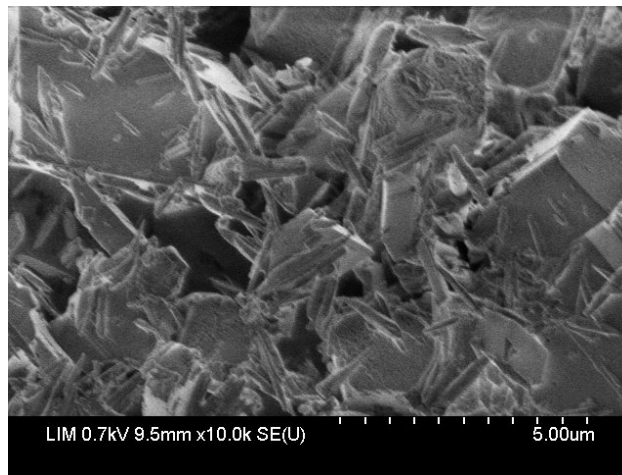


Fig.3.45 SEM micrographs of CaCO<sub>3</sub> formed in the Salvetat water after addition of inhibitor {Inhibitor = 0.1 mg/L (PASP+PESA) (1:1)}

### 3.2.2.3 Evaluation of scale inhibition performance by continuous tests

At the temperature of 40 °C, for 30 % Salvetat solution (Ca<sup>2+</sup>: 75.9 mg/L, HCO<sub>3</sub><sup>-</sup>: 246 mg/L), as shown in Fig.3.46, the ascending part of the curve corresponds to the first seven days (56 h) of tests with untreated water, the weight of scaling on tubes increases with time stably. From the 8<sup>th</sup> day, 0.2 mg/L (PASP+PESA) (1:1) was introduced into the solution, there was no weight change on tubes and the value has a bearing on the curve, that is, the scaling was totally inhibited. After the 13<sup>th</sup> day, no inhibitor was added to the solution, it was found that the increase of weight on tubes was very low for the first 2 days, which indicated that the remanent effect was remarkable. This is due to the fact that some of (PASP+PESA) (1:1) were adsorbed on the wall of the tank and pipes that connected the tubes. The normal increase of weight on tubes was recovered from the 3<sup>rd</sup> day after withdrawal of inhibitor.

When the temperature rose to 50 °C, as seen in Fig.3.47, the total inhibition of scaling was always attained during the treatment phase with 0.2 mg/L (PASP+PESA) (1:1), however, the remanent effect didn't exist any more, which indicated that the

amount of adsorbed inhibitor was insufficient. The results showed that the concentration of (PASP+PESA) (1:1) necessary for complete inhibition is even greater as the temperature rises. This is confirmed by the results shown in Fig.3.48. At the temperature of 60 °C, the weight of scaling on tubes increased slightly for the treated water adding 0.2 mg/L (PASP+PESA) (1:1), which meant that inhibition of scaling was not complete. In other words, for a total inhibition at this temperature, it would either increase the dosage of inhibitor or decrease water flow.

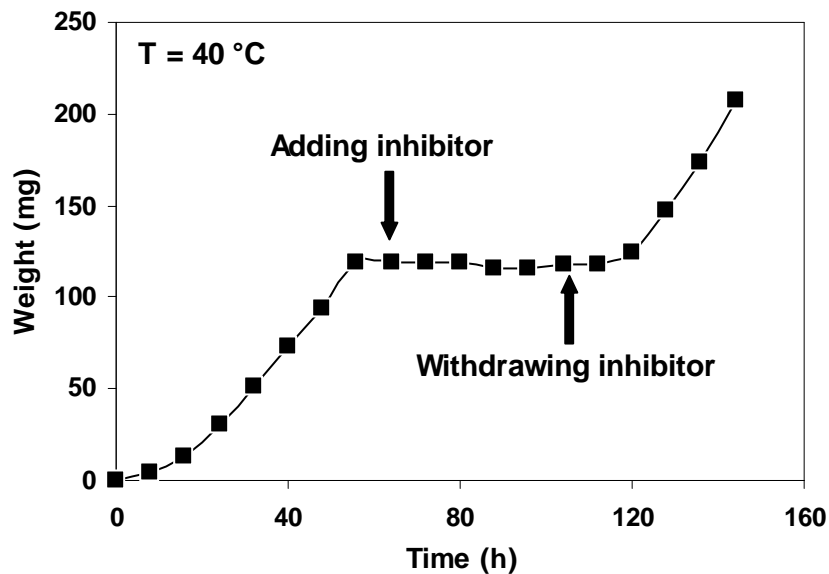


Fig. 3.46 Variation of weight of scaling on the tube wall versus time at 40°C  
{Inhibitor = 0.2 mg/L (PASP+PESA) (1:1)}

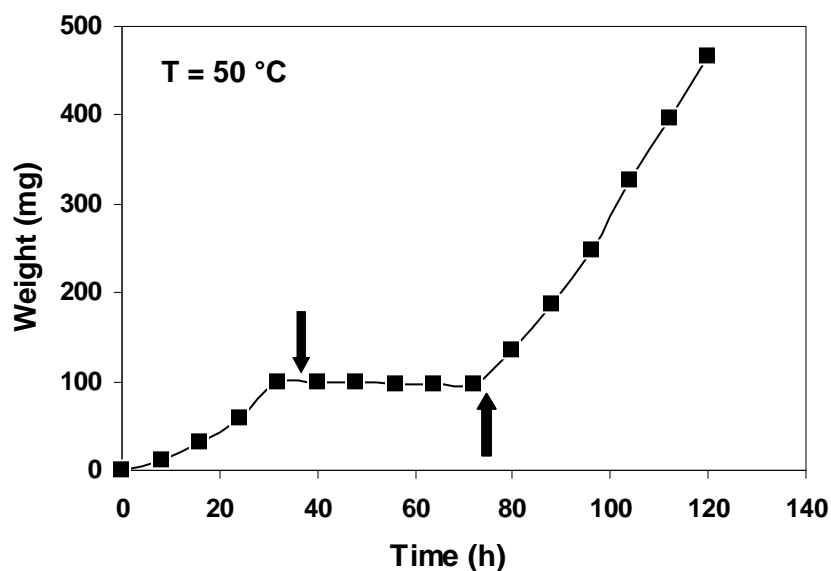


Fig.3.47 Variation of weight of scaling on the tube wall versus time at 50°C  
{Inhibitor = 0.2 mg/L (PASP+PESA) (1:1)}

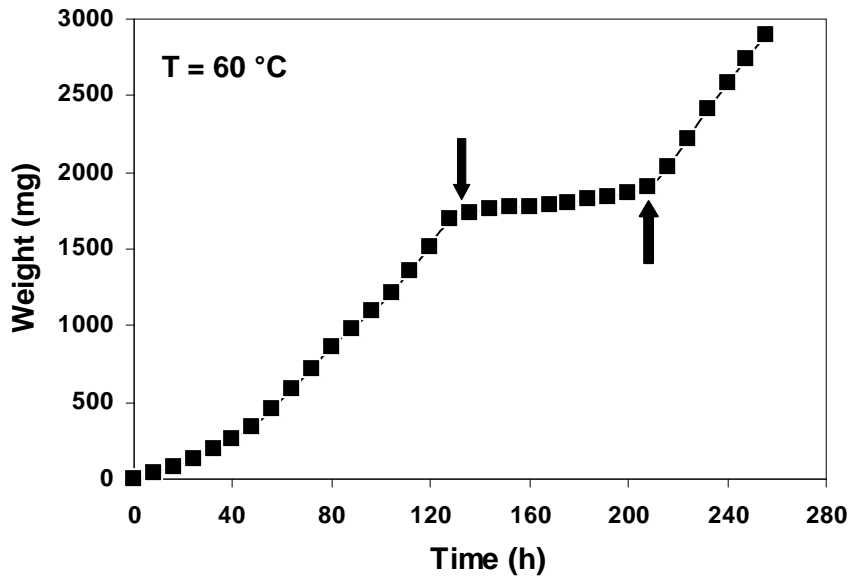


Fig.3.48 Variation of weight of scaling on the tube wall versus time at 60°C  
 {Inhibitor = 0.2 mg/L (PASP+PESA) (1:1)}

The results of SEM (Figs.3.49 and 3.50) show the different crystal habit, that is, the morphology has been modified from the uniform and compact massive forms to the loose petal shaped fragments, which indicated that the inhibitor had participated in the composition of crystal. The change in crystal morphology also showed that the inhibitor made the crystal lattice distort, as a result, the nucleus would not grow any longer, so the scaling was inhibited temporarily.

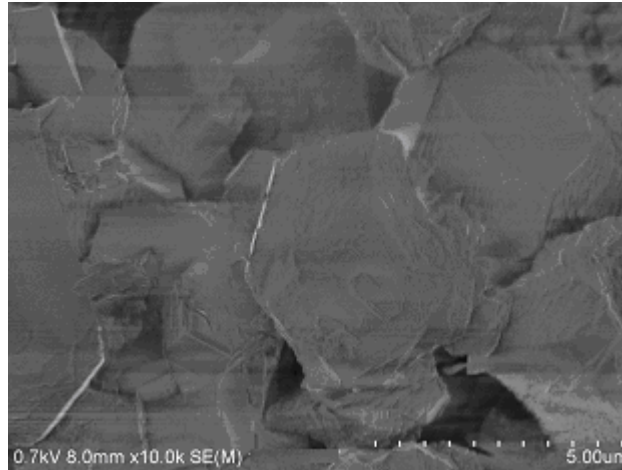


Fig.3.49 The deposit obtained from the tube wall in the Salvetat water at 60°C

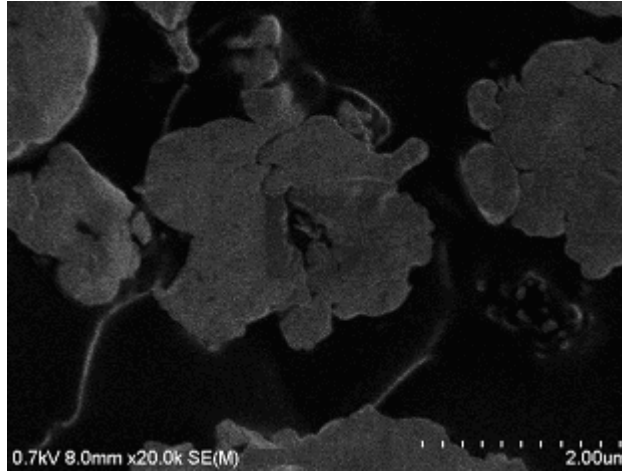


Fig.3.50 The deposit obtained from the tube wall after addition of inhibitor to the Salvetat water at 60°C {Inhibitor = 0.2 mg/L (PASP+PESA) (1:1)}

### 3.3 Summary

(1) When the green scale inhibitors, PASP and PESA, were used alone for the inhibition of  $\text{CaCO}_3$  and  $\text{SrSO}_4$ , the performance of PESA overmatched PASP; on the contrary, PASP was better than PESA in inhibiting the scale of  $\text{CaSO}_4 \cdot 2\text{H}_2\text{O}$  and  $\text{BaSO}_4$ .

RCP tests showed, when the concentrations of PESA and PASP were lower than 0.005 mg/L and 0.01 mg/L respectively, there was hardly any inhibition effect on scaling of  $\text{CaCO}_3$ . But when their dosage increased above 0.25 mg/L and 0.3 mg/L, total inhibition was reached within 60 min. PESA was remarkably better performed than PASP in inhibiting  $\text{CaCO}_3$  at a low level, but with the increase of dosage, the gap between the two became gradually narrow. Compared to PASP, PESA can attain better effect at a lower dosage; with the rise in  $\text{Ca}^{2+}$  concentration or temperature, the inhibition effect of PESA or PASP got worse at the former dosage. The inhibitor could distort the crystal lattice, destroy the compact and regular crystal structure into a loose and rough one, and thus retard the formation of precipitate. This was confirmed by studying the crystal habit of  $\text{CaCO}_3$  and  $\text{CaSO}_4$  in the absence or presence of PESA or PASP, through SEM and XRD analyses.

(2) The synergistic effect of PASP and PESA on inhibition of scaling has been studied using both static and dynamic methods. It is found that PASP combined with PESA has better anti-scaling effect than PASP or PESA alone on inhibition of  $\text{CaCO}_3$ ,  $\text{CaSO}_4 \cdot 2\text{H}_2\text{O}$  and  $\text{BaSO}_4$ , and the optimal mass ratio of PASP and PESA is 1:1 for inhibition of  $\text{CaCO}_3$  in the static tests.

The results of RCP tests showed that with the rise in dosage of (PASP+PESA) (1:1), the inhibitory efficiency of  $\text{CaCO}_3$  increased; the total efficiency of 100 % was reached when the concentration of (PASP+PESA) (1:1) was 0.2 mg/L for 50 % Salvetat solution at 30 °C; the anti-scaling performance of (PASP+PESA) (1:1) was superior to that of PASP or PESA alone, and the concentration of (PASP+PESA) (1:1) needed to attain the same efficiency was lower than that of PASP or PESA alone; as the concentration of  $\text{Ca}^{2+}$  or temperature rose, the minimum dosage of (PASP+PESA) (1:1) for achieving total

inhibition of scaling should be increased.

The results of continuous tests presented that the scaling on tubes was totally inhibited for 30 % Salvetat solution adding 0.2 mg/L (PASP+PESA) (1:1) at 40 °C, and the remanent effect was remarkable after withdrawal of inhibitor. However, with the rise in temperature, the remanent effect would disappear gradually, even the inhibition of scaling was not complete for the same dosage of inhibitor. Therefore, if (PASP+PESA) (1:1) as a synergistic scale inhibitor will be applied in a real scaling procedure, appropriate concentration of inhibitor should be considered according to the temperature in hot water circuits. Moreover, the analysis of SEM showed that (PASP+PESA) (1:1) could affect the calcium carbonate germination and change the crystal morphology, which indicated that the inhibitor had participated in the composition of crystal.

## **Chapter 4. Effects of Copper and Zinc Ion in Preventing Scaling of Drinking Water**

To prevent or inhibit the formation of scaling of water, various ways were tried and many kinds of inhibitors were widely used, which increased some economic returns in a way. However, these inhibitors were mostly organic complexes, so using them extensively would produce masses of sediments and thus cause some secondary pollution for water environment. Therefore, finding some economical and environmentally friendly inhibitors is one of the major research focuses nowadays.

The inhibiting effectiveness of metal ion in the water was shown by some literatures. Using the expensive experimental set-up and the complicated experimental procedure, the inhibition effectiveness of the scaling has been researched with metal ion in a high hardness or synthetic water in those literatures. Then, according to the last results, they have investigated the inhibition mechanism, which was successful for industrial water. However, it was not certain for drinking water as no literatures were recorded.

So the present chapter, using economical experimental set-up and simple experimental procedure, would investigate the inhibition effectiveness of copper ion and zinc ion for scaling in drinking water and give the quantitative relationship between the concentration of drinking water and that of copper and zinc ions, afterwards, according to the last results, it also would discuss the inhibition mechanism.

### **4.1 Experimental**

#### **4.1.1 Materials**

##### **4.1.1.1 Reagents**

All the chemicals were analytical pure, such as  $\text{CuCl}_2 \cdot 2\text{H}_2\text{O}$  and  $\text{Zn}(\text{NO}_3)_2 \cdot 6\text{H}_2\text{O}$  etc., and all the stocked solutions were prepared by dissolving the weighed trace amount of the respective salt into deionized water.

##### **4.1.1.2 Water studied**

Salvetat, whose characteristics are shown in Section 3.1.1.3.

#### **4.1.2 Method**

The principle, device, and procedure of RCP method are shown in Section 3.1.2.2.

### **4.2 Results and discussion**

#### **4.2.1 Anti-scaling Tests of Zinc Ions of Different Concentrations**

After the zinc ions of different concentrations (0.025; 0.05; 0.1; 0.2; 0.3; 0.4 mg/L) had been introduced into 300 mL Salvetat solutions where the concentration of calcium

ion was 126.5 mg/L, the results showed that with the increase in concentration, the calculated efficiency,  $E$  increased (Fig.4.1), the retarding pH-time curve of the treated water slowly became a line and, correspondingly, the slope of the resistivity-time curve became smaller (Figs. 4.2, 4.3 and 4.4).

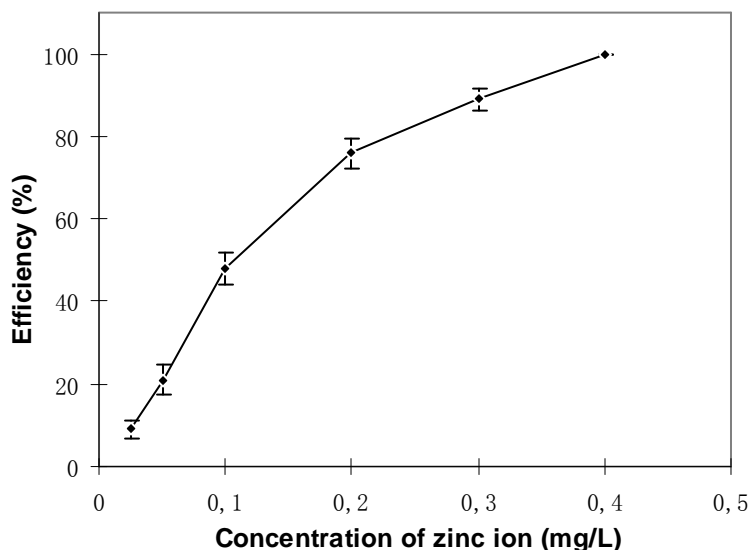


Fig.4.1 Variation of efficiency of inhibition versus concentration of zinc ion ( $t = 70$  min)

As shown in Fig.4.1, the efficiency of inhibition attained 100% in 70 min for the zinc ion concentration greater than 0.4 mg/L, however, when the concentration of zinc ion was below 0.025 mg/L, it hardly had any effect on the inhibition of scaling.

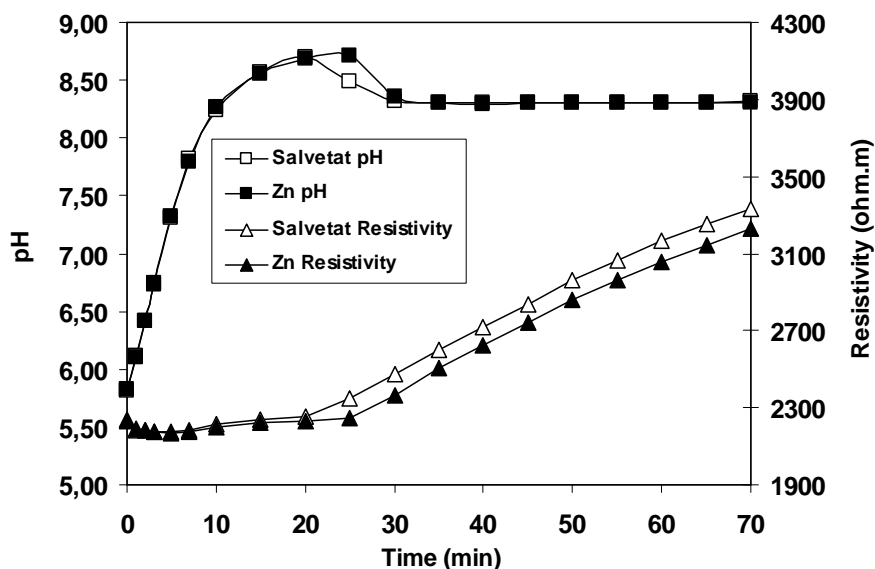


Fig.4.2 The curves of the pH and resistivity with time in the 0.05 mg/L zinc ion solution

As seen in Fig.4.2, for the untreated water, the scaling time was 20 min, after

introducing 0.05 mg/L zinc ion, the retarding time was only 5min, it had weak inhibitory effect on the scaling and its inhibition effectiveness was poor.

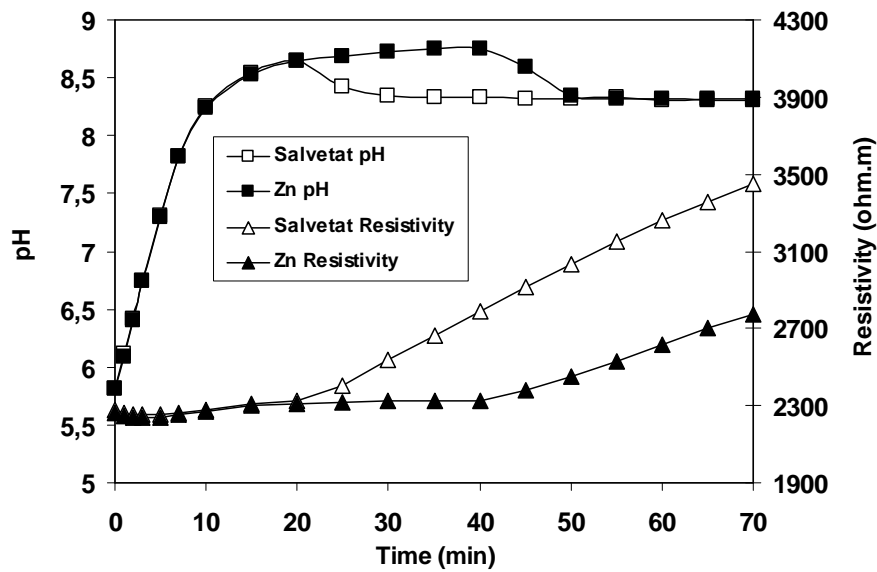


Fig.4.3 The curves of the pH and resistivity with time in the 0.2 mg/L zinc ion solution

As seen in Fig.4.3, for the treated water, the pH began to fall 20 min later that of the untreated water, and the rate of precipitation, indicated by the slope of the resistivity curve, was considerably reduced, which showed that with the increase in the concentration of zinc ion, its ability to inhibit the scaling of  $\text{CaCO}_3$  enhanced obviously.

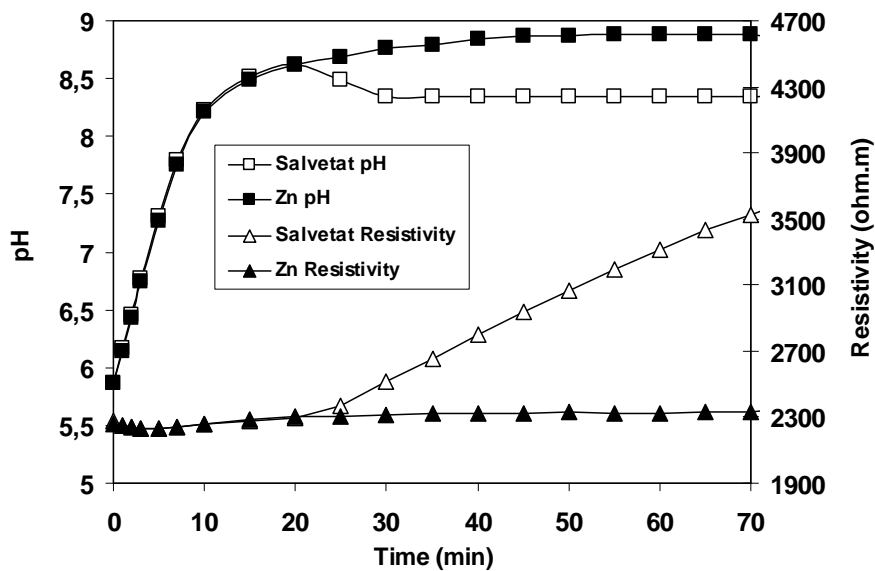


Fig.4.4 The curves of the pH and resistivity with time in the 0.4 mg/L zinc ion solution

As seen in Fig.4.4, for the untreated water, the scaling time was 20 min, but for the treated water, the curve of pH-time and that of resistivity-time extended linearly towards

the rights, any precipitate hadn't yet appeared in 70 min, which showed total inhibition effectiveness of scaling.

By the above tests of zinc ions of different concentrations, the results listed in Table 4.1 indicated that the greater the increase in concentration of zinc ion, the longer the scaling time lasted, the better its inhibition effectiveness.

Table 4.1 The results of anti-scaling tests of zinc ions of different concentrations (t = 70 min)

Concentration of Zn <sup>2+</sup> (mg/L)	Scaling time of untreated water (min)	Scaling time of treated water (min)	Efficiency (%)
0.025	20	20	9±2.0
0.05	20	25	21±3.7
0.10	20	30	48±4.0
0.20	20	40	76±3.6
0.30	20	50	89±2.6
0.40	20	70	100

#### 4.2.2 Anti-scaling Tests of Copper Ions of Different Concentrations

For the copper ions of different concentrations (0.05; 0.3; 0.5; 0.7; 0.9 mg/L) introduced into 300 mL Salvetat solutions where the concentration of calcium ion was 126.5 mg/L, their inhibition effectiveness of scaling can be seen in Figs.4.5, 4.6, 4.7 and 4.8.

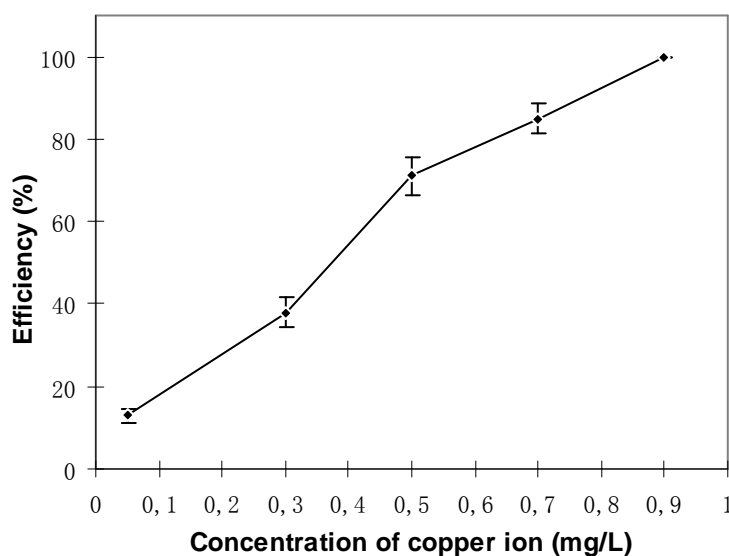


Fig.4.5 Variation of efficiency of inhibition versus concentration of copper ion (t = 70 min)

As shown in Fig.4.5, when the concentration of copper ion was lower than 0.05 mg/L, it hardly had any effect on the scaling and its inhibition effectiveness was poor. But when the copper ion concentration was above 0.9 mg/L, it showed total inhibition effectiveness in 70 min.

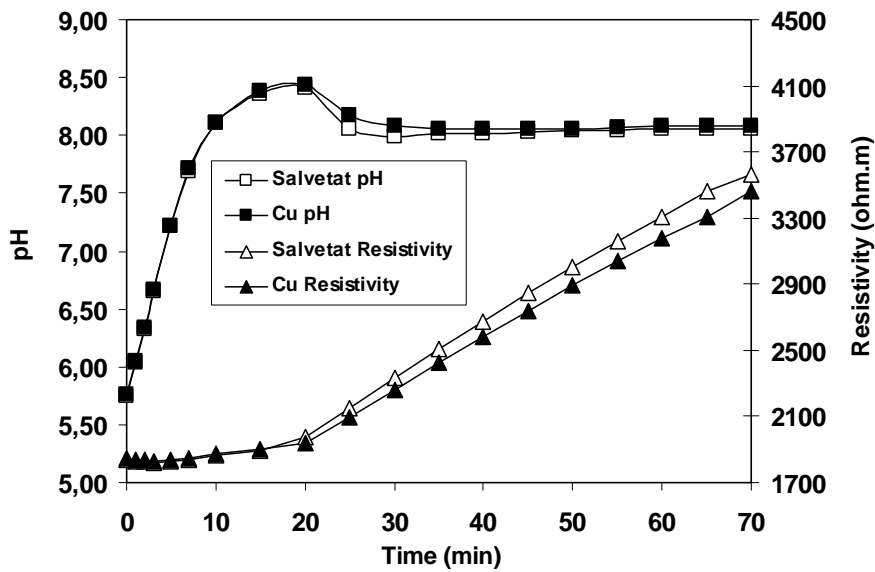


Fig.4.6 The curves of the pH and resistivity with time in the 0.05 mg/L copper ion solution

As seen in Fig.4.6, the pH-time curve of treated water and that of untreated water began to overlap, the scaling times were both 20min, which showed that 0.05 mg/L copper ion had little effect on the inhibition of scaling.

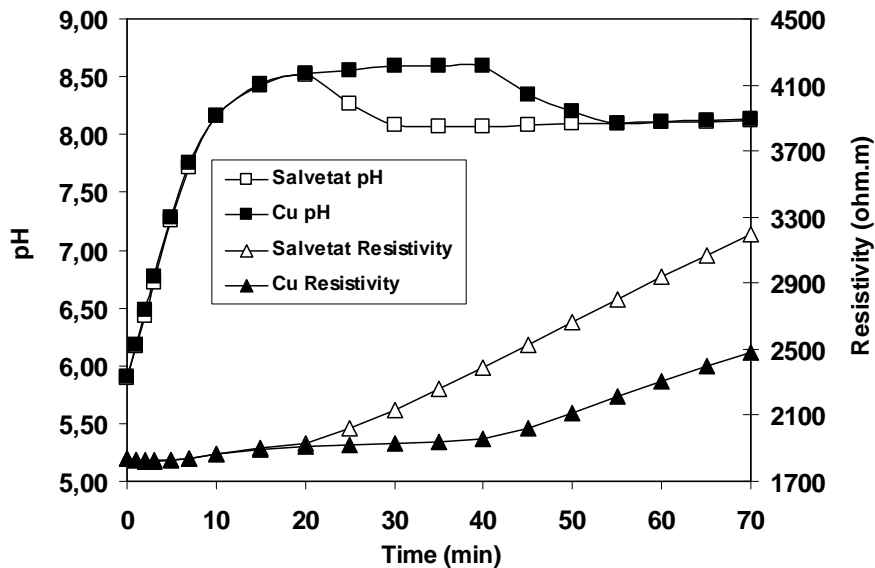


Fig.4.7 The curves of the pH and resistivity with time in the 0.5 mg/L copper ion solution

As seen in Fig.4.7, for the untreated and treated water, the scaling time was respectively 20 min and 40 min, which showed that 0.5 mg/L copper ion could significantly retard the precipitation of  $\text{CaCO}_3$ .

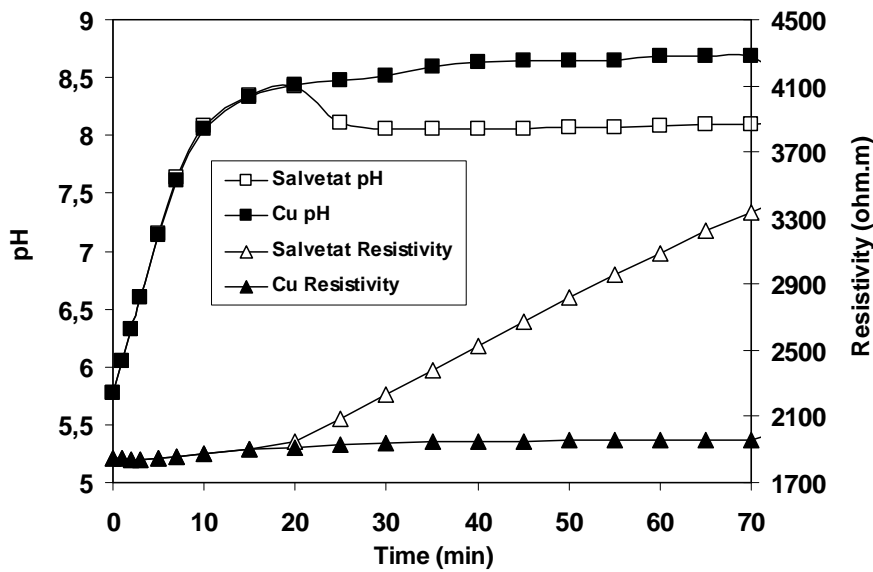


Fig.4.8 The curves of the pH and resistivity with time in the 0.9 mg/L copper ion solution

As seen in Fig.4.8, for the treated water with 0.9 mg/L copper ion, any precipitate hadn't yet appeared in 70 min, the total inhibition effectiveness of scaling was reached.

The results of the above tests of copper ions of different concentrations were listed in Table 4.2, which indicated that with the increase in concentration of copper ion, the kinetics of CaCO<sub>3</sub> precipitation was slowed greatly.

Table 4.2 The results of anti-scaling tests of copper ions of different concentrations (t = 70 min)

Concentration of Cu <sup>2+</sup> (mg/L)	Scaling time of untreated water (min)	Scaling time of treated water (min)	Efficiency (%)
0.05	20	20	13±1.7
0.30	20	30	38±3.5
0.50	20	40	71±4.4
0.70	20	50	85±3.6
0.90	20	70	100

#### 4.2.3 Comparison Between Inhibition Effectiveness of Zinc Ion and that of Copper Ion

By comparing the inhibition effectiveness of zinc ion and copper ion in the 300 mL Salvetat solution where the calcium ion concentration was 126.5 mg/L (Figs. 4.9 and 4.10), it could be found that zinc ion and copper ion showed different inhibitory strength on the scaling of CaCO<sub>3</sub>. For the zinc ions of different concentrations, their difference in inhibitory strength was relatively obvious, and the total efficiency of 100% had already reached for the zinc ion concentration of 0.4 mg/L; however, 0.9 mg/L copper ion was needed to totally inhibit the precipitation in 70 min (Table 4.3), and with the increase in

concentrations of copper ions, their inhibitory capacity displayed a slow growth rate, which indicated that the anti-scaling performance of zinc ions was superior to that of copper ions.

As seen in Table 4.3, the concentration of zinc ions needed to attain the same efficiency was lower than that of copper ions.

Table 4.3 The corresponding concentrations of ions for the efficiency of 0% and 100% (t = 70 min)

Ion	Concentration/ mg/L	Concentration/ mg/L
	(E = 0%) ≤	(E = 100%) ≥
Zn <sup>2+</sup>	0.025	0.40
Cu <sup>2+</sup>	0.05	0.90

As seen in Fig.4.9, the inhibitory efficiency of zinc ion was higher than that of copper ion when their concentrations were both 0.05 mg/L, for the untreated water and the treated water with copper ion, the scaling times were both 20 min, but for the treated water with zinc ion, the scaling time was 25 min.

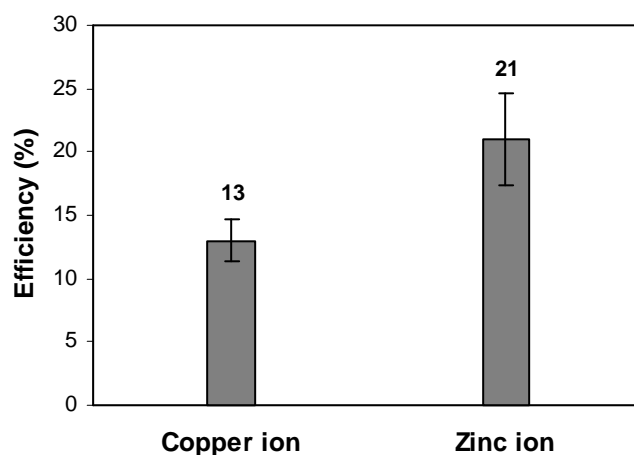


Fig.4.9 The corresponding efficiency for the ions concentration of 0.05 mg/L (t = 70 min)

As seen in Fig.4.10, the inhibitory efficiency of zinc ion was much higher than that of copper ion when their concentrations were both 0.3 mg/L, for the untreated water and the treated water with copper ion, the scaling time was respectively 20 min and 30 min, but any precipitate didn't appear until 50 min for the treated water with zinc ion.

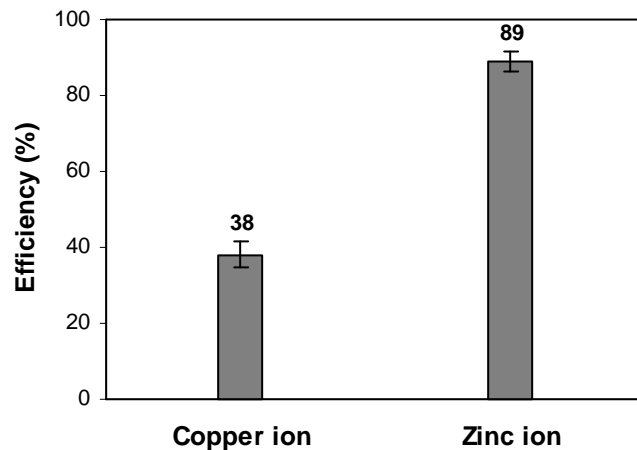


Fig.4.10 The corresponding efficiency for the ions concentration of 0.3 mg/L (t = 70 min)

#### 4.2.4 Inhibition Mechanism of Scaling by Copper and Zinc Ions

While the inhibiting effect of copper and zinc ions on scaling is undeniable, it is necessary to determine the mechanism whereby copper and zinc ions affect the calcium carbonate nucleation and growth process [71-77].

In fact, in the course of the formation of calcium carbonate germination, copper and zinc ions directly took part in the chemical reaction.  $\text{Cu}^{2+}$  and  $\text{Zn}^{2+}$  ions could associate with  $\text{Ca}^{2+}$  ions to form a mixed carbonate of the type  $\text{Cu}_x\text{Ca}_{1-x}\text{CO}_3$  or  $\text{Zn}_x\text{Ca}_{1-x}\text{CO}_3$ . The analysis with infrared absorption spectrometry (IR) of the obtained precipitate from the Salvetat solution introduced with copper and zinc ions are given in Figs.4.11 and 4.12, which showed that the white material mainly consisted of the calcium carbonate, however, no peaks showed the existence of copper or zinc ion in the precipitate. The results of scanning electron microscope (SEM) analysis of the white precipitate (Figs. 4.13, 4.14 and 4.15) showed the different crystal morphologies, which indicated that copper and zinc ions had participated in the composition of crystal, however, the quantity of copper or zinc ion was so small that it was difficult to observe them. The change in crystal morphology also showed that copper and zinc ions made the crystal lattice distort, as a result, the nucleus would not grow any longer, so the scaling was inhibited temporarily.

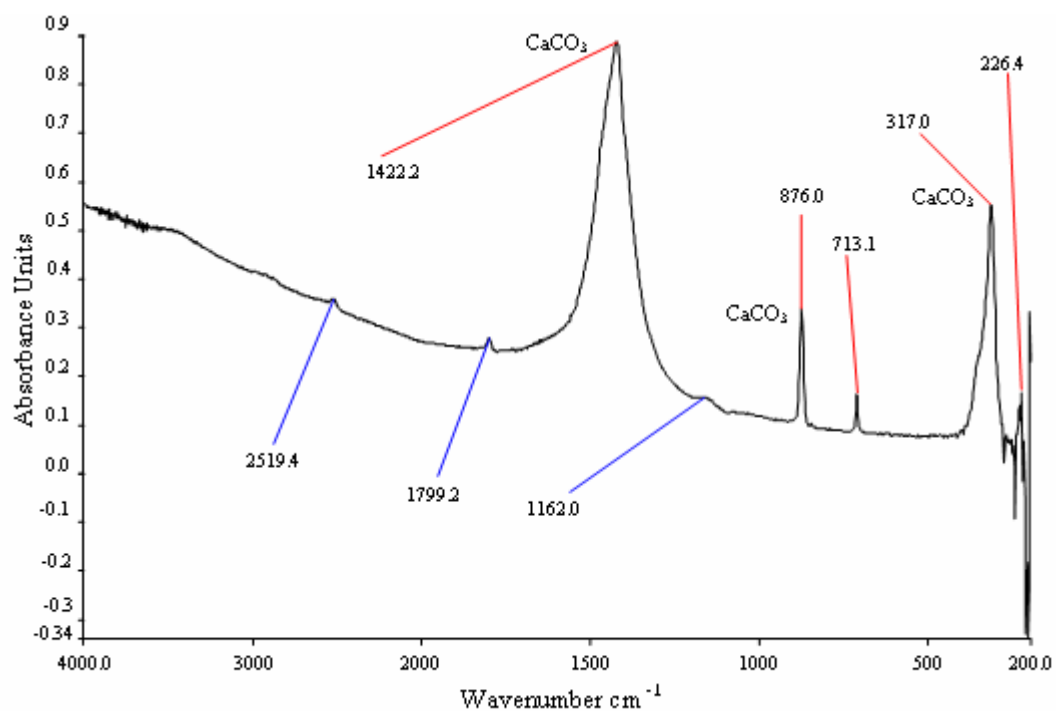


Fig.4.11 IR analysis of the precipitate obtained from the Salvetat solution of copper ion

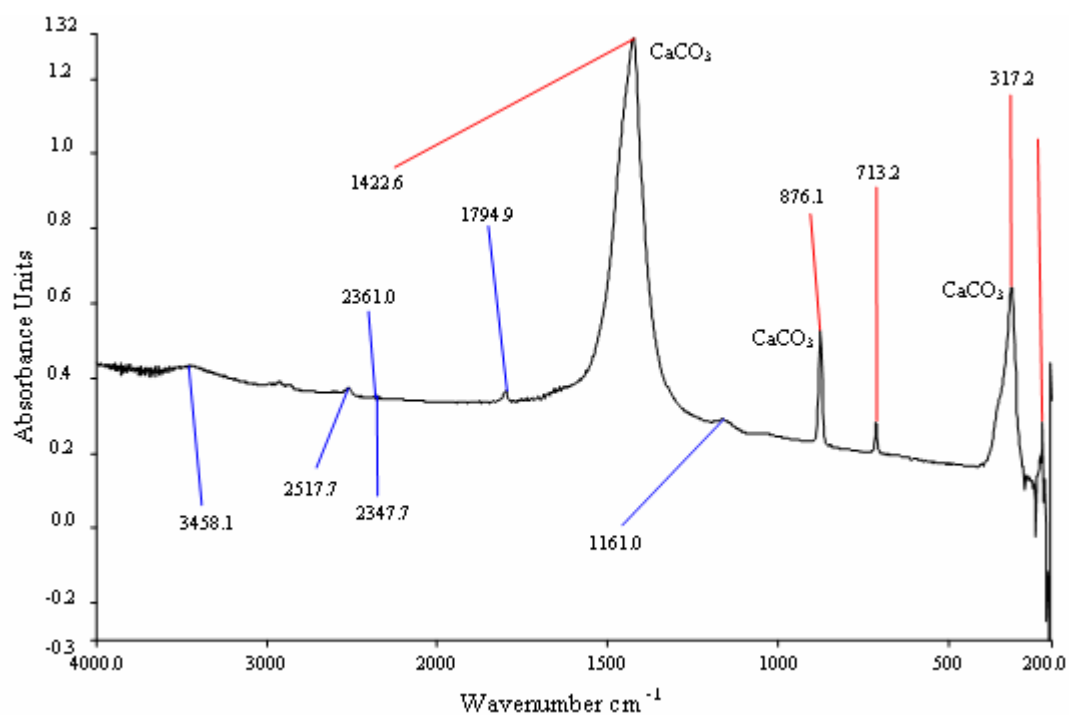


Fig.4.12 IR analysis of the precipitate obtained from the Salvetat solution of zinc ion

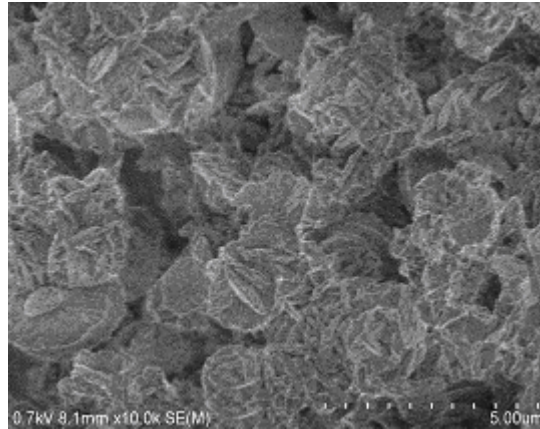


Fig.4.13 SEM analysis of the precipitate obtained from the Salvetat solution

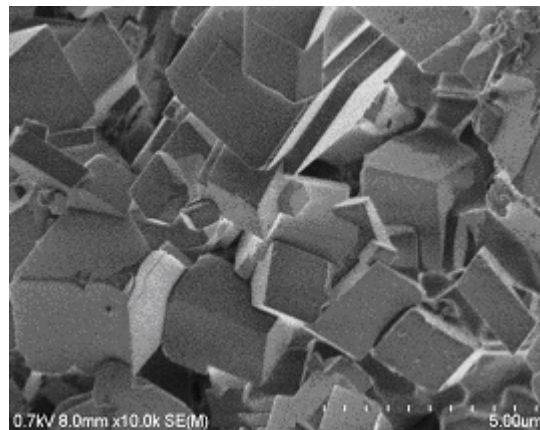


Fig.4.14 SEM analysis of the precipitate obtained from the Salvetat solution of copper ion

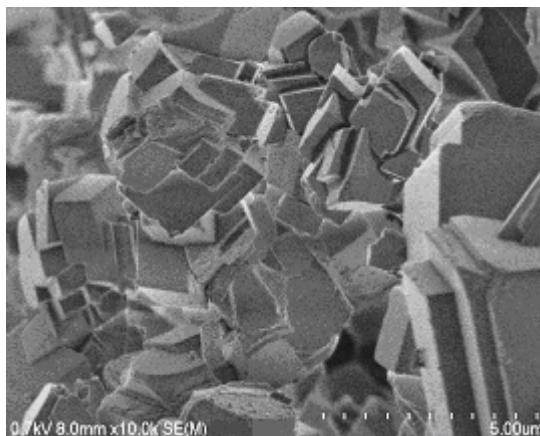


Fig.4.15 SEM analysis of the precipitate obtained from the Salvetat solution of zinc ion

#### **4.2.5 Effects of temperature and dissolved CO<sub>2</sub> on the scaling of water in the presence of copper and zinc**

In order to provide better guidance for their practical use in inhibiting scaling in mineral water, it is necessary to study how various factors affect the performance of zinc

and copper ions as inhibitors.

In RCP, temperature and dissolved CO<sub>2</sub> are two key factors; by modifying the parameters of temperature and dissolved CO<sub>2</sub> concentration, the scaling of water can be accelerated and CaCO<sub>3</sub> precipitates can be observed in a reasonable period of time.

#### 4.2.5.1 Tests on scaling capacity of Salvetat water

##### 4.2.5.1.1 The influence of temperature

For 50 % Salvetat water of different temperatures, as shown in Fig.4.16, at T= 20; 25; 30; 35; 40; 45 °C, the precipitates appeared at 40; 25; 20; 15; 15; 10 min correspondingly. As the temperature rose, 1) the initial pH of Salvetat water increased while the initial resistivity decreased; 2) both the maximum pH and its corresponding resistivity decreased; 3) the scaling time greatly decreased (comparing to 35 °C, pH fell more sharply at 40 °C); 4) the rate of precipitation, indicated by the slope of the resistivity curve, considerably increased.

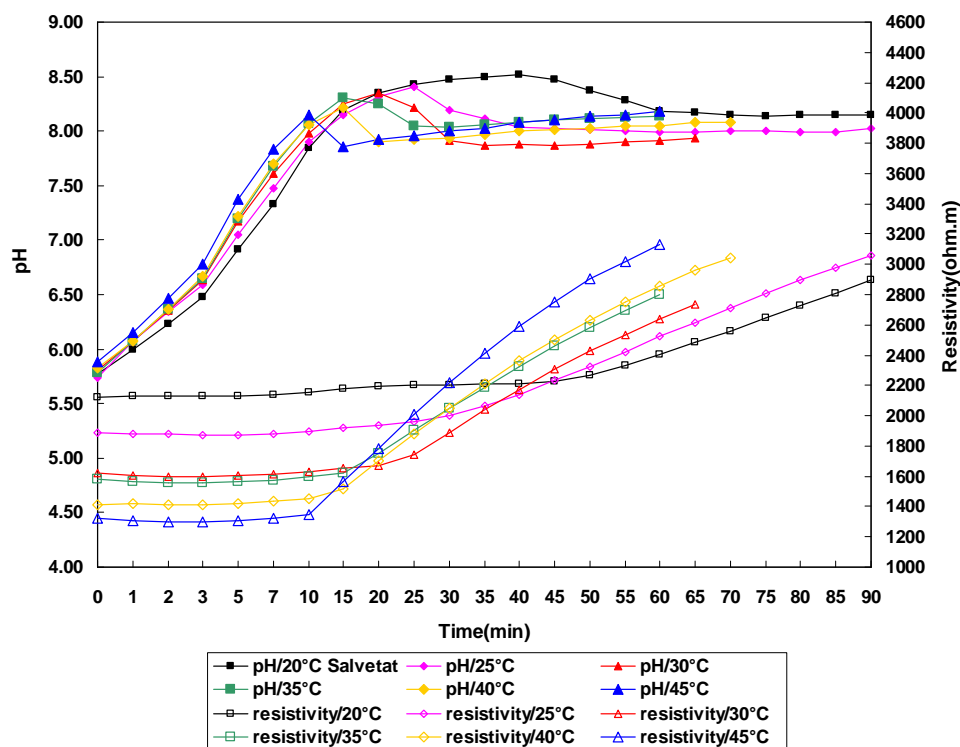


Fig.4.16 Effect of temperature on the scaling of Salvetat water

##### 4.2.5.1.2 The influence of dissolved CO<sub>2</sub>

Salvetat water of different volume percents was chosen for the factor of dissolved CO<sub>2</sub>. At T= 30 °C, as seen in Fig.4.17, for 25 % Salvetat water, no precipitate appeared in 90 min. However, for 30; 40; 50; 75; 100 % Salvetat water, the precipitation started at 70; 30; 20; 15; 10 min respectively. The results indicated that with the rise in concentration of dissolved CO<sub>2</sub>, the scaling time of Salvetat water greatly decreased and the rate of precipitation obviously increased.

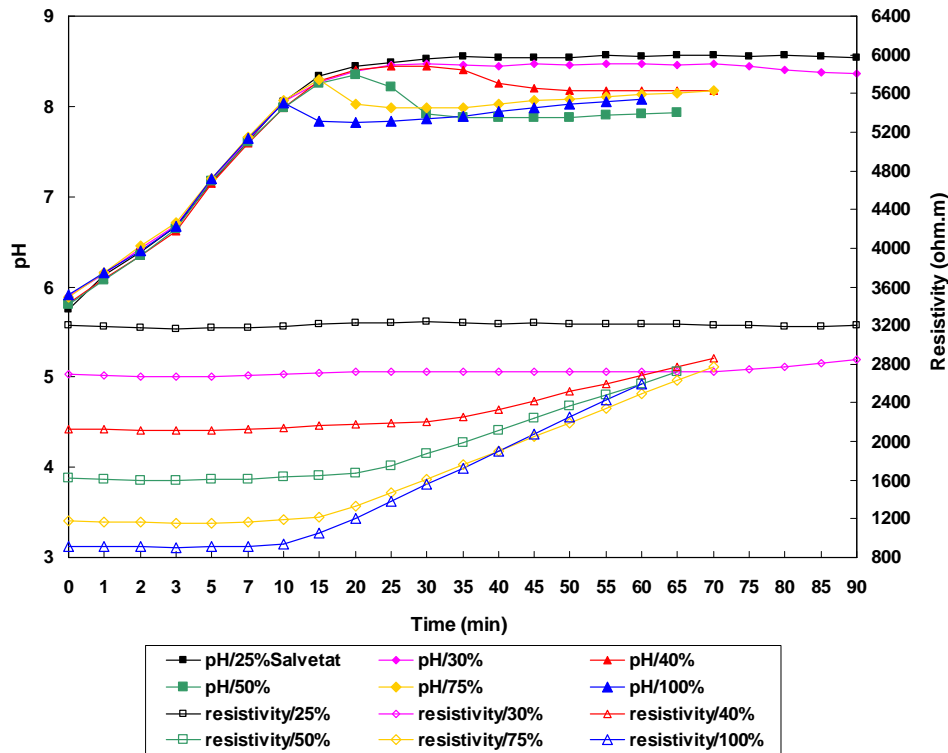


Fig.4.17 Effect of dissolved CO<sub>2</sub> concentration on the scaling of Salvetat water

## 4.2.5.2 Inhibition of scaling in the presence of copper

### 4.2.5.2.1 The influence of temperature

For 50 % Salvetat water, at different temperatures, the minimum concentration of copper ion required to achieve total inhibition of CaCO<sub>3</sub> scaling is shown in Fig.4.18. In order for the inhibition of scaling to attain an efficiency of 100 % for 70 min, the dosage of copper needed to be increased as the temperature rose. For example, as seen in Fig.4.19, at T= 30 °C, for the untreated water, the scaling time was 20 min; for the treated water adding 0.9 mg/L copper, no precipitate had yet appeared in 70 min. However, when the temperature rose to 40 °C, for the untreated and treated water, the scaling time was 15 min and 45 min respectively, that is, the precipitation of CaCO<sub>3</sub> was merely delayed for 30 min by 0.9 mg/L copper; only when the concentration of copper was higher than 1.2 mg/L, could the scaling be totally inhibited for 70 min.

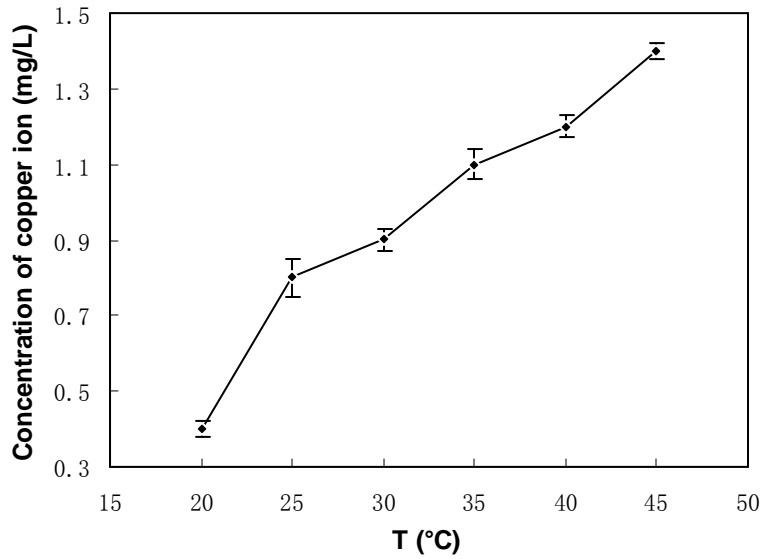


Fig.4.18 Influence of temperature on the dosage of copper ion

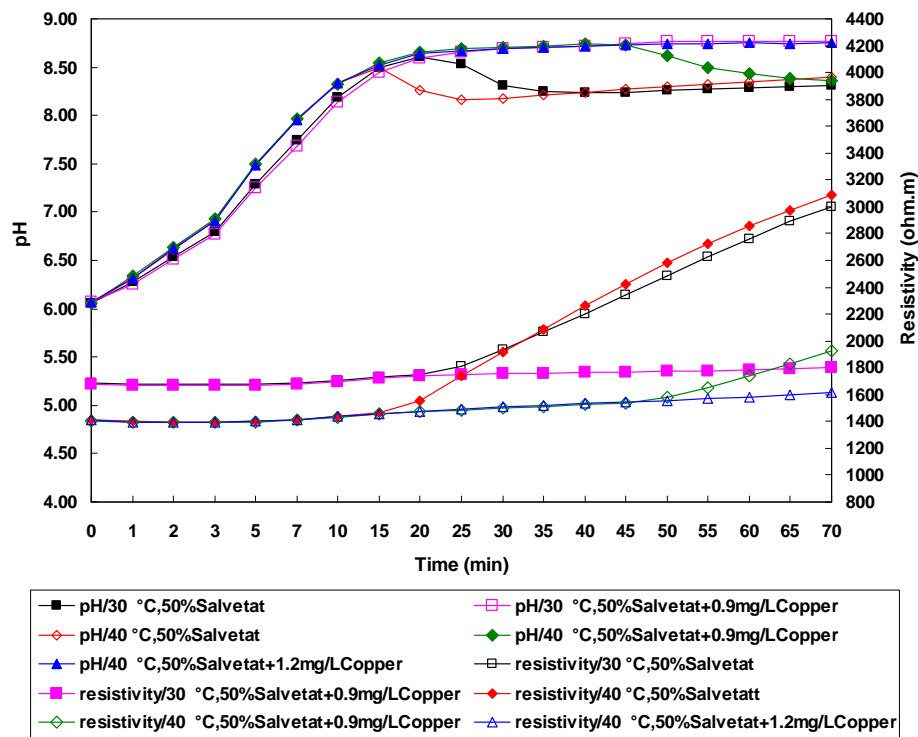


Fig.4.19 Effect of temperature on the scaling of Salvetat water in the presence of copper ion

#### 4.2.5.2.2 The influence of dissolved CO<sub>2</sub>

At T= 30 °C, for Salvetat water of different volume percents, the lowest concentration of copper needed to totally inhibit the precipitation of CaCO<sub>3</sub> is shown in Fig.4.20. The results indicated that the higher the concentration of dissolved CO<sub>2</sub>, the greater the minimum dosage of copper required to attain an inhibitory effectiveness of 100 % in 70 min. For instance, as seen in Fig.4.21, at T= 30 °C, for 50 % Salvetat water,

the scaling time of untreated water was 20 min, after introducing 0.9 mg/L copper, no precipitate appeared in 70 min. But for 75 % Salvetat water, the scaling time of untreated and treated water was 15 min and 40 min respectively, that is, precipitation was merely delayed for 25 min by 0.9 mg/L copper. However, if the copper concentration increased to 1.4 mg/L, the scaling could be totally inhibited for 70 min.

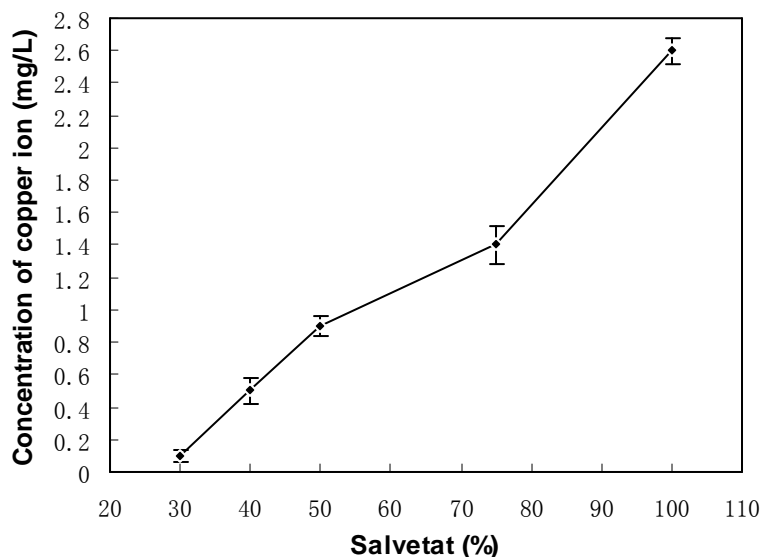


Fig.4.20 Influence of dissolved CO<sub>2</sub> concentration on the dosage of copper ion

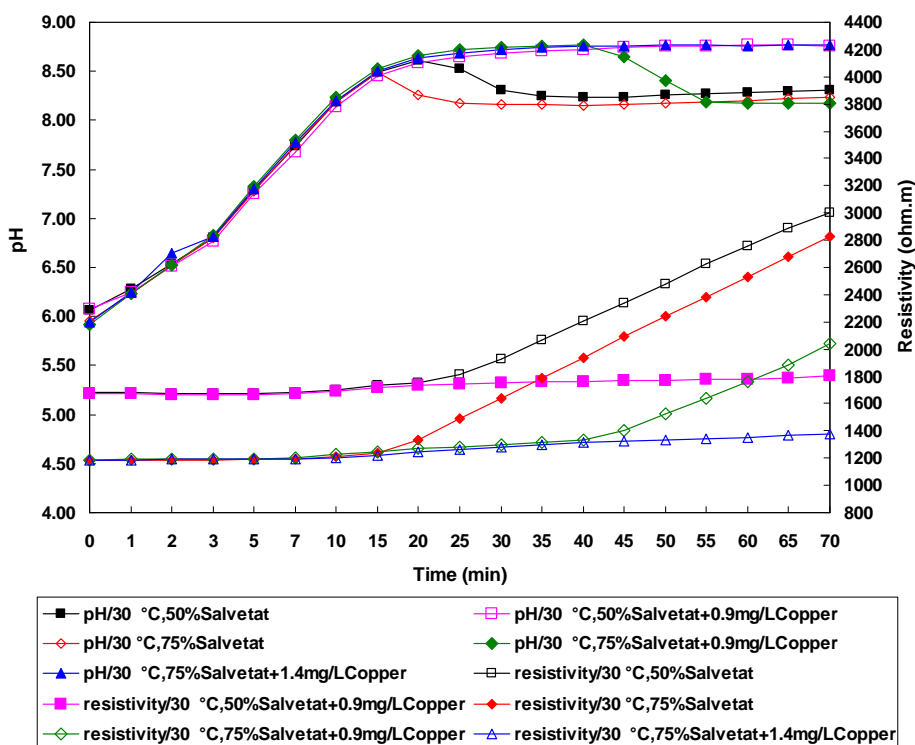


Fig.4.21 Effect of dissolved CO<sub>2</sub> on the scaling of Salvetat water in the presence of copper ion

### 4.2.5.3 Inhibition of scaling in the presence of zinc

#### 4.2.5.3.1 The influence of temperature

As shown in Fig.4.22, for 50 % Salvetat water, the minimum concentration of zinc ion for achieving total inhibition of  $\text{CaCO}_3$  scaling increased as the temperature rose. For example, as seen in Fig.4.23, at  $T= 30\text{ }^\circ\text{C}$ , in 70 min no precipitation occurred in the treated water with 0.4 mg/L zinc. However, if the temperature rose to  $40\text{ }^\circ\text{C}$ , 0.4 mg/L zinc could only delay the precipitation of  $\text{CaCO}_3$  for 35 min, but when the zinc concentration was up to 0.45 mg/L, the efficiency of inhibition attained 100% for 70 min.

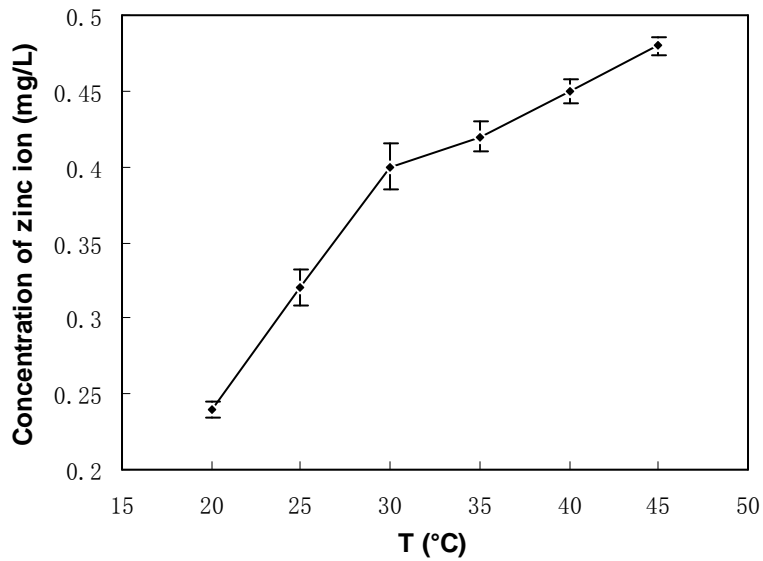


Fig.4.22 Influence of temperature on the dosage of zinc ion

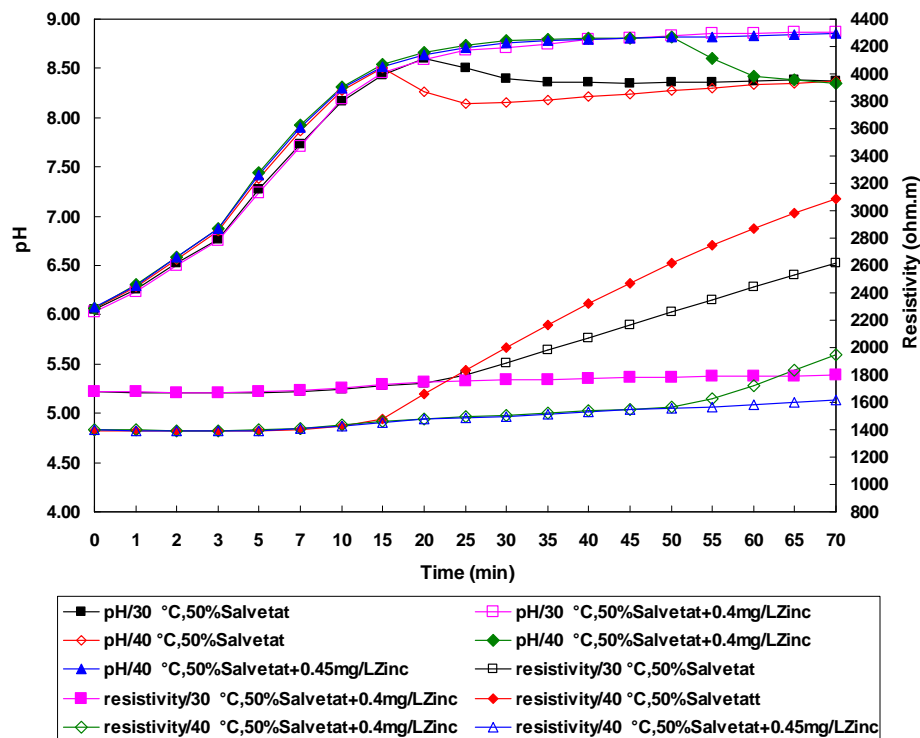


Fig.4.23 Effect of temperature on the scaling of Salvetat water in the presence of zinc ion

#### 4.2.5.3.2 The influence of dissolved CO<sub>2</sub>

As shown in Fig.4.24, at T= 30 °C, the lowest dosage of zinc ion for attaining total inhibition effectiveness of scaling needed to be increased with the rise in the concentration of dissolved CO<sub>2</sub>. For instance, as seen in Fig.4.25, at T= 30 °C, for 50 % Salvetat water, in 70 min no precipitate had yet appeared in the treated water including 0.4 mg/L zinc. But for 75 % Salvetat water, 0.4 mg/L zinc could merely retard the scaling of CaCO<sub>3</sub> for 30 min; however, if the zinc concentration reached to 0.6 mg/L, an inhibitory effectiveness of 100 % could be attained for 70 min.

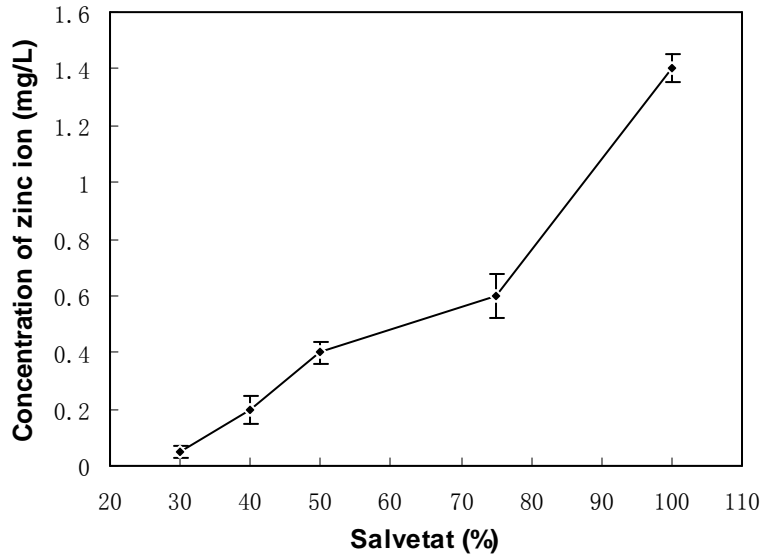


Fig.4.24 Influence of dissolved CO<sub>2</sub> concentration on the dosage of zinc ion

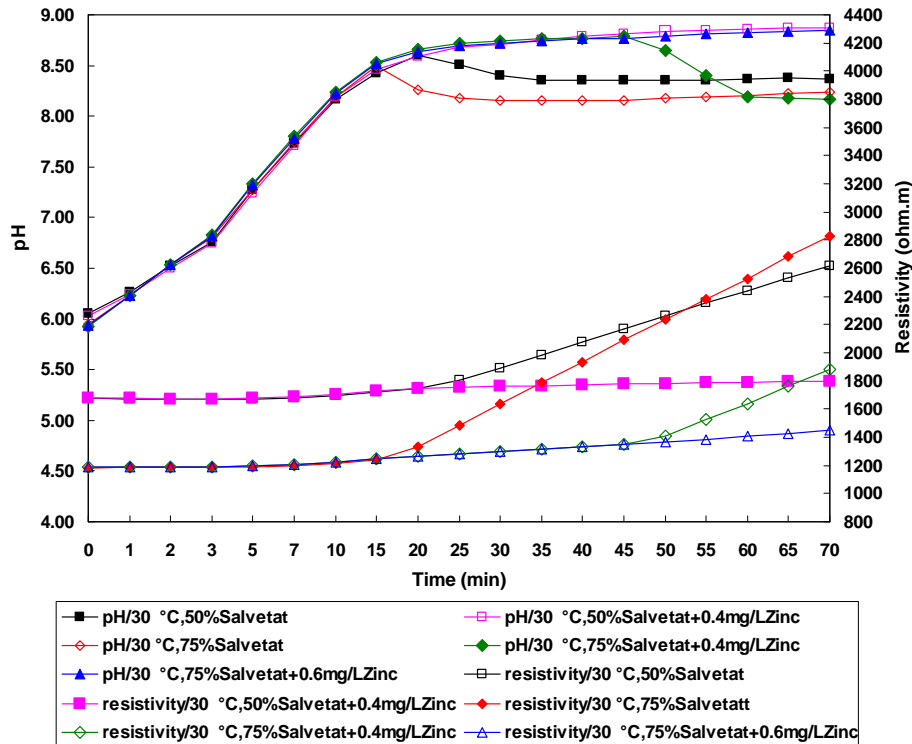


Fig.4.25 Effect of dissolved CO<sub>2</sub> on the scaling of Salvetat water in the presence of zinc ion

### 4.3 Summary

(1) The zinc ion or copper ion had great inhibition effectiveness of the scaling with a low concentration ( $<1$  mg/L), in the 300 mL solutions (calcium ion concentration of 126.5 mg/L), when the inhibition efficiency of the precipitation was 100% (in 70 min), the concentration of the copper ion was 0.9 mg/L and that of the zinc ion was 0.4 mg/L. So zinc and copper ions would be the most economical and environmentally friendly inhibitors.

(2) As the temperature rose, the scaling time of Salvetat water considerably decreased and the rate of precipitation obviously increased, so the minimum dosage of copper or zinc ion needed to totally inhibit the scaling of  $\text{CaCO}_3$  should be increased; The higher the concentration of dissolved  $\text{CO}_2$ , the shorter the scaling time of Salvetat water, and the greater the lowest dosage of copper or zinc ion needed to achieve total inhibition of scaling.

(3) By the analysis with SEM and IR of the obtained precipitate from solutions, the results showed that copper and zinc ions had participated in the composition of crystal by affecting the calcium carbonate germination and changing the crystal morphology; however, the quantity of copper or zinc ion in the precipitate was so small that it was difficult to observe them, all of which showed that zinc and copper ions were high efficient inhibitors of low concentration.

(4) The composed complexes of zinc ion or copper ion in the scaling were not known (the existing equipment such as ICP polarographic analyzer only can detect the existence of metal ions, but not determine the composition of compounds), which would be a major object of our further study.

(5) In the periodic table, we see that zinc and copper are transition metals and are closer to the metal aluminum, which showed that they had the possibility to inhibit scaling. With further research, perhaps we would discover more metals as inhibitors among these transition metals.

## **Chapter 5. Evaluation of a new “green” solid scale inhibitor with real “threshold effect”**

One of the chemical means to prevent the scaling formation consists in adding, in water to be treated, some inhibitors having “threshold effect”. However, most threshold inhibitors available nowadays are totally soluble in water. So their use generally requires two steps: first an aqueous solution of the inhibitors is prepared at a known concentration; then this solution is injected, by a dosage pump, to the water to be treated. This process is therefore onerous and often causes running troubles in practice.

An ideal scale inhibitor should be a solid form compound having a very low solubility, but the value of this solubility is big enough to ensure a total scaling inhibition.

In this chapter, we synthesized a new type of solid scale inhibitor with very poor solubility to achieve better inhibitory efficiency at a lower concentration of inhibitors.

### **5.1 Experimental**

#### **5.1.1 Materials**

##### **5.1.1.1 Test water**

Salvetat, whose characteristics are shown in Section 3.1.1.3.

##### **5.1.1.2 Synthesis of Solid inhibitor**

The procedures of precipitation, filtration, drying, pressing, etc. were carried on to prepare granular solid.

#### **5.1.2 Methods**

##### **5.1.2.1 RCP**

The principle, device, and procedure of RCP method are shown in Section 3.1.2.2.

##### **5.1.2.2 Measurement of solubility**

The supernatant solution by magnetic stirring was removed periodically followed by filtration. The active ingredient in filtrate was then measured by standard method <sup>[66]</sup>.

### **5.2 Results and discussion**

For the reason of confidentiality, the following content will be presented in another separated version.

### **5.3 Summary**

A new solid scale inhibitor was synthesized with a very low solubility (1.5 mg/L), and a complete scaling inhibition was obtained by its concentration of 30 µg/L (ppb).

# Conclusions & Perspective

## Conclusions

Using economical experimental set-up and simple experimental procedure, the method of Rapid Controlled Precipitation (RCP), which was used to estimate the scaling power of natural waters and characterise the scaling formation mechanisms, was proved to be a novel and fast evaluation method for performance of scale inhibitors.

a. Evaluation of anionic polymers as scale inhibitors on  $\text{CaCO}_3$  and Ca-phosphonate precipitates:

(1) The order of solubility of the Ca-phosphonates was found to be as follows: BHMTMP > PAPEMP > HDTMP >> PBTCa > DTPMP > EDTMP > ATMP > HEDP. The formation of Ca-phosphonates precipitates plays an important role in inhibition performance for preventing  $\text{CaCO}_3$  scale.

(2) Homopolymers of acrylic acid and epoxysuccinic acid were relatively ineffective as Ca-phosphonate precipitation inhibitors. However, copolymers and terpolymers show excellent inhibitory effectiveness. The inhibition order of the polymers for Ca-phosphonate precipitation was determined as follows: terpolymer > copolymer > homopolymer.

(3) Using the anionic AA/AMPS/HPA terpolymer as Ca-phosphonate inhibitors was found to improve inhibition efficiency for preventing  $\text{CaCO}_3$  scale and reduce the threshold effect of the inhibition by phosphates. Moreover, the molecular structure of the polymers and concentration of the polymer are critical to their performance as inhibitors of Ca-phosphonate and  $\text{CaCO}_3$  precipitation.

b. Performance of polyaspartic acid/ polyepoxysuccinic acid and their synergistic effect on inhibition of scaling:

(1) When the green scale inhibitors, PASP and PESA, were used alone for the inhibition of  $\text{CaCO}_3$  and  $\text{SrSO}_4$ , the performance of PESA overmatched PASP; on the contrary, PASP was better than PESA in inhibiting the scale of  $\text{CaSO}_4 \cdot 2\text{H}_2\text{O}$  and  $\text{BaSO}_4$ .

RCP tests showed, PESA was remarkably better performed than PASP in inhibiting  $\text{CaCO}_3$  at a low level, but with the increase of dosage, the gap between the two became gradually narrow. Compared to PASP, PESA can attain better effect at a lower dosage; with the rise in  $\text{Ca}^{2+}$  concentration or temperature, the inhibition effect of PESA or PASP got worse at the former dosage.

(2) PASP combined with PESA has better synergistic anti-scaling effect than PASP or PESA alone on inhibition of  $\text{CaCO}_3$ ,  $\text{CaSO}_4 \cdot 2\text{H}_2\text{O}$  and  $\text{BaSO}_4$ , and the optimal mass ratio of PASP and PESA is 1:1 for inhibition of  $\text{CaCO}_3$  in the static tests.

RCP tests showed that the anti-scaling performance of (PASP+PESA) (1:1) was superior to that of PASP or PESA alone, and the concentration of (PASP+PESA) (1:1) needed to attain the same efficiency was lower than that of PASP or PESA alone; as the concentration of  $\text{Ca}^{2+}$  or temperature rose, the minimum dosage of (PASP+PESA) (1:1) for achieving total inhibition of scaling should be increased.

Continuous tests indicated that with the rise in temperature, the remanent effect

would disappear gradually, even the inhibition of scaling on tubes was not complete for the same dosage of inhibitor.

c. Effects of Copper and Zinc Ion in Preventing Scaling of Drinking Water:

(1) The zinc ion or copper ion had great inhibition effectiveness of the scaling with a low concentration ( $<1$  mg/L), in the 300 mL solutions (calcium ion concentration of 126.5 mg/L), when the inhibition efficiency of the precipitation was 100% (in 70 min), the concentration of the copper ion was 0.9 mg/L and that of the zinc ion was 0.4 mg/L. So zinc and copper ions would be the most economical and environmentally friendly inhibitors.

(2) As the temperature rose, the scaling time of Salvetat water considerably decreased and the rate of precipitation obviously increased, so the minimum dosage of copper or zinc ion needed to totally inhibit the scaling of  $\text{CaCO}_3$  should be increased; The higher the concentration of dissolved  $\text{CO}_2$ , the shorter the scaling time of Salvetat water, and the greater the lowest dosage of copper or zinc ion needed to achieve total inhibition of scaling.

d. Evaluation of a new “green” solid scale inhibitor with real “threshold effect”

(1) A new type of solid inhibitor was synthesized with a very low solubility (about 1.5 mg/L) in Paris’s tap water at 20 °C, but the value of this solubility was big enough to ensure a total scaling inhibition.

(2) For 50% Salvetat at 30 °C, a complete scaling inhibition was obtained by solid scale inhibitor with a concentration of 30  $\mu\text{g/L}$ , and the temperature or  $\text{Ca}^{2+}$  concentration in water influenced inhibitive efficiency.

## Perspective

Synthesis of solid scale inhibitors is an important innovation, their solubility is very low, but the soluble parts (active ingredients) have enough inhibition effects on scaling. Solid inhibitors have following advantages comparing with traditional ones: (1) they can be added into water by a simple and convenient way without using pump. (2) Their active ingredient can release slowly, so it can protect the tube continuously for a long time. (3) Environmentally friendly and economical. Therefore, synthetic optimization, structural characterization, especially anti-scaling mechanism of “green” solid scale inhibitors will be major direction of our further research.

## References

- [1] Gabrielli C., M. Keddou, A. Khalil, R. Rosset, M. Zidoune. Study of calcium carbonate scales by electrochemical impedance spectroscopy. *Electrochim. Acta.* 1997, 42(8): 1207-1218.
- [2] Rosset, R. Les procédés physiques antitartre: mythe ou réalité? *L'actualité chimique*, 1992, 1-2: 125-148.
- [3] Aborak J, Aoki T, Ritter R B, Palen J W, Knudsen J G. Fouling: The major unsolved problem in heat transfer. *Chem. Eng.* 1972, 68(2): 59.
- [4] Elfil H., Roques H. Role of hydrate phases of calcium carbonate on the scaling phenomenon. *Desalination* 2001, 137: 177-186.
- [5] Ghizellaoui S., Euvrara M., Lédion J., Chibani A. Inhibition of scaling in the presence of copper and zinc by various chemical processes. *Desalination* 2007, 206: 185-197.
- [6] J. Ladel. Thèse de doctorat de l'Université de René Descartes de Paris V, Hydrologie appliquée, 1996.
- [7] Lin W., C. Colin, R. Rosset. Caractérisation du pouvoir incrustant d'une eau par chronoampérométrie au potentiel optimal d'entartrage. *TSM-L'eau* 1990, 12: 613-620.
- [8] Khalil A., P. Sassi, C. Colin, C. Meignen, C. Garnier, C. Gabrielli, M. Keddou, R. Rosset. Water scaling tendency characterization by coupling constant potential chronoamperometry with quartz crystal microbalance. *C. R. Acad. Sci. Paris* 1992, 314 (2): 145-149.
- [9] Gabrielli C., M., Keddou, G. Maurin, H. Perrot, R. Rosset, M. Zidoune. Estimation of the deposition rate of thermal calcareous scaling by the electrochemical impedance technique. *J. Electroanal. Chem.* 1996b, 412: 189-193.
- [10] Feitler H. The scale meter: a new method for determining the critical pH of scaling. *Mater. Prot. Proform.* 1972, 11 (1): 31-35.
- [11] Rosset R., M. Zidoune, C. Gabrielli, M. Keddou, G. Maurin, H. Perrot. Caractérisation du pouvoir entartrant d'une eau et évaluation de l'efficacité d'un traitement antitartre chimique au moyen d'une sonde thermique. *C. R. Acad. Sci. Paris* 1996, 322 (2b): 335-341.
- [12] Euvrard M., J. Lédion, Ph. Leroy. Effects and consequences of electric treatment in preventing scaling in drinking water systems. *J. Water SRT-Aqua* 1997, 46: 71-83.
- [13] Elfil H., H. Roques. Role of hydrate phases of calcium carbonate on the scaling phenomenon. *Desalination*, 2001, 137: 177-186.
- [14] Lédion J., B. François, J. Vienne. Caractérisation du pouvoir entartrant de l'eau par Précipitation Contrôlée Rapide. *Journal Européen d'Hydrologie* 1998, 28 (1): 15-35.
- [15] Hui F, Yang J, Lédion J. Evaluation gravimétrique des vitesses d'entartrage sur des tubes témoins. *J Eur Hydrol.* 2003, 34: 221-234.
- [16] Lédion J., Y. Guegnon, C. Ribal, P. Combaz, J. Verdu. L'entartrage des Matières Plastiques. *TSM l'Eau* 1993, 7-8: 355-360.
- [17] Amjad, Z. *Advances in Crystal Growth Inhibition Technologies.* Kluwer Academic/Plenum Publishers, New York, 2000.

- [18] W.J. Liu, F. Hui, J. Lédion, X.W. Wu. Inhibition of scaling of water by the electrostatic treatment. *Water Resour. Manag.* 2009, 23: 1291-1300.
- [19] M.A. Quraishi, I.H. Farooqi, P.A. Saini. Investigation of some green compounds as corrosion and scale inhibitors for cooling systems. *Corrosion.* 1999, 55: 493-497.
- [20] N. Bdel-Aal, K. Sawada. Inhibition of adhesion and precipitation of  $\text{CaCO}_3$  by aminopoly phosphonate. *J. Cryst. Growth* 2003, 256: 88-200.
- [21] I. Atamanenko, A. Kryvoruchko, L. Yurlova, E. Tsapiuk. Study of the  $\text{CaSO}_4$  deposits in the presence of scale inhibitors. *Desalination* 2002, 147: 257-262.
- [22] N. Bernd, Environmental chemistry of phosphonates, *Water Res.* 2003, 37: 2533-2546
- [23] A. Martinod, M. Euvrard, A. Foissy, A. Neville. Progressing the understanding of chemical inhibition of mineral scale by green inhibitors. *Desalination* 2008, 220: 345-352.
- [24] D. Darling, R. Rakshpal. Green chemistry applied to corrosion and scale inhibitors, *Mater. Perform.* 1998, 37: 42-45.
- [25] Zhang BR, Li FT. Versatile scale inhibition of polyepoxysuccinic acid. *Industrial Water Treatment*, 2002, 22(9): 21-24.
- [26] Zhang BR, Li FT. Study of the versatile scale inhibition of polyaspartate. *Industrial Water Treatment*, 2004, 24(2): 46-48.
- [27] Wang R, Zhang Q, Ding J, Shen ZQ. Survey of Researches on Scale Inhibition Mechanism of Scale Inhibitor. *Chemical Industry and Engineering*, 2001, 18(2): 79-92.
- [28] W. E. Gledhill, T. C. J. Feijtel, Environmental properties and safety assessment of organic phosphonate used for detergent and water treatment applications, In the *Handbook of Environmental Chemistry*, O., Ed., Springer-Verlag, Berlin, Heidelberg, 1992, 3: 261-285.
- [29] P. Pang, Y. Deslandes, S. Raymond, G. Pleizier, and P. Englezos, Surface analysis of ground calcium carbonate filler treated with dissolution inhibitor. *Ind. Eng. Chem. Res.* 2001, 40: 2445-2451.
- [30] J. Guo, S. J. Severtson, Inhibition of calcium carbonate nucleation with amino-phosphonates at high temperature, pH and ionic strength. *Ind. Eng. Chem. Res.* 2004, 43: 5411-5417.
- [31] S. J. Dyer, C. E. Anderson, G. M. Graham, Thermal stability of amine methyl phosphonate scale inhibitors. *J. Pet. Sci. Eng.* 2004, 43: 259-270.
- [32] T. H. Chong, R. Sheikholeslami, Thermodynamics and kinetics for mixed calcium carbonate and calcium sulfate precipitation. *Chem. Eng. Sci.* 2001, 56: 5391-5400.
- [33] F. Brandi, D. Bosbach, Bassanite ( $\text{CaSO}_4 \cdot 0.5\text{H}_2\text{O}$ ) dissolution and gypsum ( $\text{CaSO}_4 \cdot 2\text{H}_2\text{O}$ ) precipitation in the presence of cellulose ethers. *J. Crystal Growth*, 2001, 233: 837-845.
- [34] I. Atamanenko, A. Kryvoruchko, L. Yurlova, E. Tsapiuk, Study of the  $\text{CaSO}_4$  deposits in the presence of scale inhibitors. *Desalination.* 2002, 147: 257-262.
- [35] F. Abbona, M. Franchini-Angela, Crystallization of calcium and magnesium phosphates from solutions of Medium and low concentrations. *J. Crystal Growth.* 1990, 104: 661-671.

- [36] S. He, J. E. Oddo, M. B. Tomson, The nucleation kinetics of barium sulfate in NaCl solutions up to 6 m and 90°C. *J. Colloid Interface Sci.* 1995, 174: 319-326.
- [37] F. Jones, A. Stanley, A. Oliveira, A. L. Rohl, M. M. Reyhani, G. M. Parkinson, M. I. Ogden, The role of phosphonate speciation on the inhibition of barium sulfate precipitation. *J. Crystal Growth.* 2003, 249: 584-593.
- [38] Y. D. Yeboah, M. R. Saeed, A. K. K. Lee, Kinetics of Strontium Sulfate Precipitation from Aqueous Electrolyte Solutions. *J. Crystal Growth.* 1994, 135: 323-330.
- [39] H. Yu, R. Sheikholeslami, W. O. S. Doherty, Composite fouling characteristics of calcium oxalate monohydrate and amorphous silica by a novel approach simulating successive effects of a sugar mill evaporator. *Ind. Eng. Chem. Res.* 2002, 41: 3379-3388.
- [40] S. M. Hamza, S. K. Hamdona, Composite fouling characteristics of calcium oxalate monohydrate and amorphous silica by a novel approach simulating successive effects of a sugar mill evaporator. *J. Phys. Chem.* 1991, 95: 3149-3152.
- [41] E. Mavredaki, E. Neofotistou, and K. D. Demadis, Inhibition and dissolution as dual mitigation approaches for colloidal silica fouling and deposition in process water systems: functional synergies. *Ind. Eng. Chem. Res.* 2005, 44: 7019-7026.
- [42] A. J. Gratz, P. E. Hillner, Poisoning of calcite growth viewed in the atomic force microscope (AFM). *J. Crystal growth.* 1993, 129: 789-793.
- [43] C. M. Pina, C. V. Putnis, U. Becker, S. Biswas, E. C. Carroll, D. Bosbach, A. Putnis, An atomic force microscopy and molecular simulations study of the inhibition of barite growth by phosphonates. *Surf. Sci.* 2004, 553: 61-74.
- [44] F. Jones, A. Oliveira, A. L. Rohl, G. M. Parkinson, M. I. Ogden, M. M. Reyhani, Investigation into the effect of phosphonate inhibitors on barium sulfate precipitation. *J. Crystal Growth.* 2002, 237: 424-429.
- [45] F. Jones, A. Stanley, A. Oliveira, A. L. Rohl, M. Reyhani, G. Parkinson, M. Ogden, The role of phosphonate speciation on the inhibition of barium sulfate precipitation. *J. Crystal Growth.* 2003, 249: 584-593.
- [46] K. D. Demadis, S. D. Katarachia, M. Koutmos, Crystal growth and characterization of zinc-(amino-tris-(methylenephosphonate)) organic-inorganic hybrid networks and their inhibiting effect on metallic corrosion. *Inorg. Chem. Communications.* 2005, 8: 254-258.
- [47] X. H. To, N. Pebere, N. Pelapat, B. Boutevin, Y. Hervaud, A corrosion-protective film formed on a carbon steel by an organic phosphonate. *Corrosion Sci.* 1997, 39: 1925-1934.
- [48] M. Salasi, T. Shahrabi, E. Roayaei, M. Alifkhazraei, The electrochemical behaviour of environment-friendly inhibitors of silicate and phosphonate in corrosion control of carbon steel in soft water media. *Mater. Chem. Phys.* 2007, 104: 183-190.
- [49] S. Ramesh, S. Rajeswari, Evaluation of inhibitors and biocide on the corrosion control of copper in neutral aqueous environment. *Corrosion Sci.* 2005, 47: 151-169.
- [50] K. D. Demadis, C. Mantzaridis, P. Lykoudis, Effect of structural differences on metallic corrosion inhibition by metal-polyphosphonate thin films. *Ind. Eng. Chem. Res.* 2006, 45: 7795-7800.
- [51] S. Rajendran, B. V. Apparao, N. Palaniswamy, V. Periasamy, G. Karthikeyan,

- Corrosion inhibition by stainless complexes. *Corrosion Sci.* 2001, 43: 1345-1354.
- [52] I. Andijani, S. Turgoose, Studies on corrosion of carbon steel in deaerated saline solutions in presence of scale inhibitor. *Desalination.* 1999, 123: 223-231.
- [53] T. P. Knepper, Synthetic chelating agents and compounds exhibiting complexing properties in the aquatic environment. *Trends Anal. Chem.* 2003,22: 708-724.
- [54] B. Nowack, Environmental chemistry of phosphonates. *Water Res.* 2003, 37: 2533-2546.
- [55] J. Y. Gal, J. C. Bollinger, H. Tolosa, N. Gache, Calcium carbonate solubility: a reappraisal of scale formation and inhibition. *Talanta.* 1996, 43: 1497-1509.
- [56] N. Abdel-Aal, K. Sawada, Inhibition of adhesion and precipitation of CaCO<sub>3</sub> by aminopolyphosphonate. *J. Crystal Growth.* 2003, 256: 188-200.
- [57] A. T. Kan, G. Fu, M. B. Tomson, Adsorption and precipitation of an aminoalkylphosphonate onto calcite. *J. Colloid Interface Sci.* 2005, 281: 275-284.
- [58] F. H. Browning, H. S. Fogler, Effect of precipitating conditions on the formation of calcium HEDP precipitates. *Langmuir.* 1996, 12: 5231-5238.
- [59] R. Pairat, C. Sumeath, F. H. Browning, H. S. Fogler, Precipitation and dissolution of calcium-ATMP precipitates for the inhibition of scale formation in porous media. *Langmuir.* 1997, 13: 1791-1798.
- [60] A. T. Kan, J. E. Oddo, M. B. Tomson, Formation of Diethylenetriaminepentakis (methylene phosphonic acid) precipitates and their physical chemical properties. *Langmuir.* 1994, 10: 1450-1455.
- [61] R. Nafisur., A. Yasmin, Syed Najmul Hejaz Azmi, Kinetic Spectrophotometric Method for the Determination of Ramipril in Pharmaceutical Formulations. *AAPS PharmSciTech.* 2005, 6: 543-551.
- [62] Y.H. Sun, W.H. Xiang, Y. Wang. Study on polyepoxysuccinic acid reverse osmosis scale inhibitor. *J. Environ. Sci.* 2009, S73-S75.
- [63] B.J. Sun, W.Z. Li, P.Y. Wu. Innovative spectral investigations on the thermal-induced poly(aspartic acid). *Polymer* 2008, 49: 2704-2708.
- [64] S. Tandy, K. Bossart, R. Mueller, J. Ritschel, L. Hauser, R. Schulin, B. Nowack. Extraction of heavy metals from soils using biodegradable chelating agents. *Environ. Sci. Technol.* 2004, 38: 937-944.
- [65] F. Littlejohn, C.S. Grant, Effect of poly(aspartic acid) on the removal rates of brushite deposits from stainless steel tubing in turbulent flow. *Ind. Eng. Chem. Res.* 2002, 41: 4576-4584.
- [66] A.D. Eaton, L.S. Clesceri, E.W. Rice, A.E. Greenberg. Standard methods for examination of water and wastewater, 21st ed. American Public Health Association, Washington, 2005.
- [67] Y.X. Zhang, J.H. Wu, S.C. Hao, M.H. Liu. Synthesis and inhibition efficiency of a novel quadripolymer inhibitor. *Chin. J. Chem. Eng.* 2007, 15: 600-605.
- [68] F. Hui, J. Lédion. Evaluation methods for the scaling power of water. *Eur. J. Water Qual.* 2002, 33: 55-74.
- [69] Ghizellaoui S., Lédion J., Ghizellaoui S., Chibani A. Etude de l'inhibition du pouvoir entartrant des eaux du Hamma par précipitation contrôlée rapide et par un essai d'entartrage accéléré. *Desalination* 2004, 166: 315-327.

- [70] Q.F. Yang, Y.Q. Liu, A.Z. Gu, J. Ding, Z.Q. Shen, Investigation of calcium carbonate scaling inhibition and scale morphology by AFM. *J. Colloid Interface Sci.* 2001, 240: 608-621.
- [71] Liu W.J., Hui F., Lédion J., Wu X.W. The influence of metal ion on the scaling in the mineral water tests. *Ionics* 2008, 14: 449-454.
- [72] D'Antonio, L., Fabbricino, M., Nasso, M. and Trifuoggi, M. Copper release in low and high alkaline water. *Environ. Technol.*, 2008, 29(4): 473-478.
- [73] Dmitry, L., Yang, Q.F., David, H. and Raphael, S. Inhibition of CaCO<sub>3</sub> scaling on RO membranes by trace amounts of zinc ions. *Desalination*, 2005, 183(1-3): 289-300.
- [74] Chen, T., Neville, A., Yuan, M. Comparison of calcium carbonate scale formed in the bulk solution and on the surface of metal. 1st International Water Association Conference on Scaling and Corrosion in Water and Wastewater Systems, Bedfordshire, UK (2003).
- [75] Lédion, J., Braham, C. and Hui, F. Anti-scaling properties of copper. *J. Water Supply Res. Technol.*, 2002, 51(7): 389-398.
- [76] Parsiegla K.I., Katz J.L. Calcite growth inhibition by copper(II) I. Effect of super-saturation. *J. Crystal Growth* 1999, 200: 213-226.
- [77] Parsiegla K.I., Katz J.L. Calcite growth inhibition by copper(II) II. Effect of solution composition. *J. Crystal Growth* 2000, 213: 368-380.

## Acknowledgements

This work was funded by Laboratoire de Procédés et Ingénierie en Mécanique et Matériaux (PIMM), Arts et Métiers ParisTech (ENSAM), Centre National de la Recherche Scientifique (CNRS) & State Key Lab of Pollution Control and Resource Reuse, College of Environmental Science and Engineering, Tongji University, Science and Technology Commission of Shanghai Municipality, Ministry of Science and Technology of China.

First, I pay my highest respect and express my most sincere thanks to Professors Gérard COFFIGNAL, directeur de l'école doctorale, and Thierry BRETHERAU, directeur du PIMM, for their promoting and facilitating my study in France as a Joint PhD student.

My deepest gratitude goes foremost to Profs. Franck HUI & Jean LEDION, my supervisors in France, and Profs. Fengting LI & Bingru ZHANG, my supervisors in China, for their enthusiasm and inspiration, illuminating instruction, consistent encouragement & patient and meticulous guidance.

Second, I would like to express my heartfelt gratitude to Prof. Vincent JI, Paris-Sud 11 University, and Dr. Hongbin SONG, who have instructed and selflessly helped me a lot during my preparing dissertation.

Last my thanks would go to my beloved family for their loving considerations and great confidence in me all through these years. I also owe my sincere gratitude to my friends and fellow classmates who kindly gave me their strong support.



## Liste des publications

1. **LIU Dan**, HUI Franck, LEDION Jean, LI Fengting. Study of the scaling formation mechanism in recycling water. *Environmental Technology*, 2011, 32(9): 1017-1030.
2. **LIU Dan**, HUI Franck, LEDION Jean, ZHANG Bingru, LI Fengting,. Effects of temperature and dissolved CO<sub>2</sub> on the scaling of water in the presence of copper and zinc. *Ionics* (accepted).
3. **LIU Dan**, ZHANG Bingru, HUI Franck, LEDION Jean, LI Fengting. Comparison of performance of polyepoxysuccinic acid and polyaspartic acid on inhibition of scaling by static and rapid controlled precipitation methods, *Desalination* (accepted).
4. **LIU Dan**, ZHANG Bingru, HUI Franck, LEDION Jean, LI Fengting. Study of synergistic effect of polyaspartic acid and polyepoxysuccinic acid on scaling inhibition, *Environmental Technology* (accepted).